PHOTO-CATALYTIC DEGRADATION OF BENZENE, TOLUENE, XYLENE IN AN AQUEOUS SOLUTION

BY
ABDULLA MUSBAH ABDULLA MOHAMED KHAIR

A Thesis Presented to the
DEANSHIP OF GRADUATE STUDIES

KING FAHD UNIVERSITY OF PETROLEUM & MINERALS
DHAHRAN, SAUDI ARABIA

In Partial Fulfillment of the
Requirements for the Degree of

MASTER OF SCIENCE

In

CHEMICAL ENGINEERING

MAY 2015

KING FAHD UNIVERSITY OF PETROLEUM & MINERALS

DHAHRAN- 31261, SAUDI ARABIA

DEANSHIP OF GRADUATE STUDIES

This thesis, written by **Abdulla Musbah Abdulla Mohamed Khair** under the direction his thesis advisor and approved by his thesis committee, has been presented and accepted by the Dean of Graduate Studies, in partial fulfillment of the requirements for the degree of **MASTER OF SCIENCE IN CHEMICAL ENGINEERING.**

Dr. Reyad A. Shawabkeh
(Advisor)

Dr. Mohammed Ba-Shammakh
Department Chairman

Dr. Ibnelwaleed Ali Hussein
(Member)

Dr. Salam A. Zummo
Dean of Graduate Studies

Dr. Abdullah S. Sultan
(Member)

13/6/15
Date

Dr. Nadhir A. H. Al-Baghli
(Member)

Dr. Zuhair Omar Malaibari
(Member)

To my parents for every thing

To my brothers and sisters of their support

Acknowledgment

I would like to express my sincere gratitude to all of those who made this work possible. I am very grateful to King Fahd University of Petroleum and Minerals and to the Chemical Engineering Department for giving me the opportunity to pursue my master program. Many thanks go to my thesis advisor Prof. Reyad A. Shawabkeh and my co-advisor Prof. Ibnelwaleed Ali Hussein for fostering me and accepting me as their son. I would like also to thank my Thesis committee members Dr. Abdullah S. Sultan, Dr. Nadhir A. H. Al-Baghli and Dr. Zuhair Omar Malaibari for their valuable comments. Thanks are also due to Dr. Mustafa Nasser of University of Qatar. Thank are extended to all colleagues and friends for making my stay at KFUPM such a wonderful experience. Finally, I would like to express my sincere gratitude to my family members for their love and support.

Table of Contents

List of Tables

List of Figures

Thesis Abstract

Full Name : Abdulla Musbah Abdulla Mohamed Khair

Thesis Title : Photo-Catalytic Degradation of (BTX)

Major Field : Chemical Engineering

Date of Degree : May 2015

The daily routine of domestic activates and industrial facilities introduce tremendous amount of Hydrocarbons, among the hazardous by products volatile organic compounds (VOCs), there pollutants attract the attention for their harmful presence in environment, resulting pollution of atmosphere and water. Well known group of VOCs are Benzene, Toluene and Xylenes (BTX). The necessity for elimination follows its toxicity and highly carcinogenic, even acute contact to low concentrations can cause damage to organs. Owing to their adverse effects on human health and quite relative solubility in water; Environmental Protection Agency (EPA) and World Health Organization (WHO) environmental laws for water contaminations are more present where the latter specified the amounts of Benzene Toluene and Xylenes in potable water not to exceed 0.01, 0.7 and 0.5 mg/L respectively.

Iron doped titanium dioxide (Fe-TiO_2) is synthesized through applying Sol-Gel method. The prepared catalyst aimed for photo catalytic degradation of Benzene Toluene and Xylenes (BTX) in aqueous solution utilizing ultraviolet light. Synthesized catalyst was tested using many techniques to meet the intended synthesis procedure. N_2 adsorption/desorption suggested catalyst is mesoporous structure with relatively high surface area and narrow pore size distribution. X-ray diffraction (XRD) revealed samples possess small size grains, both phases Anatase and Rutile. X-ray fluorescence (XRF) was used for determining the elemental compositions of the

synthesized catalyst. Scanning electron microscopy along with energy dispersive X-ray (SEM-EDX) shown that morphology of samples investigated possess almost sharp corners and straight edges, mostly clusters of irregular shapes varying in size and dimension of synthesized catalyst. Photo catalytic activity of Fe-TiO_2 was evaluated for liquid phase phase photo catalytic degradation of benzene, toluene and xylenes under ultraviolet illumination, resulting optimum iron content around 1%. Moreover, Famous adsorption isotherms were suggested (Langmuir, Freundlich and Redlich–Peterson) to fit the equilibrium concentrations of benzene, toluene and xylenes, with adsorption capacity ascending benzene, toluene then xylenes the latter was found to be the maximum 92.1083 (mg/g). Further, benzene-toluene-xylenes were investigated for adsorption isotherms in binary mixture, to examine the effect on equilibrium capacity and in consideration to its influence on photo catalytic degradation.

ملخص الرسالة

الاسم الكامل: عبد الله مصباح عبدالله محمد خير

عنوان الرسالة: التحفيز الضوئي لتحليل (BTX)

التخصص: هندسة الكيميائية

تاريخ الدرجة العلمية: مايو 2015]

الروتين اليومي من النشاطات اليومية والمنشآت الصناعية تتسبب بكميات هائلة من الهيدروكربونات, ضمن المنتجات الجانبية المضرة المركبات العضوية المتطايرة (VOCs). هذه الملوثات تجذب الانتباه لضررها على البيئة, ينتج عنه تلوث الغلاف الجوي والمياه. مجموعة مشهورة من (VOCs) بنزين وتولين زالزايلين (BTX). أهمية التخلص مرتبطة بخواصها السامة والمسرطنة, حتى التعرض المزمن لكميات قليلة تتسبب بضرر للأعضاء. نظرا للآثار الضارة على صحة البشر وذوبانيتها في الماء, منطمات بيئية مثل Environmental Protection Agency (EPA) وWorld Health Organization (WHO) قوانين بيئية لملوثات الماء أصبحت أكثر وجودا حيث ان المنظمة الاخيرة حددت الكميات القصوى المسموح بها للبنزين وتولين زالزايلين في مياه الشرب 0.5-0.7-0.01 mg/L على الترتيب.

ثاني اكسيد التايتينيوم مضافا اليه الحديد قد تم تحضيره بواسطة تقنية Sol-Gel. المحفز الحضر هدفه تحليل بنزين وتولوين والزايلين بالتحفيز الضوئي في محلول مائي بتعريض الاشعة فوق البنفسجية. الحفازالمحضر قد تم اختباره بواسطة طرق عديدة لمطابقة طريقة التحضير. ادمصاص وامتزاز النايتروجين وضح ان المحفز متوسط المسامية مع مساحة سطح عالية نسبيا و محدود التنوع في مقاس المسام. حيود الاشعة السينسة (XRD) وضح ان العينات تمتاز بحجوم صغيرة, وتمتلك كلتا التكوين انانيز و روتايل. الاشعة الفلورية السينية (XRF) استعمات لتحديد التكوين العنصري للحفاز بالاضافة الى (EDX) الذي اوضح شكل الحفاز يتكون من زوايا حادة وحواف مستقيمة, معظمها تكتلات مختلفة الابعاد والاحجام. نشاط التحفيز الضوئي قد درست في الحالة السائلة للتحليل بنزين وتولوين والزايلين بالتحفيز الضوئي بتعريض الاشعة فوق البنفسجية, نتج عنه امثلة نسبة الحديد حوالي 1%. زيادة على ذلك, نماذج الادمصاص التماثلية مثل (Langmuir, Freundlich and Redlich–Peterson), قد تم استعمالها لمطابقة تراكيز الاتزان لكل من بنزين وتولوين والزايلين, مع ازدياد سعة الادمصاص

تصاعديا بنزين وتولوين والزايلين حيث الاخير اكتسب الاقصى (mg/g) 92.1083. ايضا, تم دراسة الادمصاص التماثلي المزدوج لكل من بنزين وتولوين وزايلين, لمعرفة تأثيرها على تراكيز الاتزان مع الاهتمام لتأثيرها على تحليل بالتحفيز الضوئي.

1. Chapter

1.1 Introduction

Hydrocarbons play double edged role to human life; According to Environmental Protection Agency (EPA), Agency for Toxic Substances and Disease Registry (ATSDR), International Program on Chemical Safety (IPCS-INCHEM) and other environmental agencies, the existence of certain chemicals can have adverse effect to environment then inevitably human health. Benzene, Toluene and Xylenes (BTX) are famous group produced in the petroleum and chemicals processing, among the priority pollutants to be dealt due to its severe health effects. BTX are relatively soluble in water benzene, toluene (O, M, P)-xylenes are [1800, 535 142, 146, 185] mg/L respectively (Breu et al. 2008a; Breu et al. 2008b; Breu et al. 2008c). Pollutants found in soil, water and air; e.g. leakage of hazardous compounds from underground storage tanks contaminates the soil, septic tanks, waste disposal pits and sewer lines, eventually the ground water adjacent an essential source to rural areas and finally into air hence nature volatility. As a group the BTX is harmful to human being; Benzene exposure for few minutes to high levels (10,000–20,000) ppm can cause death and for long time probably cancer, lower levels might result headaches, rapid heartbeat and unconsciousness (Wilbur and Keith 2007). Toluene also can be fatal or brain damaging; disturbing breathing and heart functions, high concentration would damage the kidney. Other symptoms confusion, nausea and decrease in mental ability (Dorsey and McClure 1989). Xylenes on the other hand, at high concentrations some casualties have been found, short exposure can result irritation, malfunction of lungs and nervous system and possible mutation to kidneys and liver (Fay and Risher 2007).

Table 1.1 National Primary Drinking Water Regulations (Oc & Ioc n.d.)

Contaminant		MCL	possible health effect	Common source contamination	Public health (mg/L)[2]
OC	**Alachlor**	0.002	Eye, liver kidney or spleen problems; anemia; increased risk of cancer	Runoff from herbicide used on row crops	Zero
IOC	**Antimony**	0.006	Increased in blood cholesterol; decrease in blood sugar	Discharge from petroleum refineries; fire retardants; ceramics; electronics; solder	0.006
OC	**Benzene**	0.005	Anemia; decrease in blood platelets increased risk of cancer	Discharge from factories; leaching from gas storage tanks and landfills	Zero
DBP	**Bromated**	0.010	Increased risk of cancer	Byproduct of drinking water disinfection	Zero
D	**Chlorine**	MRDL=4	Eye/ nose irritation; stomach discomfort	Water additive used to control microbes	MRDL=4
OC	**Toluene**	1	Nervous system, kidney or liver problems	Discharge from petroleum factories	1
OC	**Xylenes**	10	Nervous system damage	Discharge from petroleum factories; discharge from chemical factories	10

OC	organic compound	IOC	Inorganic chemical
DBP	Disinfection byproduct	D	Disinfection
MCL	Max contaminant level	MRDL	Max residual Disinfection level

Table 1.2 Critical Molecular Diameter (Ruthven et al. 1991; Newsam 1988)

Element	Diameter (nm)
Benzene	0.69
Toluene	0.69
(P,O,M)-Xylene	0.69-.074-.074

1.2 Photo catalysis

The first discovery of this phenomena also known as “Honda-Fujishima Effect” was in 1972 for water electrolysis (Fujishima 1972), the concept of catalysis in both the conventional and photo type are the same except for the conventional is activated by thermal means while the latter is by means of photonic activation via illumination **Fig 1.1**. It can be carried in either gas, aqueous or pure organic liquid phase. Similar to normal reaction steps, the process undergoes:

- Migration of the reactant(s)through the media to the catalyst surface
- Adsorption/photo-adsorption of reactant(s) to surface
- Reaction/photo-catalytic on the surface
- Desorption/photo-desorption of the product(s)
- Transfer/diffusion of the product away from surface through the fluid media

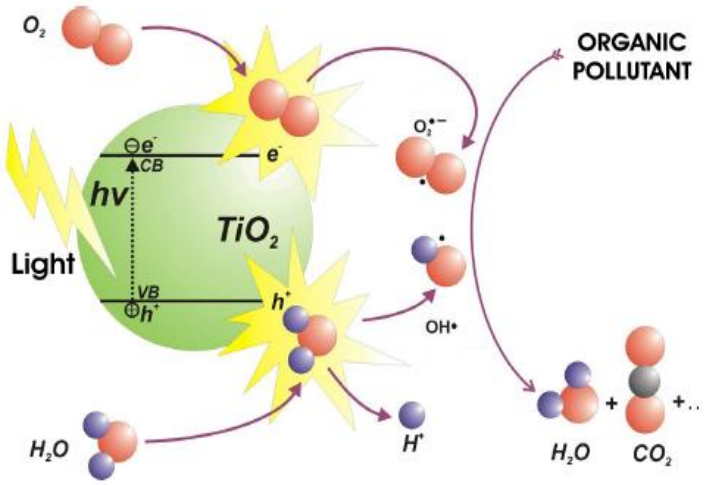

Figure 1.1 UV Photo Catalytic Activation and Free Radicals (Ibhadon and Fitzpatrick 2013)

1.2.1 Mechanism

The excitation of the semiconductor occurs from the radiation absorbance of higher or equal to energy band gap 'difference between valence and conduction bands' for specific semiconductor (E_{bg}), which for TiO_2 case is respectively large from (3.2 ~ 3.02) eV anatse to rutile respectively

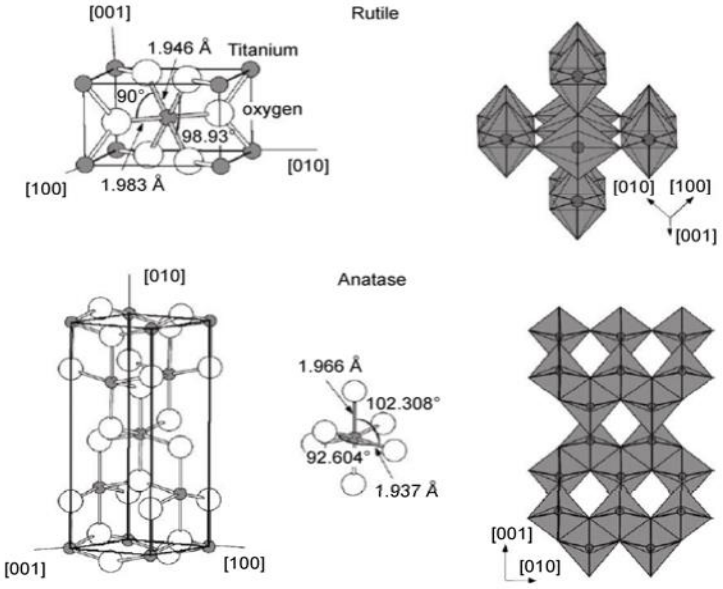

Figure 1.2 Rutile and Anatase Structures (Gupta and Tripathi 2011)

Ohno et al. (2003) found that highest activity favorable both anatase and rutile phases about 10% anatase, the valence band of TiO_2 (2p orbitals oxygen and 3d orbitals titanium) but, for titanium only 3d, irradiation approximately to Ultraviolet excites electrons in the conduction band and at 3d state, (e^-) affinity to transit into valence band probably get lower hence, less recombination of e^-/h^+ (Gupta and Tripathi 2011).

The mobile electrons at the conduction band will be generated simultaneously with positive holes in the valence band, further photo catalytic reaction will occur afterwards, photo-generated h^+/e^- contributes redox reaction on surface of catalyst for oxidation and reduction processes respectively. h^+ assists separating the water molecule into hydron (H^+) and hydroxyl radical

(OH^-), the latter generates (HO^*) strong oxidizing radical. In the meantime, e^- form other superoxide (O_2^{-*}) also contributes to (HO^*) through (HO_2^-) radicals and (H_2O_2). Recombination may arise, causing dissipation of the energy absorbed earlier hence, undesirable to the reaction sequence. On the other hand, large quantity of (HO^*) is available in TiO_2 suspension and this play important role in the mineralization of hydrocarbons. **Table 1.3** summarized the photo-catalytic reaction of irradiated TiO_2.

Table 1.3 Photo Catalytic Mechanism TiO_2 Under Illumination (Teh and Mohamed 2011)

Process	Reaction step
Photo-excited TiO_2 generates e^-/h^+ pairs ($hv>E_{bg}$)	$TiO_2 \xrightarrow{hv} e^- + h^+$
Photo-generated h^+transfer to surface thus reaction occurs with water molecules absorbed H_2O_{ad}	$TiO_2(h^+) + h_2O_{ad} \rightarrow TiO_2 + HO^* + h^+$
Photo-generated (e^-) transfer to surface where oxygen assists as an acceptor in electron reaction	$TiO_2(e^-) + O_2 \rightarrow TiO_2 + O_2^{*-}$
Reaction if superoxide anions (O_2^-)	$O_2^{*-} + H^+ \rightarrow HO_2^*$ $O_2^{*-} + 3HO_2^* \rightarrow HO^* + 3O_2 + H_2O + e^-$ $HO_2^* \rightarrow O_2 + H_2O_2$
hydrogen peroxide Photo-conversion gives (HO^*) free radical groups	$H_2O_2 + TiO_2(e^-) \rightarrow TiO_2 + HO^- + HO^*$
adsorbed pollutants (S_{ad}) are Oxidized by (HO^*) on TiO2surface	$HO_2^* + S_{ad} \rightarrow intermediates$
Overall reaction	$pollutant \xrightarrow{TiO_2(e^-)/hv} intermediates \rightarrow CO_2 + H_2O$

1.2.2 Types of photo-catalyst

Many semiconductors are available and been tested as photo-catalyst for pollutants degrading such ZnO, CdS, Fe_2O_3, TiO_2, ZrO_2, MoS_2 and WO_3. Characteristics needed to compare between plenty semiconductors based on its photo-stability, abundant and cost, the inertness nature both chemically and biologically and adsorbance of reactants under efficient photo-activation ($E_{radiation} \geq E_{bg}$). Thus, titania is considered the preferable among the diversity of semiconductors due to less E_{bg} and photo-activation wave length λ (300-388) nm. Other types such as ZnO and SnO_2 have higher E_{bg} (3.35 and 3.6) eV respectively (Gaya and Abdullah 2008). PbS and CdS rapidly lead to photo-corrosion and instability in aqueous media similar to ZnO (Bahnemann 1987) which tends to dissolves yielding $Zn(OH)_2$ and toxicity (Mills and Hunte 1997). SnO_2, Fe_2O_3 and WO_3 are naturally inherit conduction band's level of energy permits reversible hydrogen potential (Sivula et al. 2009).

In addition to the anatase and rutile phases individually or combined giving modification to photo-activity and stability. Several approaches are been developed to enhance the activity of the catalyst, and this can be categorized into Pure titanium modification (parameters), metal doping (transition metals: Co, Cr, Mo, V, Fe, Au, Pt, Cu, Ni, Mn, Nb, Ru, Ag) and nonmetal doping (N, C, P, F, S, B, I) (Zaleska 2008).

1.3 Literature Review

Photo catalysis has been an area of the interest in the recent era, one of the significant importance decomposition of organic compounds. The common semiconductors used for this specific reaction are WO_3, ZnS, Fe_2O_3, ZnO, CdS, $SrTiO_2$ and TiO_2. The latter have been numerously published as the most reliable and active in organic decomposition. Main features which titania inherit are non-toxicity, insolubility in water with or without irradiation, stability in aqueous media and weak rate of photo-corrosion. In spite of, the large band gap (3.0~3.2) eV (Thiruvenkatachari 2008) needed to be activated by UV to shift the absorption into visible region, insufficient solar energy exploit and a quite recombination generated e^-/h^+ pairs result in insufficient photon use and hinder its application in industry. Thus, improvement of TiO_2 is demanded to overcome these obstacles; suggestions modifying through noble metals, polymer, semiconductors junctions and transition metal doping. The latter was being investigated capaciously, accordingly decomposition of organic pollutants. Modification of TiO_2 to shift the absorption into visible region was investigated through doping both metals and non metals (Lee et al. 2003; Ohno et al. 2004). Also transition metals such Mn, Co, Ni, Cr, Cu and Fe were studied (Carp 2004). Fe, W and V share the similarity ionic radii to Ti cation (Ti^{4+}=74.5 pm, Fe^{3+}=78.5 pm, W^{6+}=74 pm, and V^{5+}=68 pm), causing better stable dispersion into TiO_2 matrix without phase segregation.

1.3.1 Titanium Dioxide photo-catalyst

Many studies have been conducted for photo-degradation of organic compounds, among all photo catalysis, titanium dioxide appears applicable for removal of wide range of hazardous organic compounds such as dyes (Chung and Chen 2008; Dias and Azevedo 2009), pesticides (Echavia et al. 2009; Fabbri et al. 2009), Drugs (Hapeshi et al. 2010; An et al. 2011) and pharmaceutical products (Choina and Duwensee 2010; Lin et al. 2011).

Fu et al. (1995) examined the decomposition of benzene with oxygen in gas phase using TiO_2 and platinum doped TiO_2 (0.1 wt %), observed improving in the catalyst activity towards benzene mineralization correspondingly to doping at temperature higher than (100^oC). Augugliaro et al. (1999) studied the illumination of toluene in gas solid regime using TiO_2 anatase polycrystalline in different molar ratios and compositions; air water and N_2 CO_2. Side products were detected through FT-IR, besides the importance of oxygen and water for photo-reaction and conserving catalyst activity respectively. Maira et al. (2001) modified sol-gel method to photo-oxidize toluene by TiO_2 in nano-size in both humid and dry environment, concluded mineralization of toluene efficiency related to minute particle size (6 nm) and electronic nature of TiO_2. Jeong et al. (2004) Tried to imply short wave length UV (254+185 nm) photo-oxidation of Toluene, resulting enhancement both photo-degradation and photo-chemical oxidation. Wang et al. (2003) Studied benzene degradation in gas phase at room temperature; the TiO_2 was used with UV intensity, in their work, the effect of humidity and concentration on the benzene mineralization was considered. Results were fitted using Langmuir–Hinshelwood model, they also suggested regenerating the deactivated catalyst by ozone in humid condition. Tsoukleris et al. (2007) Investigated elimination of BTX via nano-crystalline TiO_2 paste over spherical glass photo-catalytic, they reported that the light intensity was proportional to photo-

catalytic rate and stability and the results were reproducible. Xu et al. (2010) Studied carbon nano-tubes CNT/TiO_2 nano-composite photo catalyst to decompose benzene in gas phase; it revealed improvement photo catalytic activity in line to conventional Degussa P_{25}. Another attempt by mechanical mixing of conventional titania and prepared photo catalyst were developed, no improvement in activity nor decomposition was achieved. Hir et al. (2011) investigated decomposition of BTX in aqueous media by ZnO/SnO_2/WO_3 (ZSW) and ZnO/TiO_2/WO_3 (ZTW), the latter performed better as small particles in addition to H_2O_2 (10 ppm).

1.3.2 Ferrous Doped Titanium Dioxide Photo-Catalyst

As an outcome from the previous section, TiO_2 Metal doping was found favorable for degradation activity; altering the scheme of preparation or doping metals such Co(II), Ru(III), Fe(III&II) and Ag(I) under influence of ultraviolet light radiation with or without doped metals, the investigation assumed Fe^{3+} as the highest photo catalysis dopant, due to sensitivity in water when compared to others hence, essential for decomposition (Anipsitakis and Dionysiou 2004), another approach by Di Paola et al. (2002) to use doped TiO_2 powders polycrystalline with metal ions (Cr, Fe, W, Co, Cu, V and Mo). All agreed on the enhancement of photo activity compared to commercial. Among the transition metals, Fe^{3+} in particular was performing within expectations; dopant in small amounts (Ranjit and Viswanathan 1997). As a result, improvement in photo-catalytic of titania (Di Paola et al. 2002). Interestingly, Fe^{3+} cations is believed to behave as traps in TiO_2, in spite of its enhancing recombination e^-/h^+ (Hoffmann et al. 1995), where the favorable amount of Fe^{3+} was found 0.0%, 0.5% and 3.0% (Su et al. 2007).

(Zuo et al. 2006) Investigated VOCs in gas phase, by means of photolysis and photo catalysis, under illumination of germicidal lamp, which in case of direct contact of germicidal lamp with

benzene is not sufficient for degradation unlike toluene. Both means resulted proper rate of decomposition, also. Furthermore, photo catalysis synthesized by doping Sn and Fe to TiO_2; SnO_2/TiO_2 catalyst effect over benzene decomposition rate was high compared to Fe^{3+}/TiO_2 catalyst but, in case of mineralization rate it was the opposite. Hence, Fe^{3+}/TiO_2 catalyst performance was superior in both elimination and mineralization rate. Laokiat et al. (2011) Investigated degradation of Benzene, Toluene, Ethyl benzene and Xylenes (BTEX) in gas phase via doping (Fe, V and W)-TiO_2 containing both anatase (80%) and rutile produced by solvo-thermal technique and fiber glass immobilization under visible light. The results showed bare titania had less catalytic activity towards visible light than synthesized.

Jo and Lee (2013) developed sol-gel method to synthesize Fe-TiO_2 photo catalysts via tetra-*n*-butyl titanium and iron (III) nitrate. The prepared composites were oriented for low-concentration (0.1 ppm) airborne benzene, toluene, ethyl benzene, and *o*-xylene degradation. They found that the time-series ratios of outlet to inlet concentrations under illumination vary; i.e. the decomposition under the visible light is lower or similar to the reference TiO_2 photo catalyst, which was the opposite in the case of UV light. Also the optimum ratio of Fe/Ti in Fe-TiO_2 composite, assumed to perform good for low concentration aromatic organic pollutants. It follows that, enhancement in activity.

1.4 Objectives

In summary, reference to the literature review of photo-catalytic degradation of benzene, toluene and Xylenes, most studies ignore the fact BTX are dealt with in industrial case as mixture rather than individual. In addition to, their harmful presence as liquid phase in water. Therefore, in this study we aim to

- Synthesize iron doped titanium dioxide (Fe-TiO_2) photocatalytic degradation
- Characterize the prepared catalyst to verify the physical and chemical properties.
- Study the optimum iron doping into titanium dioxide accordingly photocatatalytic activity
- Examine the single adsorption isotherm of BTX and fit into famous models
- Investigate binary adsorption isotherms for BTX.
- Study the single and binary photocatalytic degradation of BTX.

1.5 Thesis Summary

This section gives a general idea of paper based manuscript.

1.5.1 Chapter Two

In this chapter, we will study the photo catalytic degradation of xylenes and toluene in aqueous solution using ultraviolet irradiation. The proposed catalyst is iron doped titanium dioxide (Fe-TiO_2). Prepared catalyst will be characterized my means of N_2 adsorption/desorption, X-ray diffraction (XRD), X-ray fluorescence (XRF) and Scanning electron microscopy along with energy dispersive X-ray (SEM-EDX). Adsorption isotherms for both mono and binary components system will be investigated. In addition to, photo catalytic degradation of binary xylenes and toluene.

1.5.2 Chapter Three

We will examine photo catalytic degradation of binary benzene and toluene in aqueous solution, using Iron doped titanium dioxide (Fe-TiO_2).under ultraviolet light illumination. The synthesized catalyst will be tested by means of X ray fluorescence (XRF), X-ray diffraction (XRD), N_2 adsorption/desorption and Scanning electron microscopy along with energy dispersive X-ray (SEM-EDX). Adsorption isotherms for both single and multi-components system will be studied. Besides, photo catalytic degradation of binary benzene and toluene.

1.5.3 Chapter Four

Benzene and xylenes will be subjected to Photo catalytic degradation in aqueous solution via synthesized iron doped titanium dioxide (Fe-TiO_2). The catalyst will be examined through X-ray diffraction (XRD), N_2 adsorption/desorption, X-ray fluorescence (XRF) and Scanning electron microscopy along with energy dispersive X-ray (SEM-EDX). Studying adsorption isotherms for

both Benzene and xylenes system individually and simultaneously. Further, study photo catalytic degradation of binary Benzene and xylenes.

1.5.4 Chapter Five

Brief conclusion of the whole work done, including recommendation for some future work

2 Chapter

Photo Catalytic Degradation of Xylenes and Toluene Binary Mixture in Aqueous Solution

Abstract

Iron doped titanium dioxide (Fe-TiO_2) was synthesized using Sol-Gel method for photo-catalytic degradation of xylenes and toluene in aqueous solution. Prepared catalyst was Characterized by means of N_2 adsorption/desorption, X-ray diffraction (XRD), X-ray fluorescence (XRF) and Scanning electron microscopy along with energy dispersive X-ray (SEM-EDX) to meet the intended synthesis procedure. The Fe-TiO_2 was found to possess both phases Anatase and Rutile, mesoporous structure, relatively high surface area and narrow pore size distribution with optimum iron doping about 1 %. Langmuir, Freundlich and Redlich–Peterson isotherm models were proposed to study adsorption capacity of toluene and xylenes with the latter resulting maximum capacity. Further investigation into xylenes-toluene binary adsorption isotherms revealed adsorption capacity of pure pollutant is influenced by the presence of coupling pollutant reducing the individual corresponding adsorption capacity. Accordingly, the photo catalytic degradation of binary xylenes and toluene since adsorption role is essential for degradation initiation.

2.1 Introduction

Environmental pollution of air, water and soil is a major concern for human beings. Therefore, environmental organizations such as Environmental Protection Agency (EPA) and World Health Organization (WHO) insisted on the importance of dealing with hazardous compounds in an effective matter to reduce the pollution. Toluene and xylenes are well known Aromatic Hydrocarbons constituents in crude oil together with Benzene, Toluene, Ethyl benzene and Xylene (BTEX). Due to its potential carcinogenic and mutagenic effect on human health (Dorsey and McClure 1989; Fay and Risher 2007), the elimination is a priority among other pollutants in water.

The daily routine of industry contributes considerable amounts that can be detected near oil & gas industries (Fahim et al. 2009) and petrochemicals (Ferrari-Lima et al. 2014) contaminating the surroundings. Hence, it is necessary to treat polluted water by effective and efficient techniques in order to diminish or completely eradicate pollutants. Numerous techniques have been published towards the removal of toluene and xylenes. Adsorption of undesired components via adsorbent's surface such as Activated Carbon (Dias et al. 2007); convenient surface characteristics & high porosity, Zeolite (Vidal et al. 2012; Gibson 2014); tunable geometry and surface properties & pore size, and Clays (Vidal & Volzone 2009; Hackbarth et al. 2014); non-toxic, high surface area and abundant. Nonetheless, previous methods are rather intermediate process where the pollutants are been transferred from liquid phase into solid surface of the adsorbent. An alternative promising method is advanced oxidation processes (AOPs), which uses hydrogen oxide to produce oxidizing agent in the presence of ultraviolet and ozone to eliminate organic pollutants. This method is considered energy and resource demanding (Arslan et al. 2000; Comninellis et al. 2008). Accordingly, the photo-degradation method emerge

as an alternative; radiation through Ultraviolet or visible light to oxidize hazardous organic pollutants (Crittenden et al. 1997).

Many studies have been conducted for photo-degradation of organic compounds, among all photo catalysts titanium dioxide (TiO_2) appears applicable for removal of wide range of hazardous organic compounds such as dyes (Chung and Chen 2008; Dias and Azevedo 2009) and pesticides (Echavia et al. 2009; Fabbri et al. 2009). Further, Blanco et al. (1996) managed to synthesize titania based monolithic catalyst for gas-solid heterogeneous photo-catalytic oxidation of toluene and xylene in the temperature range 150^o to 450^o in gas phase and impressive destruction for both pollutants was achieved. Augugliaro et al. (1999) studied the illumination of toluene in gas solid using TiO_2 anatase polycrystalline in different molar ratios and compositions and demonstrated the importance of oxygen and water for photo-reaction and conserving catalyst activity respectively. A modified sol-gel method to photo-oxidize toluene by Maira et al. (2001) via nano-size TiO_2, concluded mineralization of toluene efficiency related to minute particle size. Tsoukleris et al.(2007) investigated the elimination of (BTX) via nano-crystalline TiO_2 paste over spherical glass, they reported that the light intensity was proportional to photo-catalytic rate and stability and the results were reproducible.

Another approach is to increase the mineralization rate by adding Ferrous into Titanium dioxide. Laokiat et al. (2011) Investigated the degradation of BTEX in gas phase via doping of Fe, V and W on TiO_2 containing both anatase (80%) and rutile produced by solvo-thermal technique and fiber glass immobilization under visible light. The results showed bare titania had less catalytic activity towards visible light than synthesized. Jo and Lee (2013) developed sol-gel for Fe-TiO_2 photo catalyst, the prepared composites was oriented benzene, toluene, ethyl benzene, and *o*-xylene (BTEX) degradation. They found that activity can be induced under both visible light and

UV irradiation. Moreover, decomposition of low concentration aromatic pollutants for the synthesized catalyst exceeded the reference TiO_2, under the visible light regime. An optimal ratio of ferrous into titanium dioxide is essential for effective photo-degradation of aromatic organic pollutants.

From the previous section, it can be noticed the lack of information regarding xylenes and toluene multi component effect on photo degradation in aqueous solutions. Therefore, in this study iron doped Titanium Dioxide (Fe-TiO_2) will be synthesized using sol-gel method besides, finding optimum doping of iron in Titanium lattice, experimental photo-degradation and adsorption of Toluene and Xylenes will be investigated in both mono and binary mixture in aqueous solution, including theoretical study to determine equilibrium isotherms.

2.1.1 Experimental

2.1.1.1 Materials

The chemicals used in current study were Toluene (99.7 %), Xylenes (96 %) in high purity and Titanium (IV) Isopropoxide (97%) [$Ti(OCH(CH_3)_2)_4$] as a Titanium precursor later on for Iron doping, all obtained from (Sigma-Aldrich). Ferric Nitrate (98 %) [$Fe\ (NO_3)_3.9H_2O$] (Loba Chemie) is used as source of iron for doping into Titanium lattice. Acetic Acid glacial (99.5 %) [ACOH] (BDH Chemicals). Ethanol (99.9 %) [EtOH] (Scharlau).

2.1.1.2 Catalyst Synthesis

The synthesis of (Fe-TiO_2) followed Sol Gel method; a beaker was filled with 125 mL of Ethanol (EtOH), that was followed by 25 mL of Titanium precursor [$Ti(OCH(CH_3)_2)_4$]. The mixture was then stirred to ensure homogeneity of the solution for further processing. On the other hand, in

another beaker a 125 mL of Ethanol (EtOH) 5 mL of Acetic Acid (AcOH) and a specific amount of Ferric Nitrate [Fe $(NO_3)_3.9H_2O$] were mixed to achieve a desired percentage of doping. The latter mixture was added via a burette to the first beaker in a drop wise manner mixing with a magnetic stirrer. Then, the mixing was continued for 2 minutes. The mixture was then sonicated in ultrasonic bath for 60 minutes. The obtained orange brownish solution was left to age at room temperature for 24 hours. The solution formed a gel structure and the gel was kept into the oven and dried for 24 hrs at 70^o C. The last step was the calcination of the resulting dried powder in a furnace at 400^oC for 4 hours to produce the final powder.

2.1.1.3 Characterization

The specific surface area (S_{BET}), pore volume and other structural properties of the catalyst were carried out using nitrogen adsorption/desorption [Micrometrics ASAP 2020 – Physisorption Analyzer]. A sample of 0.4663g was degassed under vacuum for 60 minutes at 473 K before undergoing N_2 adsorption/desorption at 77 K.

X-ray diffraction (XRD) [RigakuUltima IV] of the sample was recorded for phases and crystallite sizes. The pattern was recorded over scan the range 4-80 (2 theta) with a scan speed of 3 deg/min using Cu Kα radiation with 40 kV voltage and 40 mA current.

The percentage of the doped iron on titanium dioxide surface was measured using micro X-ray fluorescence (XRF) analysis [Bruker M4 Tornado]. The XRF was used for determining the elemental compositions of the synthesized catalyst using Rh as X-ray source (50 kV, 200 μm).

Scanning electron microscopy along with energy dispersive X-ray (SEM-EDX) analysis was performed [Oxford JEOL JEM-6610LV]. The SEM and EDX were used to determine the morphology and Fe/Ti ratio, respectively.

The determination of toluene and xylenes was carried out via Gas Chromatography-Flame Ionization Detector (GC-FID) [Shimadzu GC-2010]. The GC-FID is equipped with a Velocity XPT accelerated purge and trap system (Teledyne Tekmar).Volatile organic compounds with relatively lower water solubility were purged from the sample matrix using helium gas as inert gas carrier. The trapped components were introduced into the gas chromatography for further measurement.

The optimum iron content for the photo degradation reaction was determined using a lab made set up. A number of catalysts were prepared with different amounts of doped iron. A 500 mL Erlenmeyer flask which contains 100 mg/L of toluene or xylenes was closed with a Teflon stopper to avoid volatilization. A 0.5 g of catalyst was added to the toluene and xylenes flasks and placed in orbital shaker at 150 rpm for 12 hrs under illumination of multi Ultraviolet Germicidal lamps (Sankyo Denki G20T10; 20 watts/253.7 nm).

2.1.1.4 Adsorption Equilibrium Isotherms of Toluene and Xylenes

Toluene and Xylenes adsorption isotherms were carried out in batch system **Fig 2.1** at ambient temperature and neutral pH (≈ 7.00). A number of 250 mL Erlenmeyer flasks were closed with a Teflon stopper to avoid volatilization and covered with aluminium sheet to prevent photo degradation. Each flask contain 0.02 g of catalyst and 200 mL of toluene or xylenes with a concentration of [0, 20, 40, 60, 80 and 100] mg/L, the flasks were placed in orbital shaker at 150 RPM under the dark for 12 hrs ensuring equilibrium. The concentrations were determined by Gas Chromatography-Flame Ionization Detector (GC-FID) [Shimadzu GC-2010] equipped with a Velocity XPT Accelerated Purge and Trap System (Teledyne Tekmar).

2.1.1.5 Photo Catalytic Degradation Toluene and Xylenes

The study of the degradation of toluene and xylenes was executed in a batch system **Fig 2.2**, where a 250 mL Erlenmeyer flask were closed with a Teflon stopper to avoid volatilization, containing 0.02 g of catalyst and 200 mL of [0, 20, 40, 60, 80 and 100] mg/L, concentrations of Toluene and Xylenes at neutral pH (≈ 7.00), the flask was placed in orbital shaker at 150 rpm for 12 hrs under illumination of multi Ultraviolet Germicidal lamps (Sankyo Denki G20T10; 20 watts/253.7 nm). The concentrations were determined by Gas Chromatography-Flame Ionization Detector (GC-FID) [Shimadzu GC-2010] equipped with a velocity XPT accelerated purge and trap system (Teledyne Tekmar).

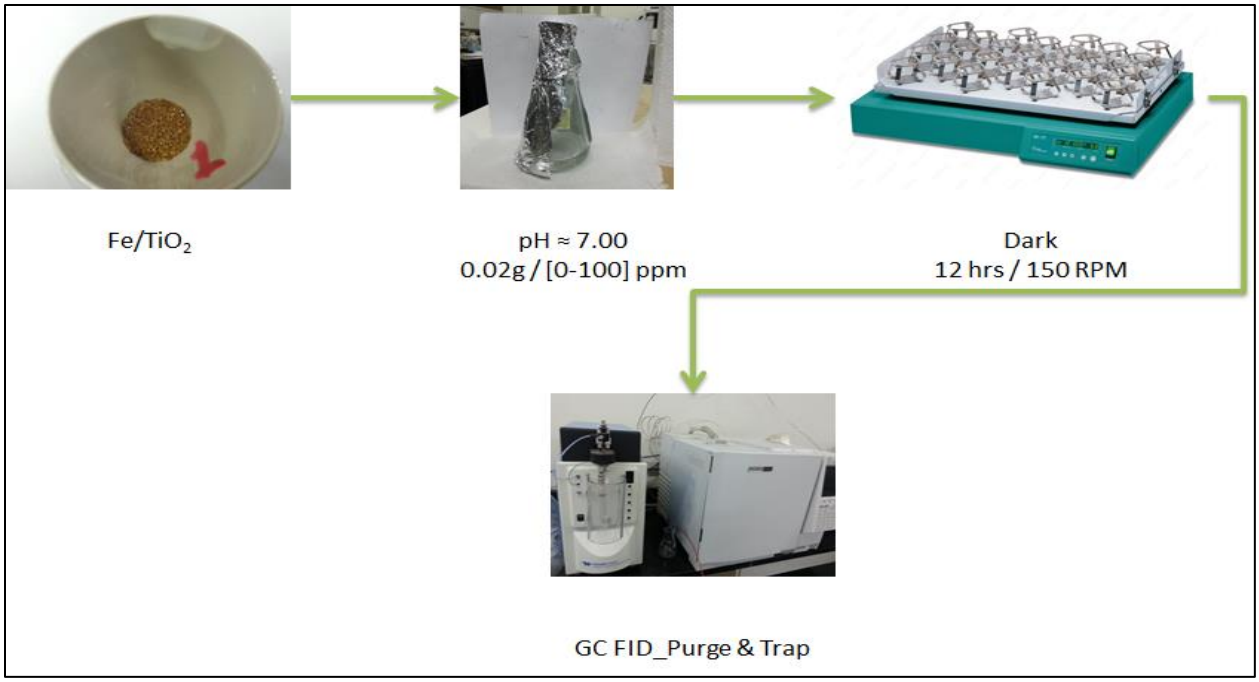

Figure 2.1 Setup for Adsorption Equilibrium Isotherm

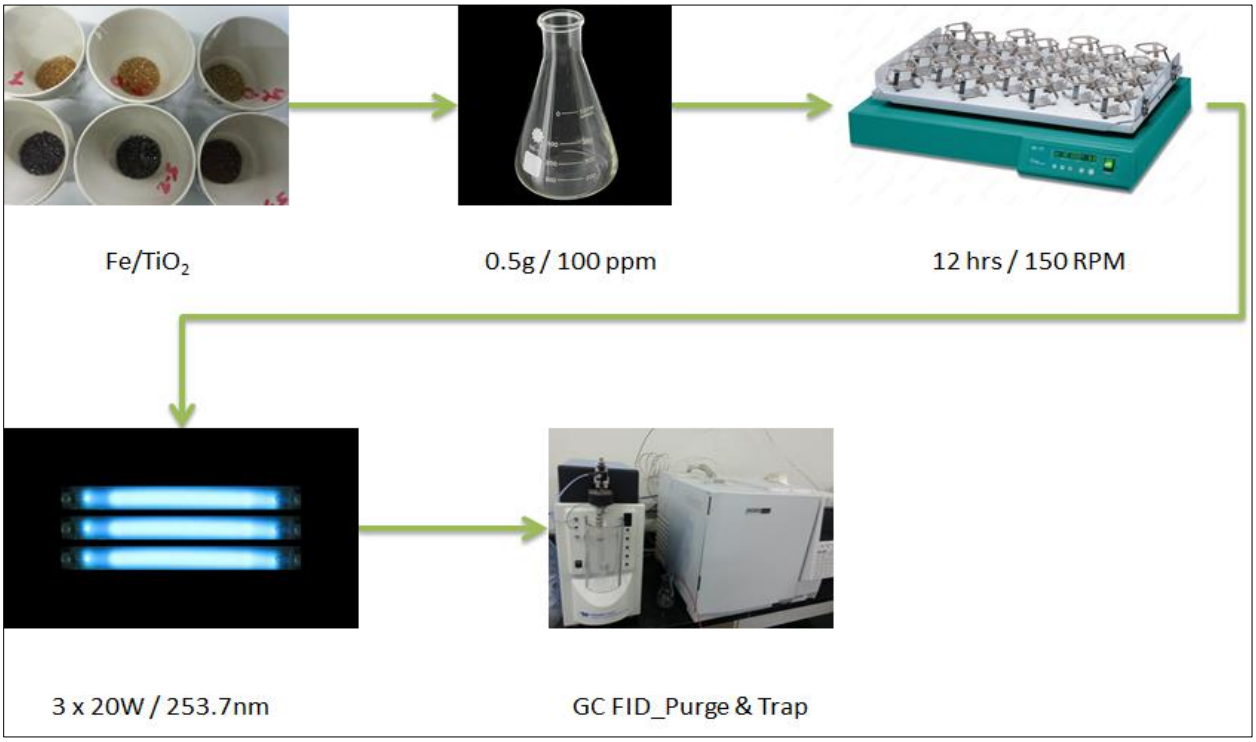

Figure 2.2 Setup for Photo-Catalytic Degradation

2.2 Results and discussions

2.2.1 Characterization

2.2.1.1 XRD

The crystalline size and phase composition for the synthesized TiO_2 doped with iron catalyst powder was examined. According to the pattern shown in **Fig 2.3** the X-ray diffraction (XRD) crystalline peaks indicated that the iron doped Titanium Dioxide displayed two phases Anatase ((1 0 1) at $2\theta=25.38^{o}$) and Rutile ((1 1 0) at $2\theta=29.54^{o}$) in agreement with previous reports (Mwangi et al. 2013; Ambrus et al. 2008) Iron characteristic peaks were not present suggesting continuous and proper dispersion of doped iron. Further investigations of the produced peaks shows proportional increase in Rutile peaks intensity with the addition of iron (Su et al. 2007), This implies that iron percentage in Titanium is a critical parameter among others, that controls the crystalline conversion of TiO_2 from Anatase to Rutile. Also, the obtained peaks were wide revealing small crystallite which was calculated using Scherrer formula. The sizes of the examined samples were in nanometer scale range (11-17) nm; attributed to Fe doping (Li et al. 2008; Sun et al. 2012). Doped iron was assumed to be dispersed homogeneously among the surface of Titanium Dioxide; due to the absence of its characteristic peak (Adán et al. 2007); This is possibly due to the limitation of the XRD detection or the resemblance in ionic radii between (Fe^{3+} = 0.79Å) and (Ti^{4+} = 0.75 Å) enabling iron substitution of Ti ions into titanium dioxide (Zhu et al. 2004; Laokiat et al. 2011).

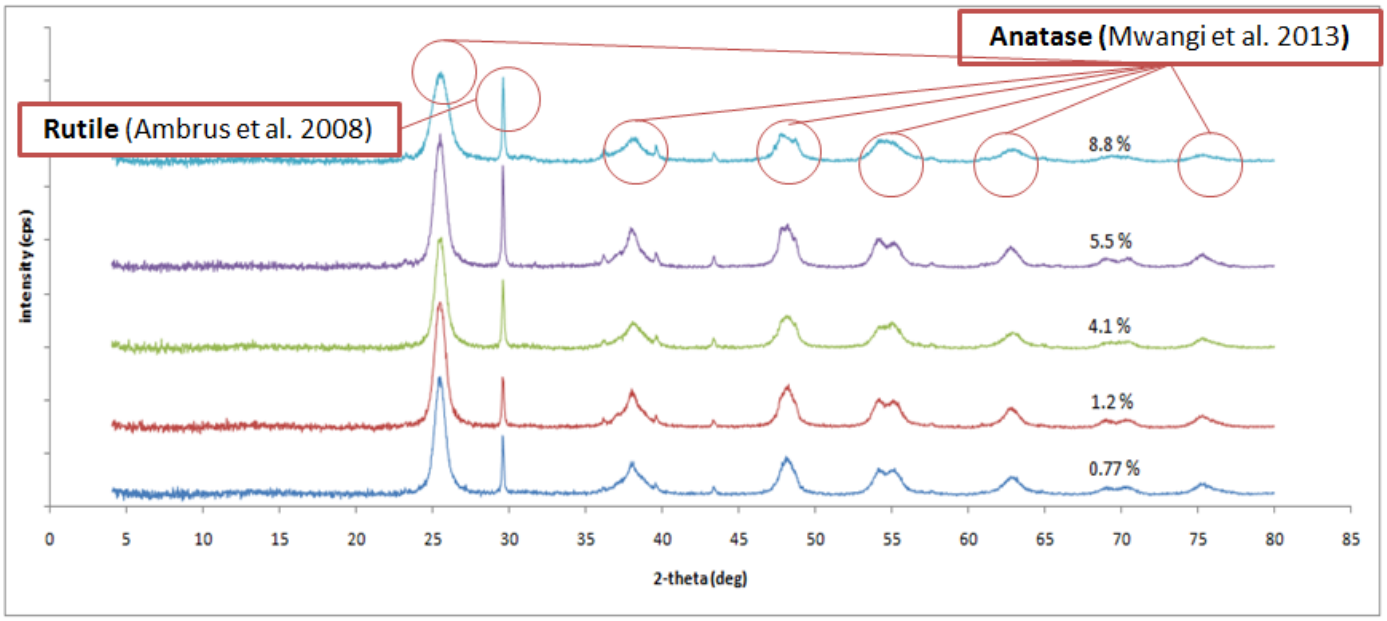

Figure 2.3 XRD Iron Doped Titanium Dioxide

2.2.1.2 N_2 adsorption-desorption

Fig 2.4 illustrates N_2 adsorption/desorption isotherms for synthesized iron doped Titanium Dioxide; the isotherms physisorption were believed to follow the classical type (IV), suggesting meoporous structure for synthesized Iron doped Titanium Dioxide. The hysteresis loop featured of slope adsorption branch followed by comparatively steep desorption realized about relative pressure (0.4-0.8), implying the characteristics of (H2) kind hysteresis loop (Sing et al. 1985); indicating the material of study experience capillary condensation associated with mesoporous structure such, synthesized catalyst suggested sophisticated pore structure and interconnected network of pores that diverse in size and shape presumably pore shape as "ink bottle" type (Wang et al. 2006). The Barret–Joyner–Halender (BJH) analysis is showed **Fig 2.4** inset, it was noticed a narrow pore size distribution in mesopore dimensions with a peak resulted at pore diameter of (4.6) nm. The results obtained fromN_2 adsorption/desorption are given in **Table 2.1**. Comparing the surface area S_{BET} of Doped Titanium Dioxide with the results found in the literature of commercial undoped TiO_2 (Tong et al. 2008; Wang et al. 2006) a remarkable increase in surface area of Fe-$TiO_2$is achieved. The addition of iron into Titanium resulted in a decrease in grain size as confirmed by XRD analysis.

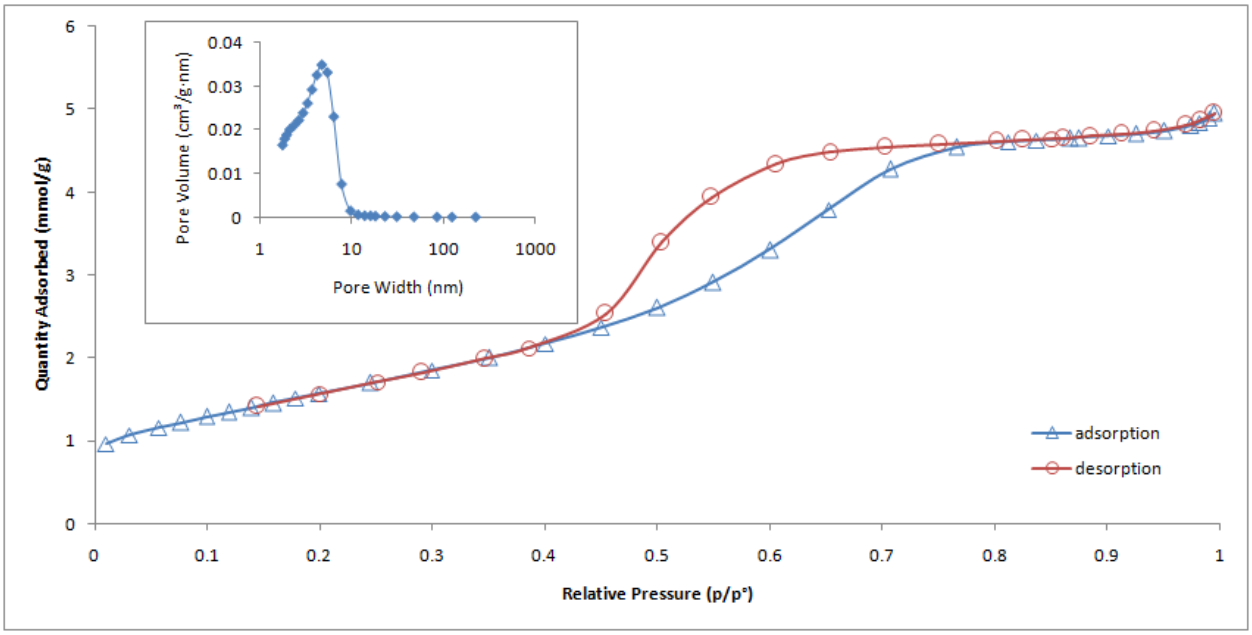

Figure 2.4 Nitrogen adsorption desorption isotherm Iron Doped Titanium Dioxide

Table 2.1 Structural Properties of Fe-TiO_2

Catalyst	Fe-TiO_2 ≈ 1 wt%
BET Surface Area (m^2/g)	129.675
Pore Volume (cm^3/g)	0.1665
Average Pore Diameter (nm)	5.14
Crystallite Size (nm)	11

2.2.1.3 SEM-EDX

The morphology of Fe doped titanium dioxide are examined via (SEM) shown in **Fig 2.5**, Clusters of irregular shapes of synthesized catalyst in different sizes are observed. The agglomerated particles are in small dimensions that can be attributed to the iron addition to titanium lattice (Ambrus et al. 2008) Accordingly, the specific surface area of catalyst samples have increased allowing enhancement in adsorption capacity thus photo-catalytic reaction. Further chemical composition was carried out by EDX and the results are given in **Fig 2.6**, the (EDX) spectra peaks of sample exhibited (C, O, Ti, Fe, Au) the latter peak was observed in high intensity as a result of sample coating for SEM clear and fine images.

2.2.1.4 Optimum Doping and Photo-Catalytic Activity

The investigation of optimum doping and photo-catalytic activity was based on detecting the remaining of the selected pollutants after illumination with UV light in different pre synthesized Fe-TiO_2 catalyst **Fig 2.7** shows the Fe doping content performance on photo degradation activity. It was found that the degradation percentage was proportional to Fe doping, reaching the highest peak at iron percentage of about 1.2 % wt. However, beyond that point the degradation decreased with further Fe addition. These findings can be attributed to the appropriate Fe doping into TiO_2 lattice. The Fe dopant can serve as charge trap hindering electron-hole combination besides, enhancing the interfacial charge transfer for pollutants degradation as long as the percentage of iron is within the adequate amount for photo-catalytic activity. On the other hand, as the concentration is beyond the optimum adverse effect takes place, dopant tend to act as recombination centers retarding charge transfer to the surface due to narrow distance between dopant traps(Cong et al. 2007) Eventually, this will result in lower photo-catalytic activity of

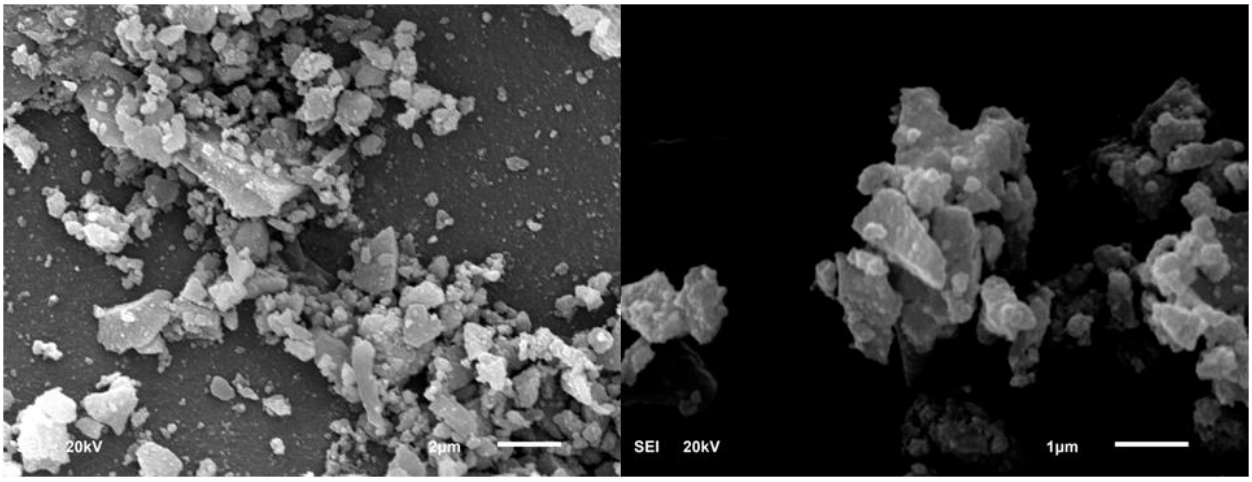

Figure 2.5 SEM of Synthesized Fe-TiO_2

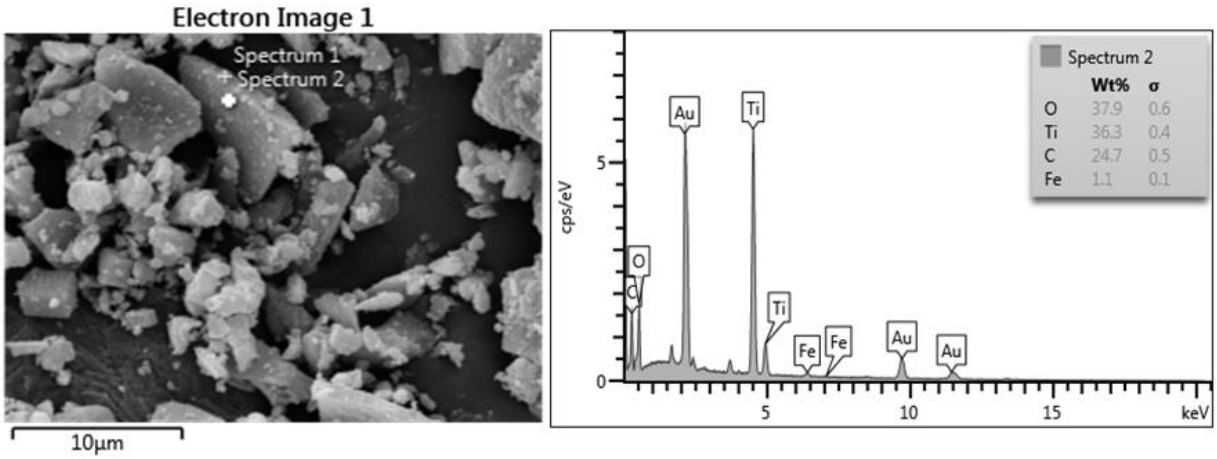

Figure 2.6 EDX of Synthesized Fe-TiO2

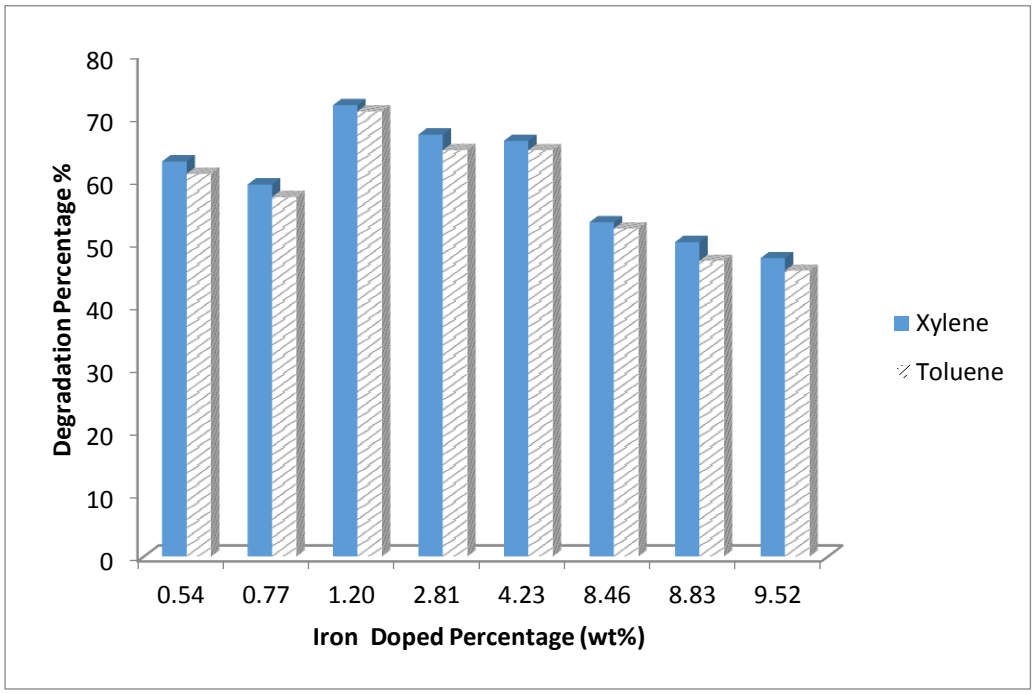

Figure 2.7 Effect of doping percentage on photo-Degradation

TiO_2 and accordingly the degradation rate of the pollutants (Xin et al. 2007; Yang et al. 2009; Lu et al. 2011). EDX analysis further demonstrates (**Fig 2.6)** iron introduced into titanium dioxide lattice because (Fe^{3+} = 0.79Å) and (Ti^{4+} = 0.75 Å) resemblance in ionic radii enabling iron substitution of Ti ions into semiconductor (Jo and Lee 2013).

2.2.2 Adsorption Equilibrium Isotherms of Toluene and Xylenes

2.2.2.1 Mono equilibrium adsorption

The photo catalytic process occurs principally on the surface of the catalyst hence, it is essential to study adsorption of Toluene and Xylenes from aqueous solution onto the catalyst surface. The objective is to determine the equilibrium concentrations (Ce) that represent the initial concentration for photo-catalytic process. The quantity of Toluene and Xylenes adsorbed, (q_e) (mg/g) onto the surface is calculated through mass balance with the assumption that the decrease of contaminants in liquid phase is related to adsorption onto the catalyst surface.

$$q_e = \frac{(C_o - C_e)V}{M} \qquad \textbf{Equation 1}$$

Where C_o (mg/L) is pollutants initial concentration in solution, C_e (mg/L) equilibrium concentration, V (L) volume of solution and M (g) mass of adsorbent added for experiment. Famous adsorption isotherm models such Langmuir, Freundlich and Redlich–Peterson equations **Table 2.2** were applied to the experimental data of Toluene and Xylenes mono component adsorption isotherms individually. The constants among suggested adsorption isotherms were obtained using Wolfram Mathematica 8. Fitted constants and correlation coefficient (R^2) are listed in **Table 2.3**. Graphs **Fig 2.8** and **Fig 2.9** illustrate experimental results along with the

adsorption model isotherms. The isotherms fit the experimental data and accordingly the correlation coefficients for all models are near unity. The maximum adsorption capacity is determined as $[56.1159 - 92.1083]$ (mg/g) for Toluene and Xylenes respectively. The latter among the examined pollutants achieved the highest adsorption capacity in agreement with (de Souza et al. 2012; Shahalam et al. 1997); This is likely due to the physical properties; relatively large molar mass, molecular structure and less tendency towards water solubility. For verification, experimental results follow Langmuir adsorption isotherm. A dimensionless constant, separation factor or equilibrium factor R_L defined **Table 2.4**:

$$R_L = \frac{1}{1 + b_L\, C_o} \qquad \textbf{Equation 2}$$

The obtained R_L values range from 0.6868 to 0.9164 Toluene and from 0.7263 to 0.9299 for Xylenes. Hence, R_L lies between 0 and 1 implying the adsorption processes are favorable. A low value (<1) of Freundlich's n_F parameter, an index that relates adsorption affinity and capacity between adsorbent and adsorbate, suggests weak interaction between adsorbate and adsorbent. However, at a value close to unity, the assumption is that energetic sites are equivalent. Experimental data fit Langmuir adsorption model for Toluene and Xylenes (Valente et al. 2006).

Table 2.2 Adsorption Isotherm Models used for Mono component adsorption

Isotherm Model	Equation
Langmuir	$q_e = \frac{q_{max} b_L C_e}{1 + b_L C_e}$
Freundlich	$q_e = k_F\, C_e^{\,1/n_F}$
Redlich–Peterson	$q_e = \frac{K_{PR}\, C_e}{\left(1 + C_e^b\, a_{PR}\right)}$

Table 2.3 Values for Adsorption Isotherm Model fitted parameters of BTX in Mono Component System

	Toluene	Xylenes
Langmuir		
$q_{max}\ (mg/g)$	56.1159	92.1083
$b_L\ (L/mg)$	0.00456	0.00376
R^2	0.9973	0.9998
R_L	0.6868	0.7263
Freundlich		
k_F	14.8128	20.5321
n_F	1.0900	1.0886
R^2	0.9971	0.9997
Redlich–Peterson		
$K_{PR}\ (L/mg)$	12.7989	17.3585
$a_{PR}\ (L/mg)$	0.00464	0.00381
b	0.9954	0.9970
R^2	0.9973	0.9998

Table 2.4 Dimensionless Constant Separation Factor or Equilibrium Factor, R_L

Langmuir equilibrium parameter	R_L
$R_L > 1$	Unfavorable
$R_L = 1$	Linear
$0 < R_L < 1$	Favorable
$R_L = 0$	irreversible

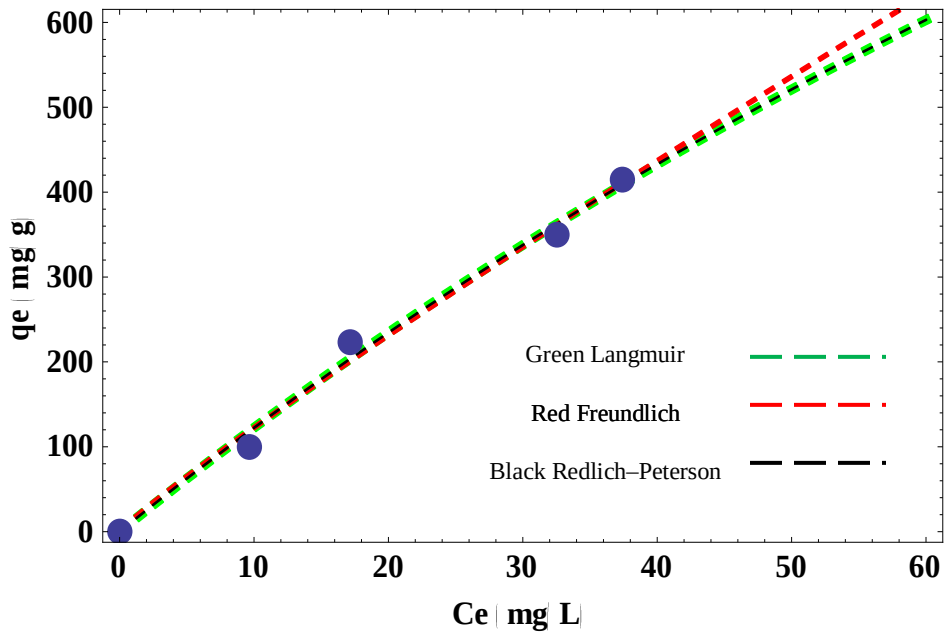

Figure 2.8 Fitting Experimental data of Toluene

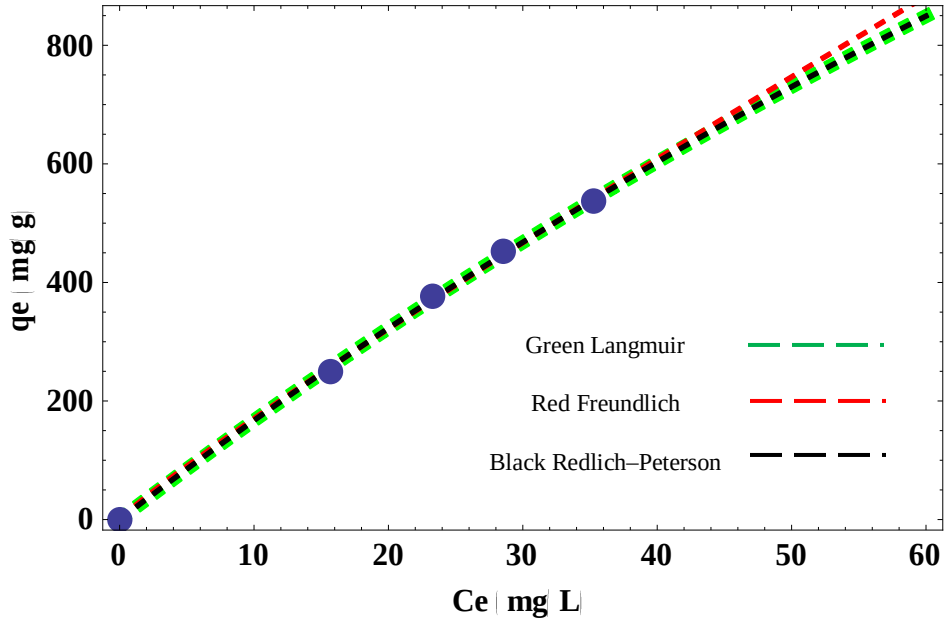

Figure 2.9 Fitting Experimental data of Xylenes

The Redlich–Peterson combined both features of Langmuir and Freundlich adsorption models, with parameter b as limiting factor. The model follows Henry's law as b approaches zero thus, the parameter reaching unity strongly suggests that the experimental data fits Langmuir model (Moura et al. 2011).

2.2.2.2 Binary equilibrium adsorption

In present set of experiments on Toluene and Xylenes binary systems were carried out in batch system at room temperature and neutral pH (≈ 7.00), the outcome of each set of experiment are shown in **Fig 2.10** and **Fig 2.11**. For comparison purposes, the experimental data from the previous section for single adsorption isotherm for the relevant compound is also included. In the first set, Toluene adsorption isotherms in binary solution with Xylenes is shown in **Fig 2.10**, The adsorption capacity of pure Toluene is influenced by the presence of Xylenes and reduced the individual pollutant adsorption capacity by about 40 % in multi component system (Al-Degs et al. 2007). Further looking into the experimental data reveals the occurrence of behavior of Xylenes on Toluene adsorption. Toluene adsorption in the presence of Xylenes (**Fig 2.10)** is mostly appreciably lower than the corresponding results in the absence of Xylenes (circle).Therefore, Toluene adsorption capacity is affected by increasing Xylenes equilibrium concentration. In addition, **Fig 2.11** demonstrates Xylenes adsorption isotherms in binary solution with Toluene. A similar effect is recognized mimicking the previous one. The adsorption capacity of pure Xylenes is influenced by the presence of Toluene reducing individual pollutant adsorption capacity about 50 % in multi component system. Similar observation (**Fig 2.11)** among the binary pollutants occurred where Xylenes values of adsorption capacity is lower than the corresponding values in the absence of Toluene (circle). Keeping in mind that the single and

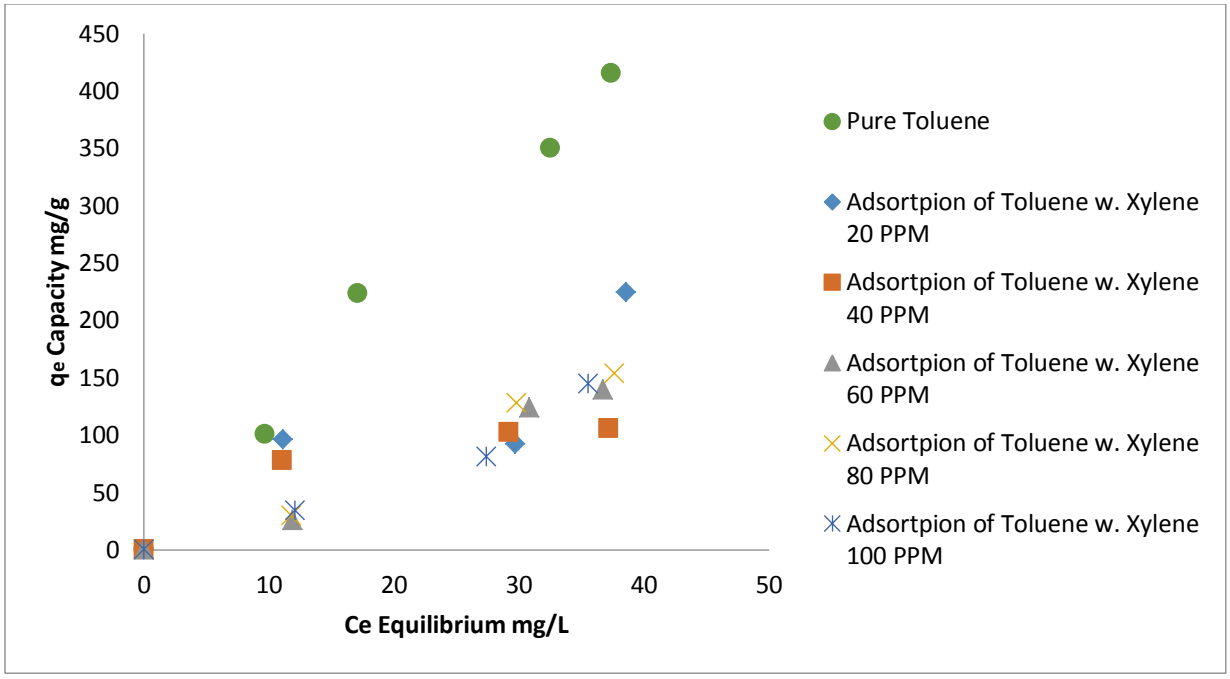

Figure 2.10 Binary Adsorption of Toluene with Different Concentrations of Xylenes

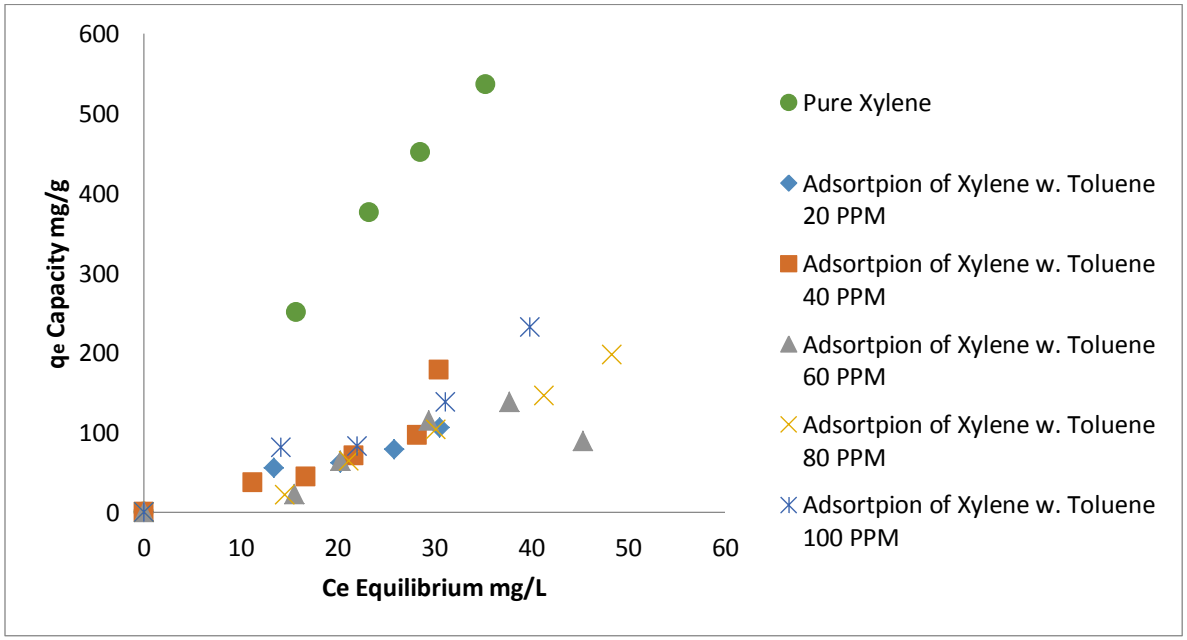

Figure 2.11 Binary Adsorption of Xylenes with Different Concentrations of Toluene

binary adsorption experiments are performed under the same conditions verifying the base of comparison (Erto et al. 2011; Erto et al. 2010). This indicates percentage of both pollutants simultaneously introduced into the adsorbate surface while the remaining in solution, Presumably, that in binary mixture solutions for the studied case, the pollutants have no effect towards each other adsorption but rather independent and that adsorption of the pollutants are related to its own affinity towards same active sites.

2.2.3 Photo-catalytic Degradation of Toluene and Xylenes

Toluene and Xylenes binary system experiment was carried out in batch system at room temperature and neutral pH (≈ 7.00), the degradation percentage is calculated

$$Degradation\ Percentage\ Reduction\ \% = \left[\frac{C_o - C_e}{C_0}\right] * 100 \qquad \textbf{Equation 3}$$

Where C_o (mg/L) pollutants initial concentration in solution, C_e (mg/L) equilibrium concentration the results are shown in **Fig 2.12** There is a clear gap between pure Toluene degradation and the degradation of binary Toluene and Xylene mixture by nearly 40%. Monitoring experimental data shows a resemblance to adsorption isotherms pattern. Toluene degradation (triangle) in the absence of Xylenes (**Fig 2.12)** is greatly higher that in the presence of Xylenes. Which is expected; since photo catalytic process occurs principally on the surface of catalyst, role of adsorption is essential for degradation initiation. Accordingly, within the investigated range of concentrations the presence of Xylenes hinders the photo catalytic degradation efficiency throughout incremental Xylene equilibrium concentration. That agrees with the assumption made regarding adsorption; where the surface of catalyst is perhaps filled with a portion of the first pollutant to initiate degradation leaving the rest in solute. Unfilled sites

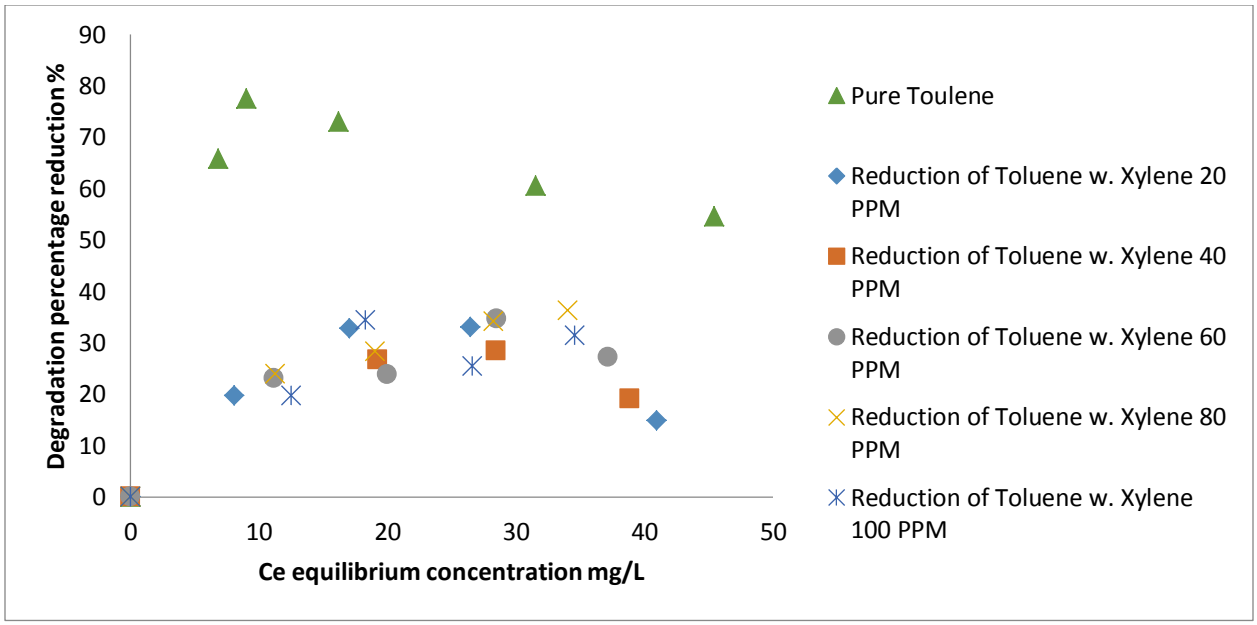

Figure 2.12 Binary Degradation of Toluene with Different Concentrations of Xylenes

will accommodate fraction of other pollutant simultaneously degraded hence, prediction of no interaction between pollutants them self but could be referred characteristics of studied pollutants tendency towards same active sites adsorption then degradation.

2.3 Conclusion

Photo-catalytic mesoporous Iron is doped on Titanium Dioxide (Fe-TiO_2). The synthesis applied Sol-Gel method for photo degradation of Toluene and Xylenes. The activity was enhanced via doping Titanium Dioxide with Fe^{+3} by about 1% enabling the dopant to act as charge trap hindering electron-hole combination. The grain size decreased to nano scale resulting in high increase in surface area. Further investigation into pollutants adsorption isotherm fitted the proposed isotherm models, while parameters strongly suggested Langmuir model fitting the experimental data with Xylenes more favorable over Toulene. Binary mixture adsorption capacities of examined pollutants showed lower values in comparison to their corresponding individual equilibrium concentrations almost 40% and 50% less capacity for Toluene and Xylenes respectively. Accordingly was the case for photo catalytic degradation since photo catalytic process occurs principally on the surface of catalyst, role of adsorption is essential for degradation initiation.

3 Chapter

Photo Catalytic Degradation of Benzene and Toluene Binary Mixture in Aqueous Solution

Abstract

Photo catalytic degradation of binary benzene and toluene was conducted via iron doped titanium dioxide (Fe-TiO_2). Sol-Gel procedure was applied for preparing the semiconductor. The catalyst was characterized by X-ray diffraction (XRD), N_2 adsorption/desorption, X-ray fluorescence (XRF) and Scanning electron microscopy along with energy dispersive X-ray (SEM-EDX). The photo catalytic activity was evaluated for the liquid phase photo catalytic degradation of benzene and toluene under ultraviolet light and about 1% Fe^{+3} was found to be the optimum value. The catalyst experienced mesoporous structure, both Anatase and Rutile phases and relatively high surface area. Famous adsorption isotherms were suggested (Langmuir, Freundlich and Redlich–Peterson) to fit the equilibrium concentrations of benzene and toluene. Adsorption capacity of toluene was greater than benzene. The binary mixture adsorption revealed nearly similar adsorption isotherms in comparison to their corresponding individual equilibrium concentrations. Subsequently, upon photo catalytic degradation since photo catalytic process fundamentally takes place on catalyst surface, adsorption is crucial part for pollutants degradation.

3.1 Introduction

Nowadays, environmental pollution is a major concern to human, notably industrial countries because of their massive production hence, large quantities of effluents containing different types of contaminants. Some of the famous hazardous pollutants are Aromatic Hydrocarbons. It attracts the attention due to its migration nature in soil, water and air inevitably human health. The group that received a great deal of awareness are Benzene Toluene and Xylenes (BTX). The necessity for elimination follows its toxicity and highly carcinogenic, even acute contact to low concentrations can cause damage to organs (Wilbur and Keith 2007; Dorsey and McClure 1989). Owing to their adverse effects on human health and quite relative solubility in water; Environmental Protection Agency (EPA) and World Health Organization (WHO) environmental laws for water contaminations are more present where the latter specified the amounts of Benzene Toluene and Xylenes in potable water not to exceed 0.01, 0.7 and 0.5 mg/L respectively. Occurrence of those pollutants are adjacent to oil & gas facilities (Fahim et al. 2009), solvent industries, petrochemicals (Ferrari-Lima et al. 2014) coating and painting applications (Palau et al. 2012). Thereby, prompted techniques for effective elimination should meet the health concerns in cooperation with environmental institutes. The removal methods of Benzene and Toluene (BT) from aqueous solutions in literature are quite prosperous some examples are adsorption of pollutants through number of adsorbents such Zeolite; surface properties and tunable geometry & pore size (Vidal et. al., 2012; Gibson 2014), Activated Carbon; convenient high porosity and surface characteristics (Dias et. al., 2007) and clays; high surface area, non-toxic and abundant (Vidal and Volzone 2009; Hackbarth et. al., 2014). However, one of the treatments is the conversion of the hazardous liquid waste to solid phase for further treatment. Other promising maneuver is advanced photo oxidation (AOPs); which

production of oxidizing agent via hydrogen oxide, ozone and UV light to completely destroy wide range of organic hazardous wastes (Arslan et. al., 2000; Comninellis et. al., 2008), unfortunately, it's energy and resources intensive. Appealing photo-catalytic process as an alternative; illumination by UV or Visible light, creating hydroxyl radical highly reactive to oxidize the compounds (Crittenden et. al., 1997). Plenty of semiconductors are available and been tested as photo-catalyst for pollutants degrading such as ZnO, CdS, Fe_2O_3, TiO_2, ZrO_2, MoS_2 and WO_3. Characteristics needed to compare between plenty semiconductors based on its photo-stability, abundance and cost, the inertness nature both chemically and biologically and absorbance of reactants under efficient photo-activation ($E_{radiation} \geq E_{bg}{}^{*}$). Thus, titanium is considered the preferable among the different semiconductors (Bahnemann 1987; Mills and Hunte 1997; Gaya and Abdullah 2008; Sivula et. al., 2009).

Reported studies in literature for (BT) degradation such as (Fu et. al., 1995) examined the decomposition of benzene with oxygen in gas phase using TiO_2 and platinum doped TiO_2 (0.1 wt %), observed improving in the catalyst activity towards benzene mineralization correspondingly to doping at temperatures higher than (100^{o}C). Also, Wang et. al., (2003) studied benzene degradation in the gas phase at room temperature; the TiO_2 was used with UV intensity, in their work, the effect of humidity and concentration on the benzene mineralization was considered. Results were fitted using Langmuir–Hinshelwood model. Another involving carbon nano-tubes CNT/TiO_2 nano-composite photo catalyst to decompose benzene in gas phase; (Xu et. al., 2010) it revealed improvement photo catalytic activity in line to conventional Degussa P_{25}.

On the other hand, Augugliaro et al., (1999) examined toluene photo-oxidation via TiO_2 anatase polycrystalline, suggesting O_2 and H_2O are important factors to maintain catalyst's activity and enhance photo reaction. Maira et al., (2001) prepared nano size TiO_2 through modified sol-gel

method, showing the enhancement of toluene mineralization because of minute TiO_2 grain size. (Jeong et. al., 2004) tried to imply short wave length UV (254+185 nm) photo-oxidation of Toluene, resulting enhancement both photo-degradation and photo-chemical oxidation. For both (BT) (Zuo et. al., 2006) Investigated VOCs in gas phase, by means of photolysis and photo catalysis, under illumination of germicidal lamp, which in case of direct contact of germicidal lamp with benzene is not sufficient for degradation unlike toluene. Both means resulted proper rate of decomposition. Furthermore, photo catalysis synthesized by doping Sn and Fe to TiO_2; SnO_2/TiO_2 catalyst effect over benzene decomposition rate was high compared to (Fe-TiO_2) catalyst but, in case of mineralization rate it was the opposite. Hence, Fe^{3+}/TiO_2 catalyst performance was superior in both elimination and mineralization rate.

Many published work in the literature dealt with Benzene and toluene individually in gas phase, in spite of the multi component nature of effluent streams. In this study, photo-catalytic degradation of Benzene and Toluene via prepared Fe^{3+}/TiO_2 catalyst will be investigated, both mono and binary mixture in aqueous solution, including simultaneous equilibrium adsorption isotherm, experimentally and theoretically.

3.1.1 Experimental

3.1.1.1 Materials

The chemicals used in the current study were Benzene (99.7 %), Toluene (99.7 %) in high purity and Titanium (IV) Isopropoxide (97%) [$Ti(OCH(CH_3)_2)_4$] as a Titanium precursor later on for Iron doping, all obtained from (Sigma-Aldrich). Ferric Nitrate (98 %) [$Fe(NO_3)_3.9H_2O$] (Loba Chemie) is used as source of iron for doping into Titanium lattice. Acetic Acid glacial (99.5 %) [ACOH] (BDH Chemicals). Ethanol (99.9 %) [EtOH] (Scharlau).

3.1.1.2 Catalyst Synthesis

The synthesis of (Fe-TiO_2) followed Sol Gel method; a beaker was filled with 125 mL of Ethanol (EtOH), that was followed by 25 mL of Titanium precursor [$Ti(OCH(CH_3)_2)_4$]. The mixture was then stirred to ensure homogeneity of the solution for further processing. On the other hand, in another beaker a 125 mL of Ethanol (EtOH) 5 mL of Acetic Acid (AcOH) and a specific amount of Ferric Nitrate [Fe $(NO_3)_3.9H_2O$] were mixed to achieve a desired percentage of doping. The latter mixture was added via a burette to the first beaker in a drop wise manner mixing with a magnetic stirrer. Then, the mixing was continued for 2 minutes The mixture was then sonicated in ultrasonic bath for 60 minutes. The obtained orange brownish solution was left to age at room temperature for 24 hours. The solution formed a gel structure and the gel was kept into the oven and dried for 24 hrs at 70^o C. The last step was the calcination of the resulting dried powder in a furnace at 400^oC for 4 hours to produce the final powder.

3.1.1.3 Characterization

The specific surface area (S_{BET}), pore volume and other structural properties of the catalyst were carried out using nitrogen adsorption/desorption [Micrometrics ASAP 2020 – Physisorption Analyzer]. A sample of 0.4663g was degassed under vacuum for 60 minutes at 473 K before undergoing N_2 adsorption/desorption at 77 K.

X-ray diffraction (XRD) [RigakuUltima IV] of the sample was recorded for phases and crystallite sizes. The pattern was recorded over scan the range 4-80 (2 theta) with a scan speed of 3 deg/min using Cu Kα radiation with 40 kV voltage and 40 mA current.

The percentage of the doped iron on titanium dioxide surface was measured using micro X-ray fluorescence (XRF) analysis [Bruker M4 Tornado]. The XRF was used for determining the elemental compositions of the synthesized catalyst using Rh as X-ray source (50 kV, 200 μm).

Scanning electron microscopy along with energy dispersive X-ray (SEM-EDX) analysis was performed [Oxford JEOL JEM-6610LV]. The SEM and EDX were used to determine the morphology and Fe/Ti ratio, respectively.

The determination of benzene and toluene was carried out via Gas Chromatography-Flame Ionization Detector (GC-FID) [Shimadzu GC-2010]. The GC-FID is equipped with a Velocity XPT accelerated purge and trap system (Teledyne Tekmar).Volatile organic compounds with relatively lower water solubility were purged from the sample matrix using helium gas as inert gas carrier. The trapped components were introduced into the gas chromatography for further measurement.

The optimum iron content for the photo degradation reaction was determined using a lab made set up. A number of catalysts were prepared with different amounts of doped iron. A 500 mL Erlenmeyer flask which contains 100 mg/L of benzene or toluene was closed with a Teflon stopper to avoid volatilization. A 0.5 g of catalyst was added to the benzene and toluene flasks and placed in orbital shaker at 150 rpm for 12 hrs under illumination of multi Ultraviolet Germicidal lamps (Sankyo Denki G20T10; 20 watts/253.7 nm).

3.1.1.4 Adsorption Equilibrium Isotherms of Benzene and Toluene

Benzene and toluene adsorption isotherms were carried out in batch system at ambient temperature and neutral pH (≈ 7.00). A number of 250 mL Erlenmeyer flasks were closed with a Teflon stopper to avoid volatilization and covered with aluminium sheet to prevent photo degradation. Each flask contain 0.02 g of catalyst and 200 mL of benzene or toluene with a concentration of [0, 20, 40, 60, 80 and 100] mg/L, the flasks were placed in orbital shaker at 150 RPM under the dark for 12 hrs ensuring equilibrium. The concentrations were determined by

Gas Chromatography-Flame Ionization Detector (GC-FID) [Shimadzu GC-2010] equipped with a Velocity XPT Accelerated Purge and Trap System (Teledyne Tekmar).

3.1.1.5 Photo Catalytic Degradation Benzene and Toluene

The study of the degradation of benzene and toluene was executed in a batch system, where a 250 mL Erlenmeyer flask were closed with a Teflon stopper to avoid volatilization, containing 0.02 g of catalyst and 200 mL of [0, 20, 40, 60, 80 and 100] mg/L, concentrations of benzene and toluene at neutral pH (≈ 7.00), the flask was placed in orbital shaker at 150 rpm for 12 hrs under illumination of multi Ultraviolet Germicidal lamps (Sankyo Denki G20T10; 20 watts/253.7 nm). The concentrations were determined by Gas Chromatography-Flame Ionization Detector (GC-FID) [Shimadzu GC-2010] equipped with a velocity XPT accelerated purge and trap system (Teledyne Tekmar).

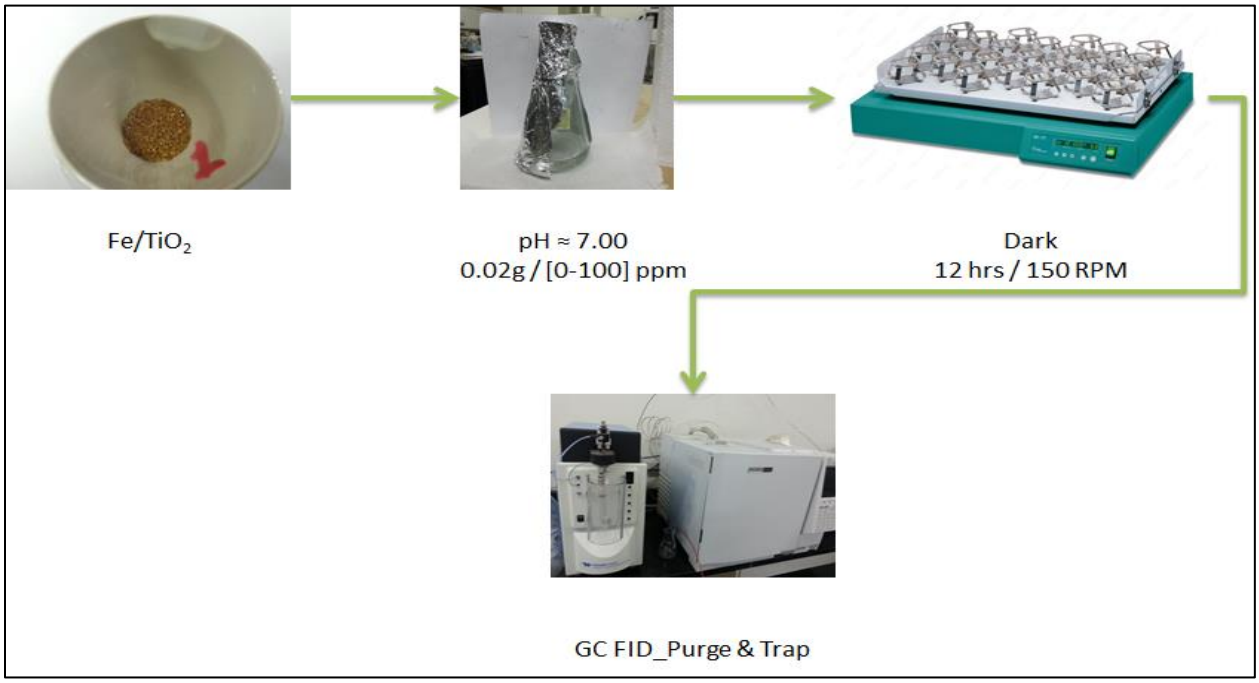

Figure 3.1 Setup for Adsorption Equilibrium Isotherm

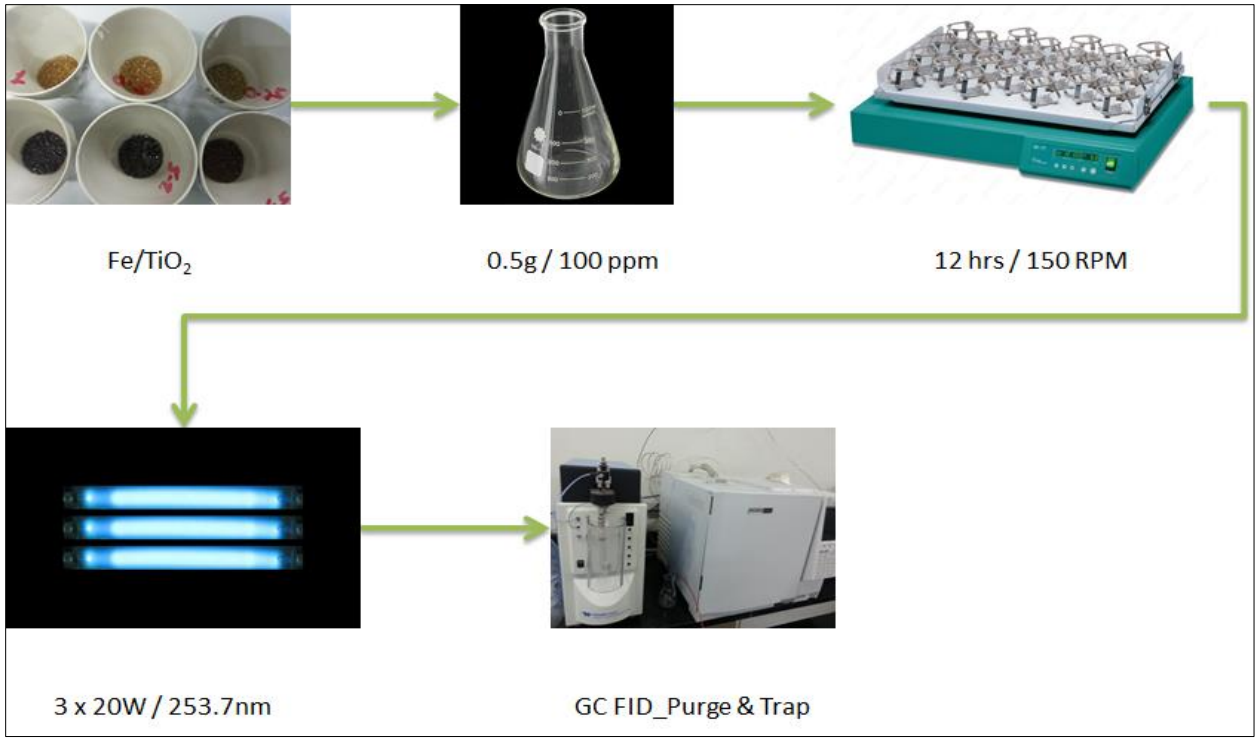

Figure 3.2 Setup for Photo-Catalytic Degradation

3.2 Results and discussions

3.2.1 Characterization

3.2.1.1 XRD

According to X-ray diffraction (XRD) analysis, the obtained Iron doped Titanium Dioxide catalyst powder reveals two phases. In **Fig 3.2**, the first characteristic peak represents the Anatase phase ((1 0 1) at $2\theta=25.38^{o}$) that agrees with work done by (Ambrus et. al., 2008; Navío et. al., 1999), while the other peak is Rutile ((1 1 0) at $2\theta=29.54^{o}$) (Mwangi et. al., 2013). Deep look into the crystalline peaks shows the absence of the Iron characteristic peaks, indicating continuous and proper dispersion of doped iron into Titanium lattice of the synthesized catalyst. In **Fig 3.2,** a clear increase in Rutile intensity peak accompanies the incremental percentage of iron into titania (Su et. al., 2007; Nasralla et. al., 2013), suggesting iron content is a major contributor in changing Anatase TiO_2 phase into Rutile. Diffraction peaks were relatively broaden; implying small grain size in the nanometer scale range (11-17) nm another preferable effect from Iron doping (Li et. al., 2008; Sun et. al., 2012). Fortunately, the diffraction peaks did not detect iron either due to the limitation of the XRD detection or the resemblance in ionic radii between (Fe^{3+} = 0.79Å) and (Ti^{4+} = 0.75 Å) enabling iron substitution of Ti ions into titanium dioxide (Zhu et. al., 2004; Laokiat et. al., 2011).

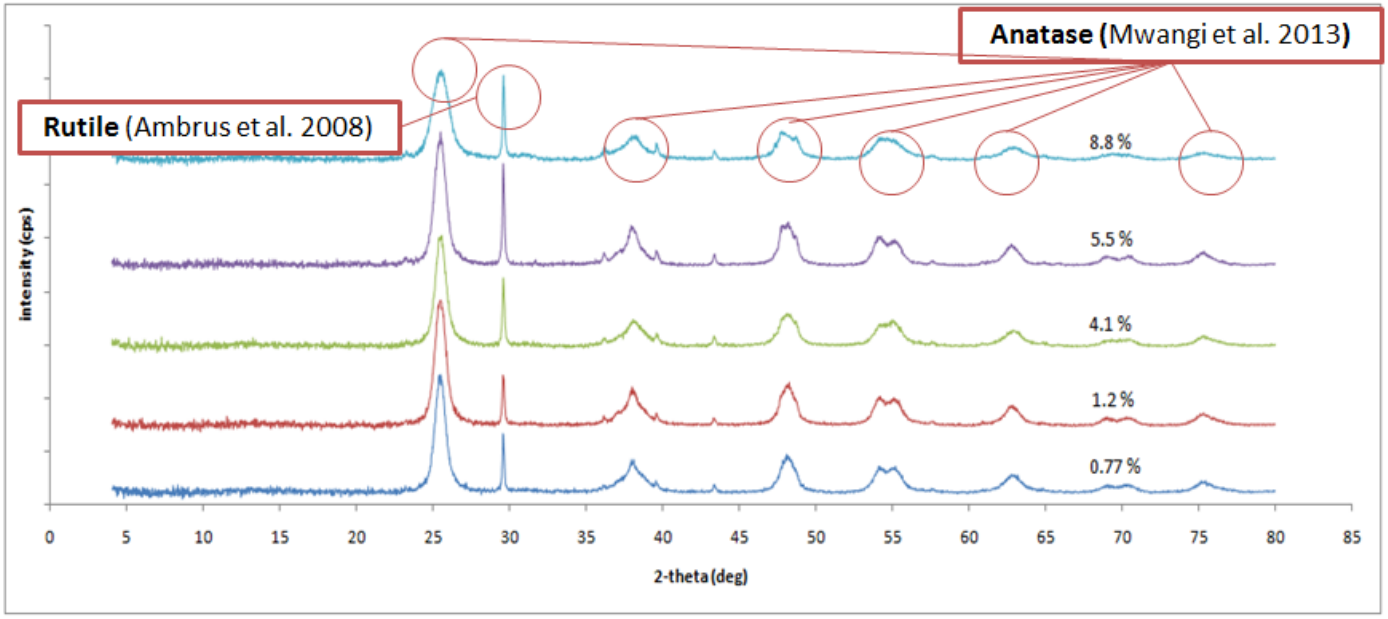

Figure 3.3 XRD Iron Doped Titanium Dioxide XRD Iron doped Titanium Dioxide

3.2.1.2 N_2 adsorption-desorption

Fig 3.4 exhibits the N_2 adsorption/desorption isotherms for synthesized Iron doped Titanium Dioxide, the specific area was determined by applying Brunaer–Emmett– Teller (BET) method **Table 3.1** shows the surface area S_{BET} of commercial undoped Titanium Dioxide in literature (Tong et. al., 2008; Wang et. al., 2006) were less in comparison to Fe-TiO_2; Iron incorporation into Titanium created smaller grains as realized in the XRD analysis, resulting into a noticeable increase in the surface area which is beneficial to photo catalytic (Zhu et. al., 2004). Synthesized Iron doped Titanium Dioxide physisorption isotherms were type (IV) and (H2) kind hysteresis loop (Sing et. al., 1985); slant branch of adsorption accompanied steep desorption realized about a relative pressure of (0.4-0.8), presumably, the material experiencing capillary condensation associated with mesoporous structure such, synthesized catalyst suggested sophisticated pore structure and interconnected network of pores that diverse in size and shape could be described as “ink bottle” type pore (Wang et. al., 2006). The pore size distribution is shown inset in **Fig 3.4** and is estimated by applying Barret–Joyner–Halender (BJH) model. The pore size distribution was narrow and in the mesopore dimensions with a peak at pore diameter of (4.6) nm.

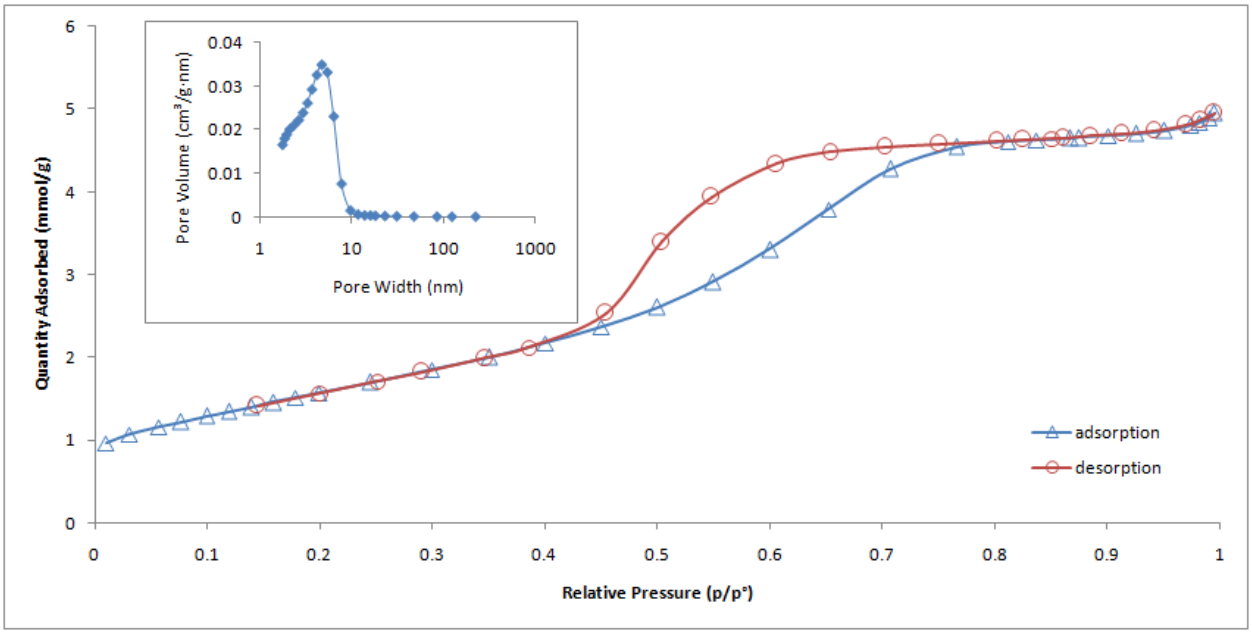

Figure 3.4 Nitrogen adsorption desorption isotherm Iron Doped Titanium Dioxide

Table 3.1 Structural Properties of Fe-TiO_2

Catalyst	Fe-TiO_2 ≈ 1 wt%
BET Surface Area (m^2/g)	129.675
Pore Volume (cm^3/g)	0.1665
Average Pore Diameter (nm)	5.14
Crystallite Size (nm)	11

3.2.1.3 SEM-EDX

The morphology shown in **Fig 3.5** is obtained for Fe doped Titanium Dioxide. The examined samples consist of clusters of irregular shapes of synthesized catalyst in diverse sizes and dimensions mostly possess sharp corners and straight edges, agglomerated particles are in small dimensions that can be attributed the iron addition to titanium lattice (Ambrus et. al., 2008) as a result mentioned in XRD, development in the specific surface area of catalyst samples allowing enhancement in adsorption capacity thus photo-catalytic reaction. Energy Dispersive X-ray (EDX) **Fig 3.6** was applied to obtain chemical composition and its percentages, the (EDX) spectra peaks of sample exhibited (C, O, Ti, Fe, Au) the latter peak was in high intensity in spite of the absence while synthesizing due to coating the sample to receive clear and fine images.

3.2.1.4 Optimum Doping and Photo-Catalytic Activity

Photo-catalytic degradation of Benzene and Toluene in **Fig 3.7** describes degradation percentage against different pre synthesized doping of Fe-TiO_2, evaluation was based on detecting the non degraded Benzene and Toluene in solution after illumination with UV light. Observation upon doping suggested proportional relation to photo catalytic activity; the degradation percentage of selected pollutants increased with Fe doping into TiO_2 until it reached maximum degradation about 70 % corresponding iron dosage 1.2 % wt; perhaps the role of doped iron is to create active sites that enhance titania activity, through capturing electrons or holes to retard electron-hole combination, expanding photo generated charges lifetime then photo catalytic degradation efficiency besides, developing the interfacial charge transfer for pollutants degradation in consideration of adequate percentage of doped iron. However, iron content exceeding 1 % results

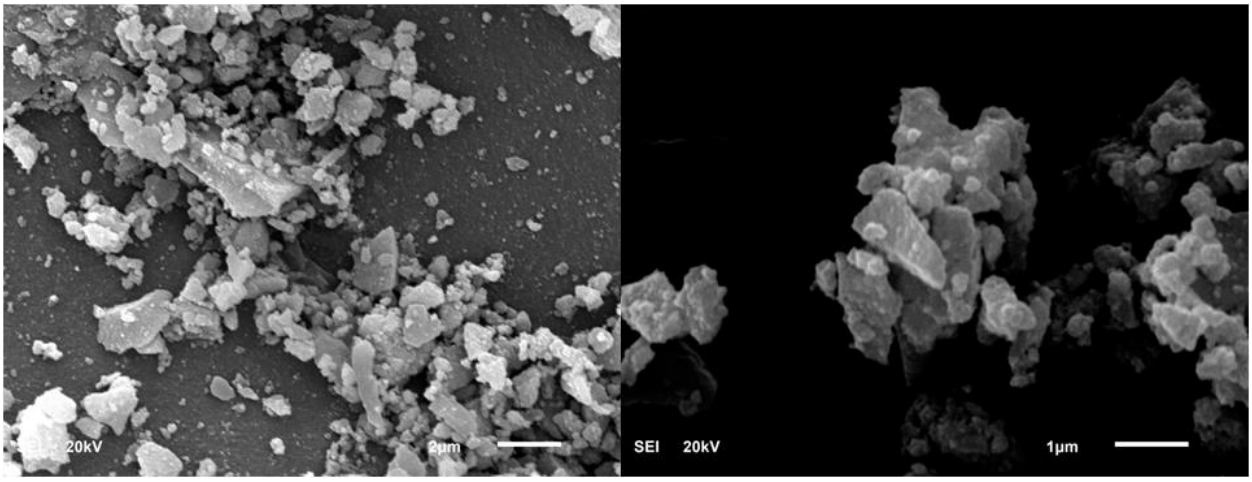

Figure 3.5 SEM of Synthesized Fe-TiO_2

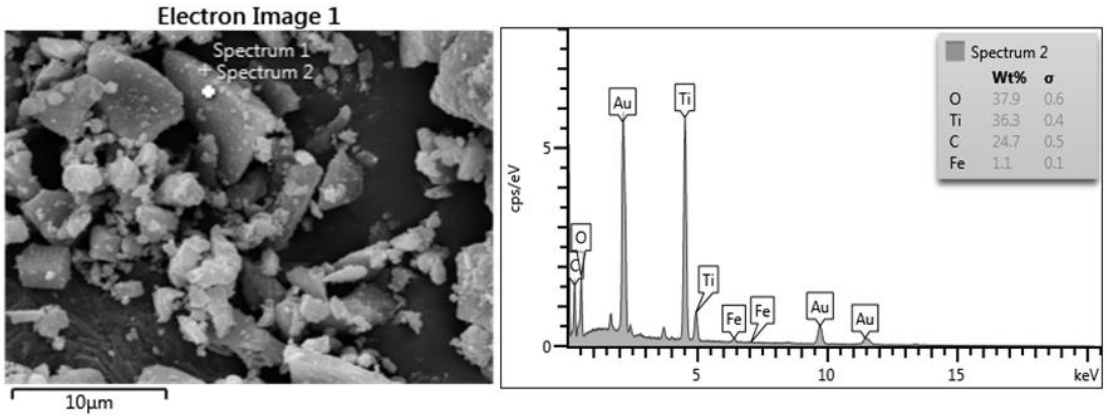

Figure 3.6 EDX of Synthesized Fe-TiO_2

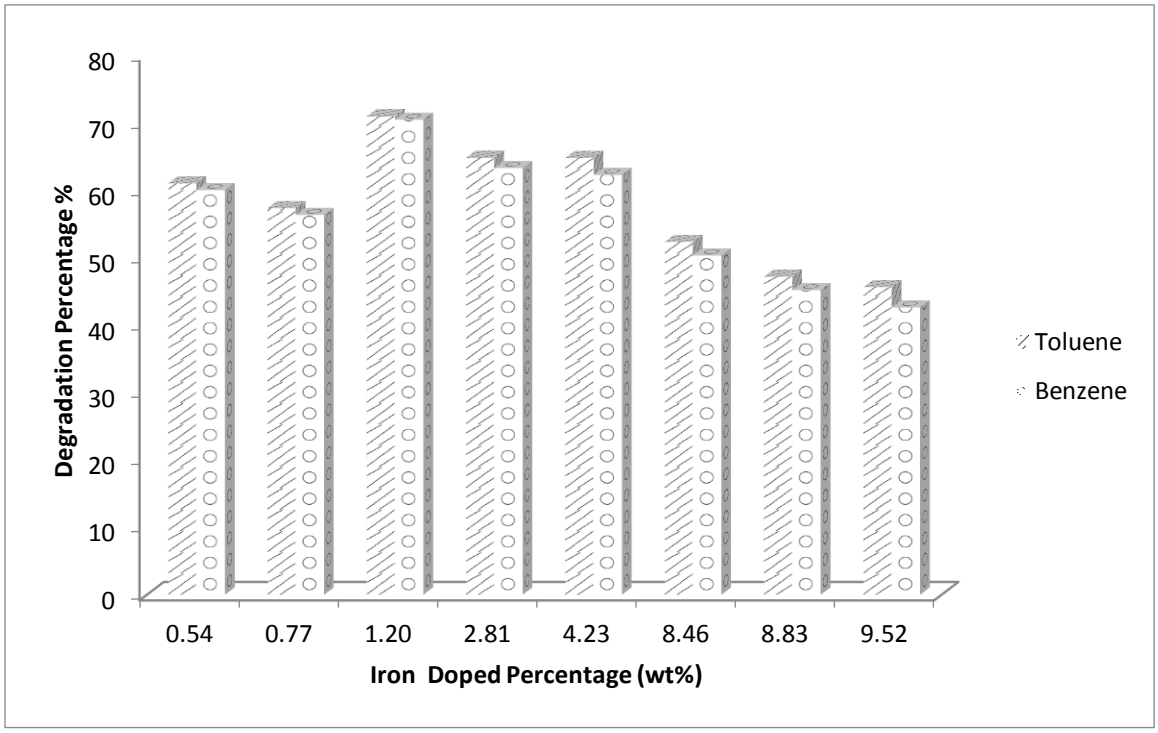

Figure 3.7 Effect of doping percentage on photo-Degradation

unfavorable recombination centers hindering charge transfer to the surface due to narrow distance between dopant trap consequently, weaken photo-catalytic activity of TiO_2 accordingly the degradation rate of the pollutants (Cong et. al., 2007; Xin et. al., 2007; Yang et. al., 2009; Lu et. al., 2011). (EDX) analysis **Fig 3.6** supports iron is incorporated in Titanium Dioxide lattice due to closeness of ionic radii (Fe^{3+} = 0.79Å, Ti^{4+} = 0.75 Å) implementing iron substitution of Ti ions into semiconductor (Jo and Lee 2013).

3.2.2 Adsorption Equilibrium Isotherms of Benzene and Toluene

3.2.2.1 Mono equilibrium adsorption

The initiative step for photo catalytic degradation is adsorption into catalyst surface therefore, it is important to investigate adsorption capacity of Fe-TiO_2 towards Benzene and Toluene from aqueous solution to identify the equilibrium concentrations (Ce) that represent the initiative concentration for photo-catalytic process. The quantity of Benzene and Toluene adsorbed, (qe) (mg/g) onto the surface is calculated through mass balance with the assumption that decrease of contaminants in liquid phase is related to adsorption onto catalyst solid surface.

$$q_e = \frac{(C_o - C_e)V}{M} \qquad \textbf{Equation 4}$$

Where Co (mg/L) is pollutants initial concentration in solution, Ce (mg/L) equilibrium concentration, V (L) volume of solution and M (g) mass of adsorbent added for experiment.

Commonly employed isotherm models to describe the mono component adsorption isotherms individually were Langmuir, Freundlich and Redlich–Peterson equations in **Table 3.2**. The parameters obtained from suggested adsorption isotherms were fitted using Wolfram Mathematica 8. The constants and correlation coefficient (R^2) were listed in **Table 3.3**. The

adsorption models isotherm and experimental data are presented simultaneously in **Fig 3.8** and **Fig 3.9**, it can be noticed the quite representation of the isotherms to the experimental data which is confirmed through correlation coefficient clearly closing up to unity. From fitted parameters we found the maximum adsorption capacity $[13.5508 - 56.1159]$ (mg/g) for Benzene and Toluene respectively. Toluene adsorption capacity was found higher than Benzene (Guelli Ulson de Souza et. al., 2012; Shahalam et. al., 1997) presumably, toluene greater than Benzene in molecular mass and less solubility towards water promote its adsorption tendency into Fe-TiO_2. Since all proposed isotherms quite represented the experimental data, further investigation of fitted parameter is needed to decide the best among chosen models. Introducing a dimensionless constant named separation factor or equilibrium factor defined $R_L = 1/[1 + b_L C_0]$, in case of $R_L > 1$ the adsorption is not favorable, $R_L = 1$ is considered linear, $R_L = 0$ the adsorption is regarded as irreversible and finally favorable if $0 < R_L < 1$. The calculated R_L was 0.6770 – 0.9129 Benzene and 0.6868 – 0.9164 Toluene thereby, the adsorption processes were favorable. The value of Freundlich's n_F parameter is an index that relates adsorption affinity and capacity between adsorbent and adsorbate. In case of n_F lower than 1 indication of weak interaction between adsorbate to adsorbent while the opposite arise at n_F greater than 1. However, at value close to unity, an assumption to equivalent energetic sites take place promotes experimental data preferably be fitted to Langmuir adsorption model, was the case for Benzene and Toluene (Valente et. al., 2006). The Redlich–Peterson model is combination of Langmuir and Freundlich aspects, with parameter b as limiting factor; lower b value reaching zero suggests Henry's law

Table 3.2 Adsorption Isotherm Models used for Mono component adsorption

Isotherm Model	Equation
Langmuir	$q_e = \frac{q_{max} b_L C_e}{1 + b_L C_e}$
Freundlich	$q_e = k_F \, C_e^{\,1/n_F}$
Redlich–Peterson	$q_e = \frac{K_{PR} \, C_e}{\left(1 + C_e^b \, a_{PR}\right)}$

Table 3.3 Values for Adsorption Isotherm Model fitted parameters of BTX in Mono Component System

	Benzene	Toluene
Langmuir		
$q_{max}\ (mg/g)$	13.5508	56.1159
$b_L\ (L/mg)$	0.00477	0.00456
R^2	0.99904	0.9973
R_L	$0.6770 - 0.9129$	$0.6868 - 0.9164$
Freundlich		
k_F	5.5992	14.8128
n_F	1.24566	1.0900
R^2	0.9987	0.9971
Redlich–Peterson		
$K_{PR}\ (L/mg)$	3.2465	12.7989
$a_{PR}\ (L/mg)$	0.00520	0.00464
b	0.9834	0.9954
R^2	0.9990	0.9973

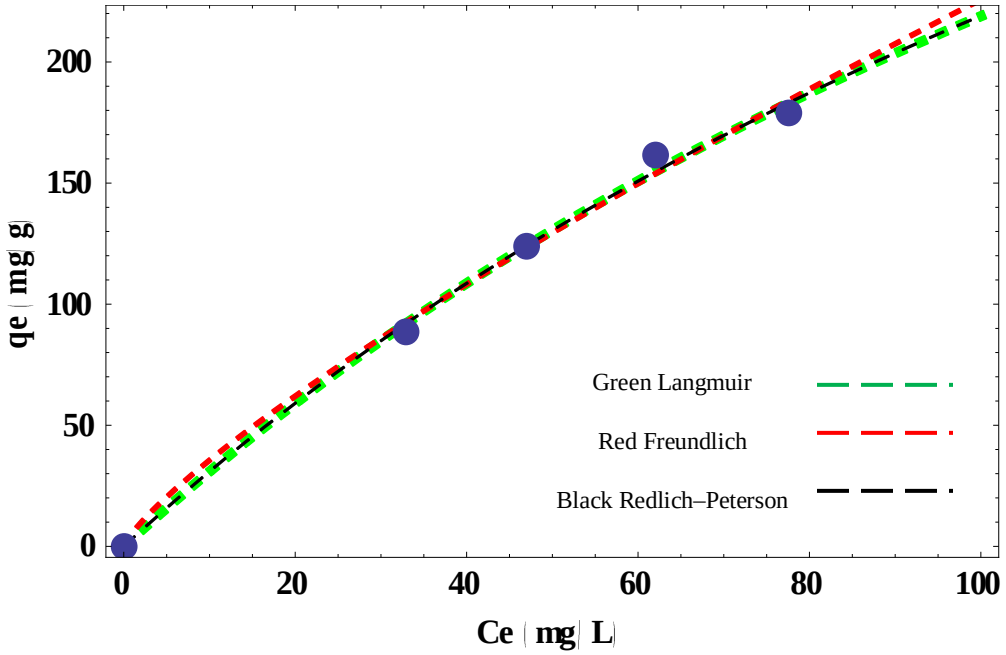

Figure 3.8 Fitting Experimental data of Benzene

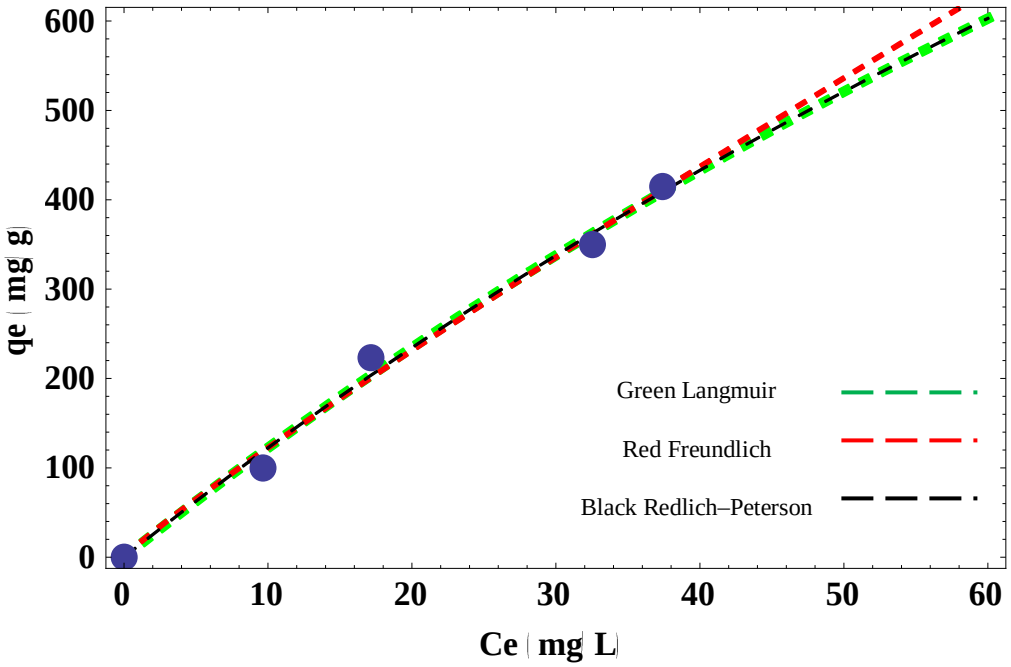

Figure 3.9 Fitting Experimental data of Toluene

feature hence, the parameter reaching unity strongly suggests Langmuir model fitting the experimental data (Moura et. al., 2011)

3.2.2.2 Binary equilibrium adsorption

The binary system set of experiments of Benzene and Toluene were carried out in batch system at room temperature and neutral pH (≈ 7.00) **Fig 3.10** and **Fig 3.11**. As for monitoring the effect of binary pollutants, single adsorption isotherm experimental data from previous section is plotted for comparison with binary data. One of the sets investigated Benzene adsorption isotherms in binary solution with Toluene **Fig 3.10**, from which we observe no major effect upon Benzene mono adsorption isotherm via existence of Toluene in binary component system. Looking deep through to experimental data, it revealed that Benzene adsorption isotherm nearly embedded among Benzene and Toluene binary adsorption isotherms **Fig 3.10**. The Benzene adsorption points (rectangular) appealing not much difference along other data of binary pollutants and may assume to be coincide therefore, within the examined range of concentrations, Benzene adsorption capacity is probably independent on Toluene existence. Moreover, **Fig 3.11** shows Toluene adsorption isotherms in binary solution with Benzene. It can be realized same pattern as in previous discussion; there is no remarkable influence over Toluene mono adsorption capacity while Benzene presence, approximately Benzene adsorption isotherm (diamond) is placed within equilibrium concentrations of binary Benzene and Toluene, indicating Toluene adsorption isotherm does not depend on Benzene. With mentioning that single and binary adsorption

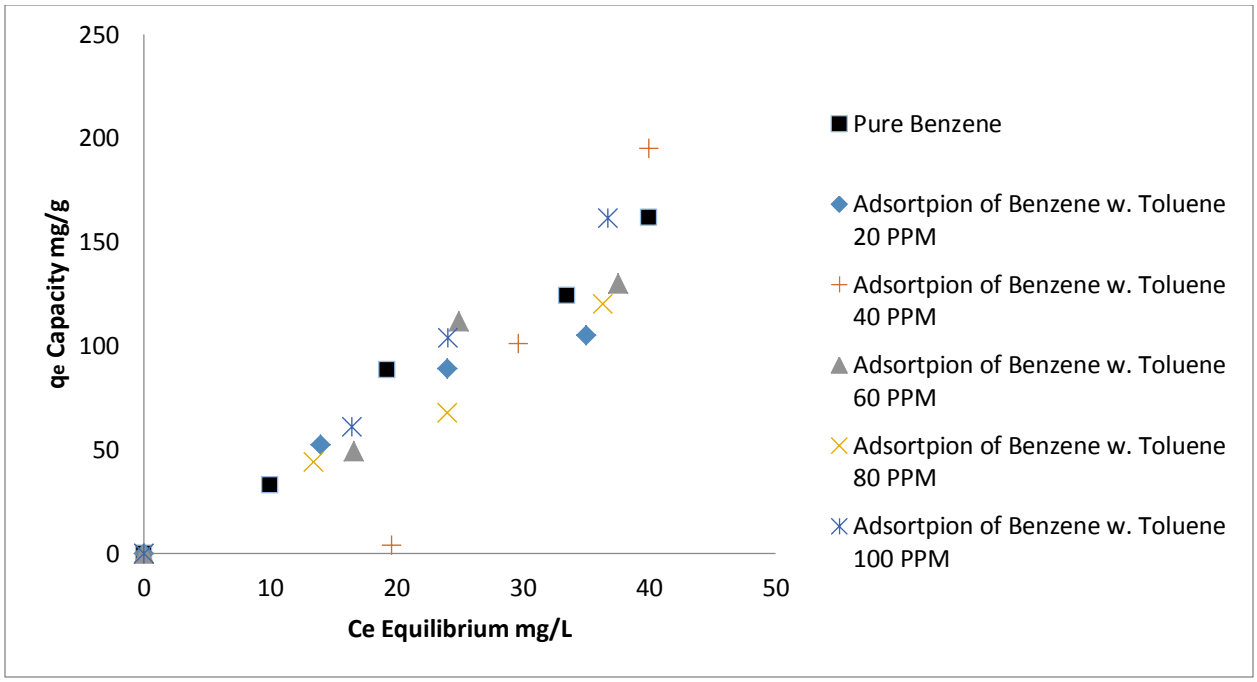

Figure 3.10 Binary Adsorption of Benzene with Different Concentrations of Toluene

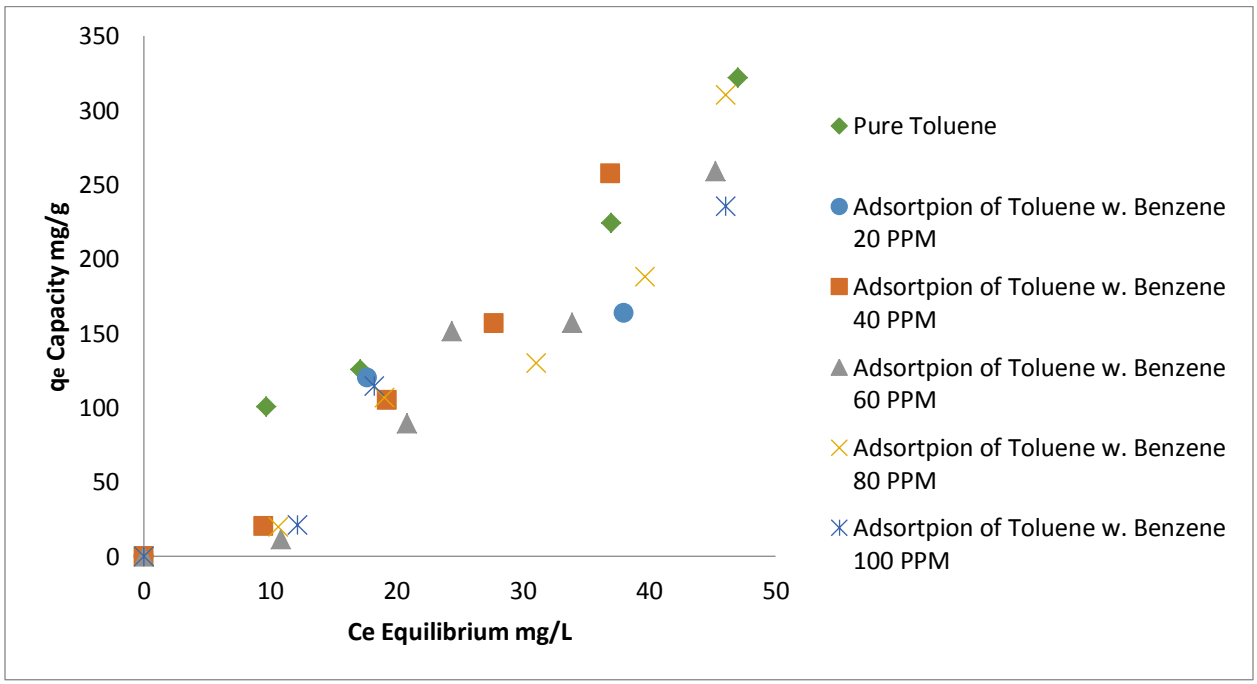

Figure 3.11 Binary Adsorption of Toluene with Different Concentrations of Benzene

experiments are performed in the same conditions verifying the base of comparison (Erto et. al., 2012; Erto et. al., 2011; Erto et. al., 2010). That point out observation of catalyst surface is considered to be covered with both pollutants independently on same active sites, attraction of investigated pollutants is expected to have no effect towards each other adsorption capacities but rather independent and that equilibrium concentrations of the pollutants are related to its own affinity towards same active sites.

3.2.3 Photo-catalytic Degradation of Benzene and Toluene

In the present set of experiment, Benzene and Toluene binary system experiment was carried out in batch system at room temperature and neutral pH (≈ 7.00), the degradation percentage is calculated

$$Degradation\ Percentage\ Reduction\ \% = \left[\frac{C_o - C_e}{C_0}\right] * 100 \qquad \textbf{Equation 5}$$

Where Co (mg/L) is pollutants initial concentration in solution, Ce (mg/L) is equilibrium concentration. **Fig 3.12** shows the percentage reduction against equilibrium concentrations. Experimental data suggested no influence for Toluene on Benzene in binary solution degradation. These results confirm the previous adsorption findings for the same system. Benzene degradation (asterisk) is considered almost coincident to Benzene and Toluene binary degradation experimental data, arising the point Toluene does not exert much considerable influence on Benzene degradation in binary mixtures. This supports the essential relation between adsorption and degradation; adsorption role is crucial for the initiation of the photo catalytic process on catalyst surface. Therefore, for the range of concentrations covered in this

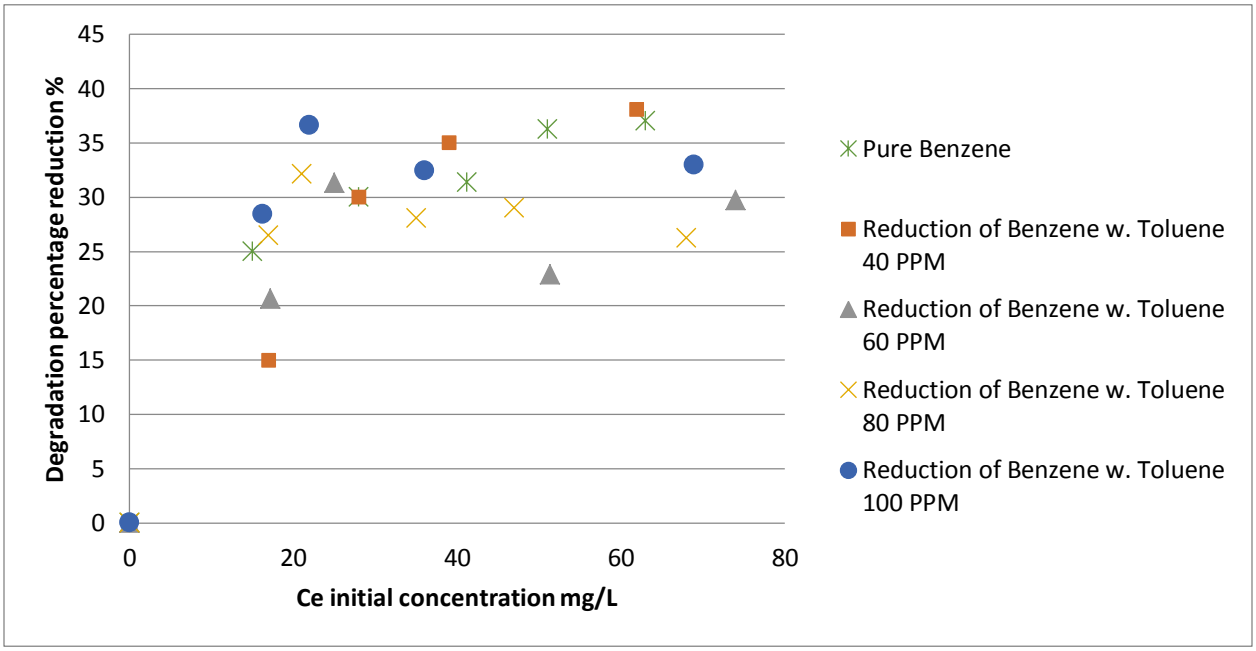

Figure 3.12 Binary Degradation of Benzene with Different Concentrations of Toluene

study Benzene mono degradation is independent of Toluene in binary degradation. The outcome verifies adsorption assumptions; catalyst surface is probably occupied by both pollutants independently on the same active sites at degradation initiation leaving the rest at solution. Attraction of investigated pollutants is expected to have no effect towards each other adsorption capacities. Hence, the degradation rate is independent of the pollutant but rather the affinity of the adsorbate towards the active sites.

3.3 Conclusion

Successfully, the Sol-Gel method was used to synthesize mesoporous Iron doped Titanium Dioxide (Fe-TiO_2) for application in photo degradation of Benzene and Toluene. The catalyst activity was enhanced by doping about 1% Fe^{+3} on titania. The dopant acts as charge trap delaying electron-hole combination which lengthens catalyst photo catalytic life. Besides, the decreasing the grain size to nano scale that results high increase in the surface area. Moreover, adsorption isotherms of studied pollutants are coincident with the proposed isotherm models. Langmuir model is found to be the best model that fits the experimental data. Further, binary mixture adsorption revealed nearly similar adsorption isotherms in comparison to their corresponding individual equilibrium concentrations.

4 Chapter

Photo Catalytic Degradation of Benzene and Xylenes Binary Mixture in Aqueous Solution

Abstract

Sol-Gel method was applied for iron doped titanium dioxide (Fe-TiO_2) for benzene and xylenes photo catalytic degradation purposes. The structure and properties of the catalyst were characterized by X-ray fluorescence (XRF), X-ray diffraction (XRD), N_2 adsorption/desorption and Scanning electron microscopy along with energy dispersive X-ray (SEM-EDX). The photo catalytic activity was evaluated by photo catalytic degradation of benzene and xylenes under ultraviolet illumination in liquid phase, indicating iron proper doping percentage of around 1 %. Results suggested catalyst in mesoporous structure, exhibit both Anatase and Rutile phases, less crystalline size, increased surface area and narrow pore size distribution. Adsorption capacity for benzene and xylenes was tested and equilibrium concentrations were fitted using common adsorption isotherm models (Langmuir, Freundlich and Redlich–Peterson). Furthermore, adsorption capacity of pure xylene is observed to be influenced by benzene presence in binary adsorption isotherms, reducing adsorption capacity of individual pollutant. That was not the case for benzene in binary mixture with xylenes, no influence upon mono adsorption benzene isotherm from xylenes presence in binary system. Consequently, the photo catalytic degradation of binary benzene and xylenes as photo catalytic process principally occurs on catalyst surface, adsorption is essential for photo catalytic degradation.

4.1 Introduction

The daily routine of domestic activates and industrial facilities either introduce or process tremendous amount of Hydrocarbons, among the hazardous by products volatile organic compounds (VOCs), it attract the attention for their harmful presence in environment, resulting pollution of atmosphere and water. Well known group of VOCs are Benzene, Toluene and Xylenes (BTX), several sources responsible for emitting BTX into environment such petrochemical, leakage from underground storage tanks, food processing, chemical, pharmaceutical and paints. The acute exposure to BTX could pose a serious threat such toxic, carcinogenic and mutagenic on health (Fay and Risher, 2007; Wilbur and Keith, 2007). Environmental bodies such Agency for Toxic Substances and Disease Registry (ATSDR), Environmental Protection Agency (EPA) and International Programme on Chemical Safety (IPCS-INCHEM), raised the awareness and restrictions upon pollutants availability in environment. Therefore, it necessary to develop techniques that remove pollutants efficiently and effectively also, meet the policies and restrictions issued by environmental agencies.

Plenty of promising methods have been published in literature, among them is adsorptive process e.g. activated carbon (Alvim-Ferraz et.al., 2007), zeolite (Gibson, 2014; Vidal et. al., 2012) and clays (de Souza et. al., 2014; Vidal and Volzone, 2009). Despite its convenient surface characteristics, adsorptive methods are considered reallocation of pollutants from initial phase into adsorbent solid phase. Other approach is advanced photo oxidation (AOPs), addition of hydrogen oxide to produce oxidizing agent eliminating undesired pollutants with the assistant of ultraviolet or ozone (Balcioğlu et. al, 2000; Comninellis et al., 2008). However, it is considered energy and resource demanding. Therefore, photo-degradation comes forth as an alternative, degradation of pollutants by adding semiconductors, activated through ultraviolet or visible

illumination to oxidize hazardous organic pollutants (Crittenden et. al., 1997). Several semiconductors have been studied such (TiO_2, ZnO, SnO_2, PbS, CdS, Fe_2O_3 and WO_3), among them TiO_2 arise as promising alternative due to the inertness nature, abundant, photo-stability and cost. In comparison, others such ZnO and SnO_2 have higher energy band gap (3.35 and 3.6) eV respectively (Gaya and Abdullah 2008). PbS and CdS rapidly lead to photo-corrosion and instability in aqueous media (Bahnemann 1987), ZnO instability in water yielding toxic $Zn(OH)_2$ (Mills and Hunte, 1997). SnO_2,Fe_2O_3 and WO_3 are naturally inherit conduction bands' level of energy permits reversible hydrogen potential (Sivula and Grätzel, 2009).

Application of titanium dioxide as photo-degradation catalyst for organic compounds is prosperous e.g. Drugs (Hapeshi et. al., 2010; An et. al., 2011) and pharmaceutical products (Choina and Duwensee 2010; Lin et. al., 2011). Moreover, Fu et al., (1995) enhanced TiO_2 activity through doping platinum, the mineralization rate of benzene was realized higher at temperatures exceeding 100^o C. Other work examined the degradation of benzene at room temperature via TiO_2 with ultraviolet (Wang et. al., 2003), humidity and pollutant concentration effect were considered for benzene mineralization. Photo-catalytic degradation of benzene using titanium dioxide into carbon nano-tubes CNT/TiO_2 nano-composite (Xu et. al., 2010), results showed developed activity over conventional titanium Degussa P_{25}. Nano-crystalline TiO_2 paste over spherical glass was used by Tsoukleris et. al., (2007) for benzene, toluene and xylene photo-catalytic elimination, catalytic rate was proportional to light intensity. Zuo et. al., (2006) implied degradation of toluene using ultraviolet germicidal lamps but hardly achieved on benzene, that overcome by addition Sn and Fe to TiO_2, results indicated Fe^{3+}/TiO_2 superior performance in mineralization. Titania doped with (Fe, V and W) and immobilized onto fiber glass cloth, was evaluated for benzene, toluene, ethyl benzene and xylene degradation (Laokiat et. al., 2011),

results suggested improvement in titania catalytic activity in comparison to commercial Degussa P_{25}. Sun et al., (2011) synthesized M-TiO_2 (M = Fe, Ag, Co, Cu) by sol-gel method, examined *O*-xylene degradation including humidity, Fe-TiO_2 was the best activity among other synthesized photo catalysts. Degradation of benzene, toluene, ethyl benzene, and *o*-xylene via sol-gel iron doped titanium dioxide (Jo and Lee 2013), activity was developed under visible light or UV irradiation, also degradation performance was greater to conventional titanita within proper percentage of Fe/ TiO_2.

In this work, iron doped Titanium Dioxide (Fe-TiO_2) will synthesized through sol-gel method for benzene and xylenes degradation along with, seeking the proper ratio of Fe/ TiO_2 to enhance the photo catalytic activity. Observe benzene-xylenes adsorption and photo-degradation in aqueous solution simultaneously, testing appropriate adsorption isotherm models to fit the equilibrium concentration data.

4.1.1 Experimental

4.1.1.1 Materials

The chemicals used in current study were Benzene (99.7 %), Xylenes (96 %) in high purity and Titanium (IV) Isopropoxide (97%) [$Ti(OCH(CH_3)_2)_4$] as a Titanium precursor later on for Iron doping, all obtained from (Sigma-Aldrich). Ferric Nitrate (98 %) [$Fe\ (NO_3)_3.9H_2O$] (Loba Chemie) is used as source of iron for doping into Titanium lattice. Acetic Acid glacial (99.5 %) [ACOH] (BDH Chemicals). Ethanol (99.9 %) [EtOH] (Scharlau).

4.1.1.2 Catalyst Synthesis

The synthesis of (Fe-TiO_2) followed Sol Gel method; a beaker was filled with 125 mL of Ethanol (EtOH), that was followed by 25 mL of Titanium precursor [$Ti(OCH(CH_3)_2)_4$]. The mixture was

then stirred to ensure homogeneity of the solution for further processing. On the other hand, in another beaker a 125 mL of Ethanol (EtOH) 5 mL of Acetic Acid (AcOH) and a specific amount of Ferric Nitrate [Fe $(NO_3)_3.9H_2O$] were mixed to achieve a desired percentage of doping. The latter mixture was added via a burette to the first beaker in a drop wise manner mixing with a magnetic stirrer. Then, the mixing was continued for 2 minutes The mixture was then sonicated in ultrasonic bath for 60 minutes. The obtained orange brownish solution was left to age at room temperature for 24 hours. The solution formed a gel structure and the gel was kept into the oven and dried for 24 hrs at 70^o C. The last step was the calcination of the resulting dried powder in a furnace at 400^oC for 4 hours to produce the final powder.

4.1.1.3 Characterization

The specific surface area (S_{BET}), pore volume and other structural properties of the catalyst were carried out using nitrogen adsorption/desorption [Micrometrics ASAP 2020 – Physisorption Analyzer]. A sample of 0.4663g was degassed under vacuum for 60 minutes at 473 K before undergoing N_2 adsorption/desorption at 77 K.

X-ray diffraction (XRD) [RigakuUltima IV] of the sample was recorded for phases and crystallite sizes. The pattern was recorded over scan the range 4-80 (2 theta) with a scan speed of 3 deg/min using Cu Kα radiation with 40 kV voltage and 40 mA current.

The percentage of the doped iron on titanium dioxide surface was measured using micro X-ray fluorescence (XRF) analysis [Bruker M4 Tornado]. The XRF was used for determining the elemental compositions of the synthesized catalyst using Rh as X-ray source (50 kV, 200 μm).

Scanning Electron Microscopy along with Energy Dispersive X-ray (SEM-EDX) analysis was performed [Oxford JEOL JEM-6610LV]. The SEM and EDX were used to determine the morphology and Fe/Ti ratio, respectively.

The determination of benzene and xylenes was carried out via Gas Chromatography-Flame Ionization Detector (GC-FID) [Shimadzu GC-2010]. The GC-FID is equipped with a Velocity XPT accelerated purge and trap system (Teledyne Tekmar).Volatile organic compounds with relatively lower water solubility were purged from the sample matrix using helium gas as inert gas carrier. The trapped components were introduced into the gas chromatography for further measurement.

The optimum iron content for the photo degradation reaction was determined using a lab made set up. A number of catalysts were prepared with different amounts of doped iron. A 500 mL Erlenmeyer flask which contains 100 mg/L of benzene or xylenes was closed with a Teflon stopper to avoid volatilization. A 0.5 g of catalyst was added to the benzene and xylenes flasks and placed in orbital shaker at 150 rpm for 12 hrs under illumination of multi Ultraviolet Germicidal lamps (Sankyo Denki G20T10; 20 watts/253.7 nm).

4.1.1.4 Adsorption Equilibrium Isotherms of Benzene and Xylenes

Benzene and xylenes adsorption isotherms were carried out in batch system at ambient temperature and neutral pH (≈ 7.00). A number of 250 mL Erlenmeyer flasks were closed with a Teflon stopper to avoid volatilization and covered with aluminium sheet to prevent photo degradation. Each flask contain 0.02 g of catalyst and 200 mL of benzene or xylenes with a concentration of [0, 20, 40, 60, 80 and 100] mg/L, the flasks were placed in orbital shaker at 150 RPM under the dark for 12 hrs ensuring equilibrium. The concentrations were determined by

Gas Chromatography-Flame Ionization Detector (GC-FID) [Shimadzu GC-2010] equipped with a Velocity XPT Accelerated Purge and Trap System (Teledyne Tekmar).

4.1.1.5 Photo Catalytic Degradation Benzene and Xylenes

The study of the degradation of benzene and xylenes was executed in a batch system, where a 250 mL Erlenmeyer flask were closed with a Teflon stopper to avoid volatilization, containing 0.02 g of catalyst and 200 mL of [0, 20, 40, 60, 80 and 100] mg/L, concentrations of benzene and xylenes at neutral pH (≈ 7.00), the flask was placed in orbital shaker at 150 rpm for 12 hrs under illumination of multi Ultraviolet Germicidal lamps (Sankyo Denki G20T10; 20 watts/253.7 nm). The concentrations were determined by Gas Chromatography-Flame Ionization Detector (GC-FID) [Shimadzu GC-2010] equipped with a velocity XPT accelerated purge and trap system (Teledyne Tekmar).

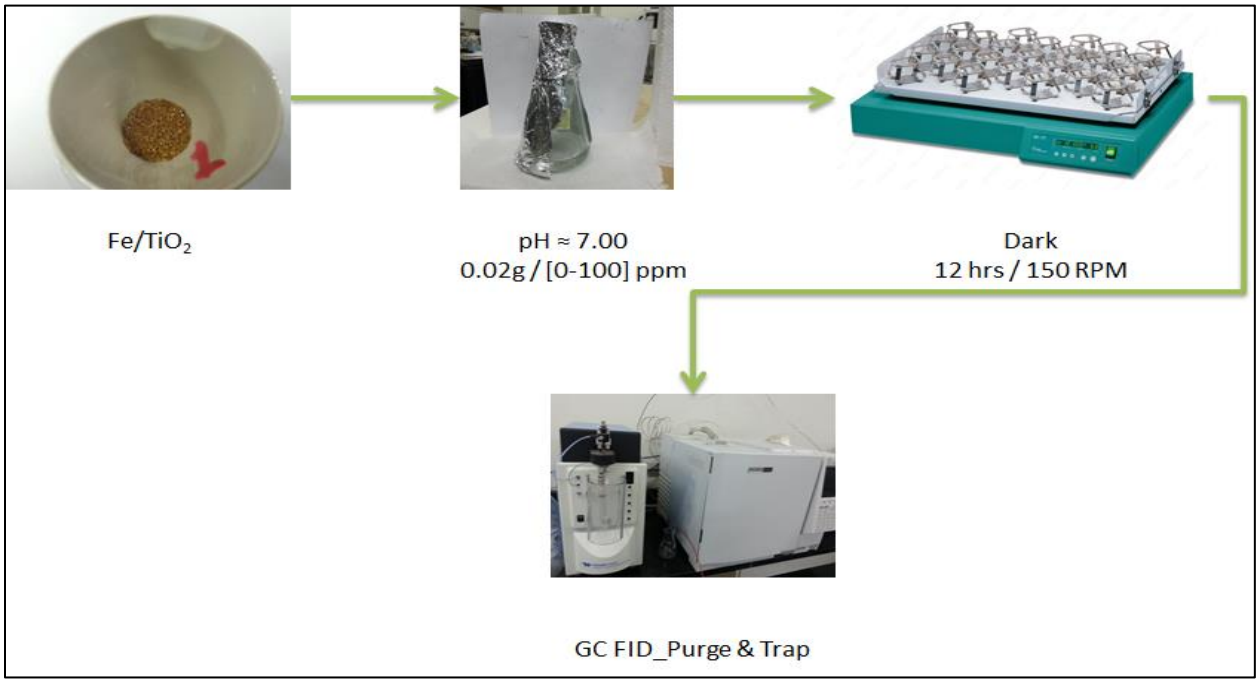

Figure 4.1 Setup for Adsorption Equilibrium Isotherm

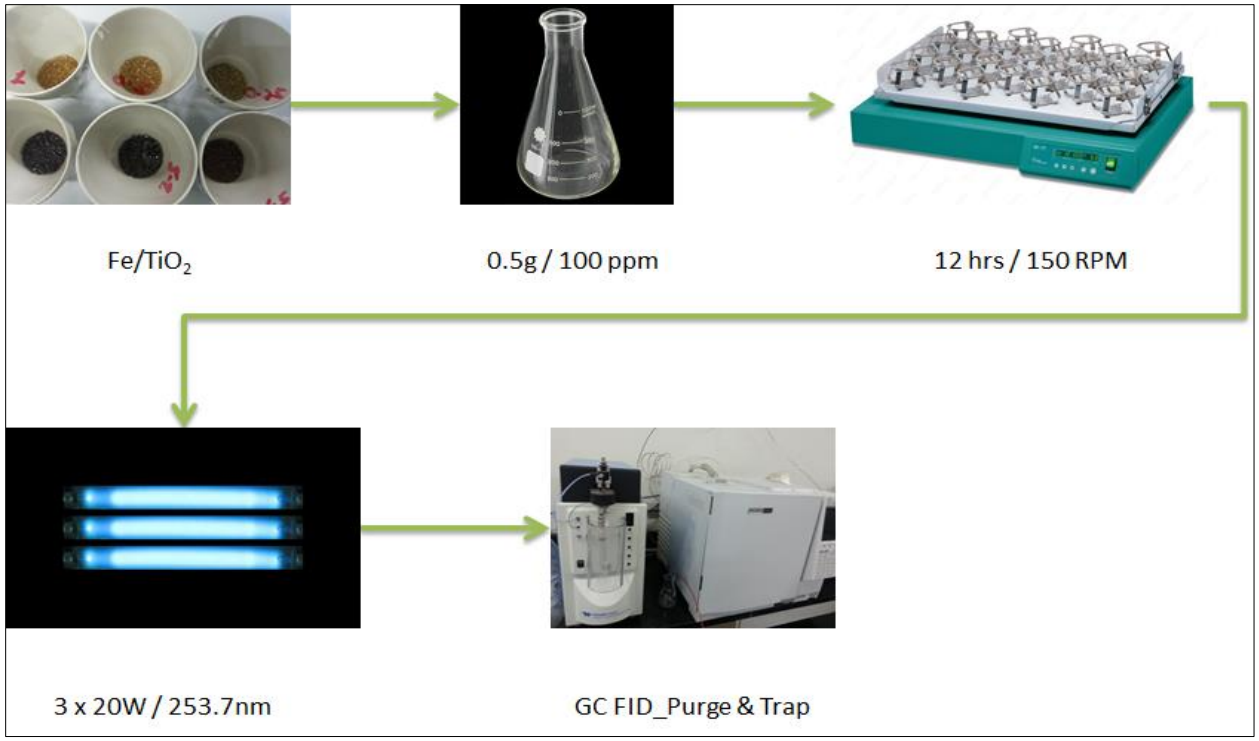

Figure 4.2 Setup for Photo-Catalytic Degradation

4.2 Results and discussions

4.2.1 Characterization

4.2.1.1 XRD

In **Fig 4.3**, shows the X-ray Diffraction (XRD) for synthesized powder of iron doped titanium dioxide. The examination of crystalline peaks pattern suggested the existence of two phases, Anatase (1 0 1) at $2\theta=25.38^{o}$ (Ambrus et. al., 2008; Navío et. al., 1999) and Rutile (1 1 0) at $2\theta=29.54^{o}$ (Mwangi et. al., 2013). Further investigation into the crystalline peaks point out the inexistence of iron characteristic's peak, implying sol-gel method followed for catalyst synthesis disperse iron properly and continuously into titania lattice. Another observation is Rutile intensity peak incremental along with iron percentage in titanium dioxide (Su et al. 2007; Nasralla et al. 2013), that gives an indication of iron crucial role as a parameter controlling the change of titania phase from Anatase to Rutile. Moreover, the crystallite size is considered small due to relatively broad diffraction peaks, an outcome from iron doping (Li et al. 2008; Sun et al. 2012). The grain sizes were in nanometer scale (11-17) nm. Iron is presumably distributed homogeneously into titanium dioxide surface, since no iron diffraction peaks was spotted. Probably to XRD detection limitation or the resemblance in ionic radii between (Fe^{3+} = 0.79Å) and (Ti^{4+} = 0.75 Å) enabling iron substitution of Ti ions into titanium dioxide (Zhu et al. 2004; Laokiat et al. 2011).

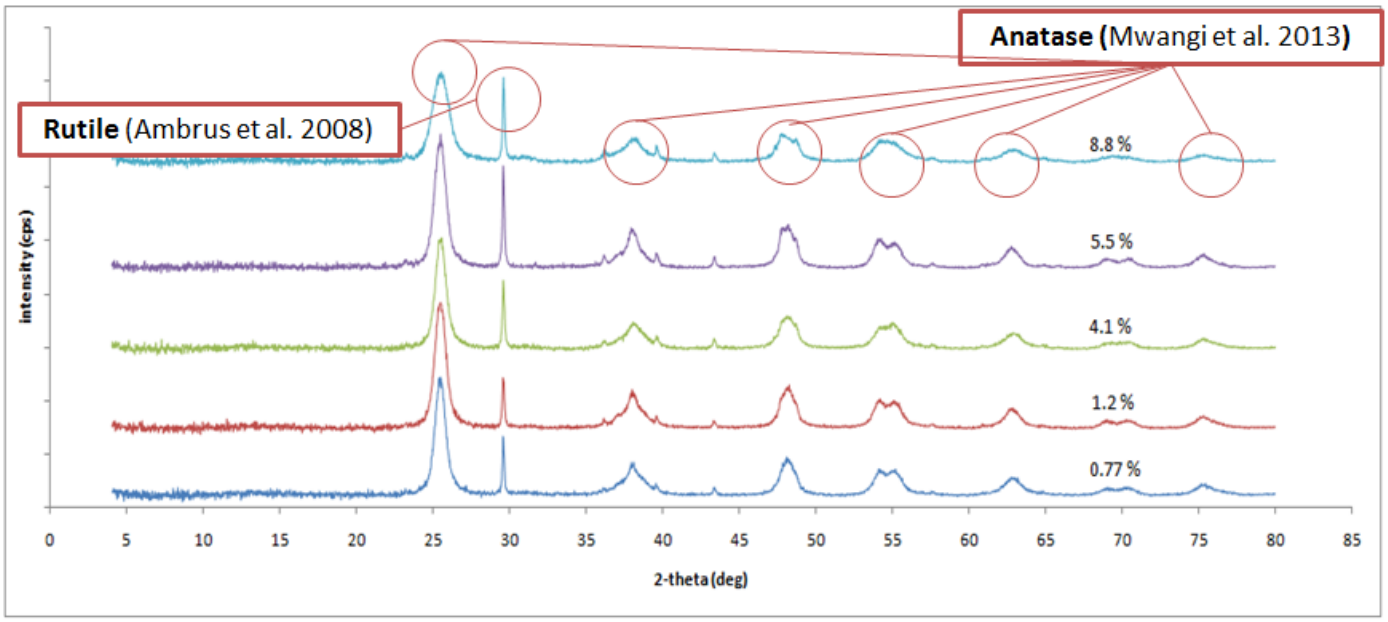

Figure 4.3 XRD Iron Doped Titanium Dioxide XRD Iron doped Titanium Dioxide

4.2.1.2 N_2 adsorption-desorption

N_2 adsorption/desorption was applied for synthesized iron doped titanium dioxide **Fig 4.4**, the physisorption isotherms suggested synthesized material to follow the classical type (IV), implying meoporous structure. Moreover, the hysteresis loop relatively steep desorption after slope adsorption branch about relative pressure (0.4-0.8), indicating the adsorption/desorption curves feature (H2) kind hysteresis loop (Sing et al. 1985). Hence, the material is supposed to experience capillary condensation associated with mesoporous structure such, synthesized catalyst suggested sophisticated pore structure and interconnected network of pores that diverse in size and shape presumably pore shape as "ink bottle" type (Wang et al. 2006). Brunaer–Emmett– Teller (BET) method was used to obtain the surface area **Table 4.1**. Reference to literature (Tong et. al., 2008; Wang et. al., 2006), the surface area of synthesized Fe-TiO_2 was found conveniently larger than commercial titania, it can be attributed to iron doping into titania lattice resulting smaller grain in size that was confirmed in XRD analysis consequently, beneficial to adsorption and photo catalytic degradation (Zhu et. al., 2004). The pore size distribution analysis was applied through Barret–Joyner–Halender (BJH) method, the results are inset in **Fig 4.2** revealing noticed a narrow pore size distribution in mesopore dimensions with a peak resulted at pore diameter of (4.6) nm.

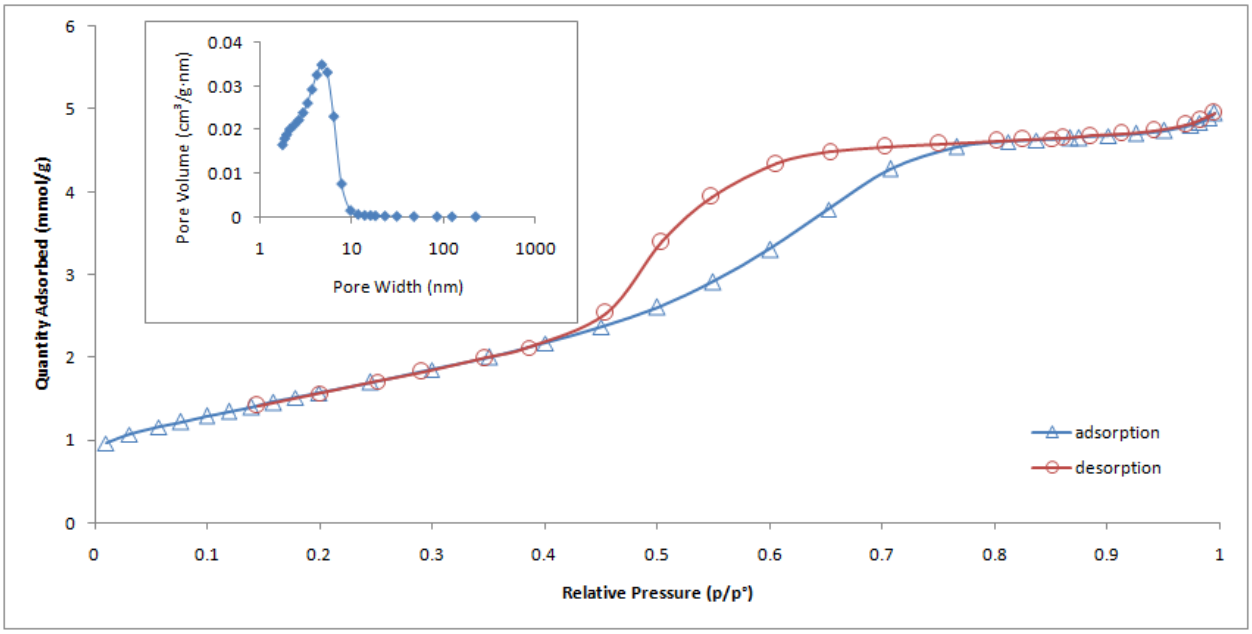

Figure 4.4 Nitrogen adsorption desorption isotherm Iron Doped Titanium Dioxide

Table 4.1 Structural Properties of Fe-TiO_2

Catalyst	Fe-TiO_2 ≈ 1 wt%
BET Surface Area (m^2/g)	129.675
Pore Volume (cm^3/g)	0.1665
Average Pore Diameter (nm)	5.14
Crystallite Size (nm)	11

4.2.1.3 SEM-EDX

The SEM images of the reference Fe-TiO_2 are seen in **Fig 4.5**. The morphology of samples investigated possess almost sharp corners and straight edges, mostly clusters of irregular shapes varying in size and dimension of synthesized catalyst, the iron addition to titanium lattice (Ambrus et. al., 2008) perhaps responsible for particles agglomeration in small dimensions as predicted in XRD analysis. As a result, enhancement in the specific surface area of catalyst samples accordingly, adsorption capacity and photo-catalytic reaction. Energy Dispersive X- ray (EDX) **Fig 4.6** was carried out to obtain chemical composition and its percentages, the EDX spectra peaks of sample detected (C, O, Ti, Fe, Au) the latter intensity peak was clearly high despite the absence while synthesizing the catalyst, due to sample coating generating clear and fine images.

4.2.1.4 Optimum Doping and Photo-Catalytic Activity

Fig 4.7 demonstrates photo-catalytic degradation activity of benzene and xylenes versus various iron percentage dopings in Fe-TiO_2. The assessment was based on detecting benzene and xylenes left in solution after irradiation with ultraviolet light with several doped Fe-TiO_2 percentages. It is noticeable the pattern between doping and photo degradation, the photo-catalytic degradation activity is proportional to iron content in titania, till it reached iron percentage near 1.2 % wt. corresponding about 70 % degradation reduction. Unfortunately, further increase of iron percentage resulted adverse effect upon photo-catalytic degradation activity. Presumably, iron incorporated into titanium dioxide create active sites to improve titania activity, by means of capturing electrons or holes to hinder electron-hole combination, which develop photo charges

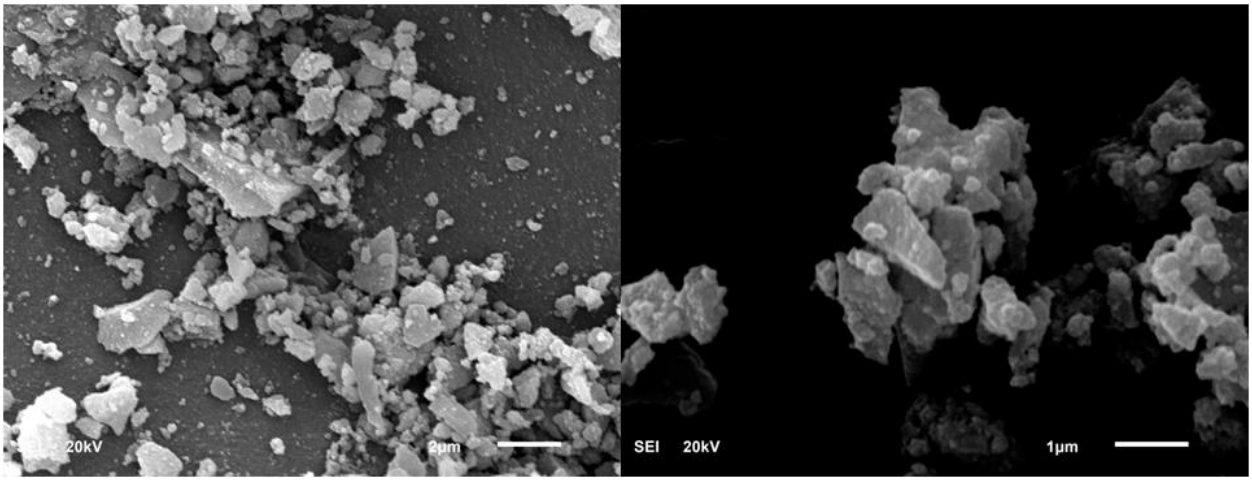

Figure 4.5 SEM of Synthesized Fe-TiO_2

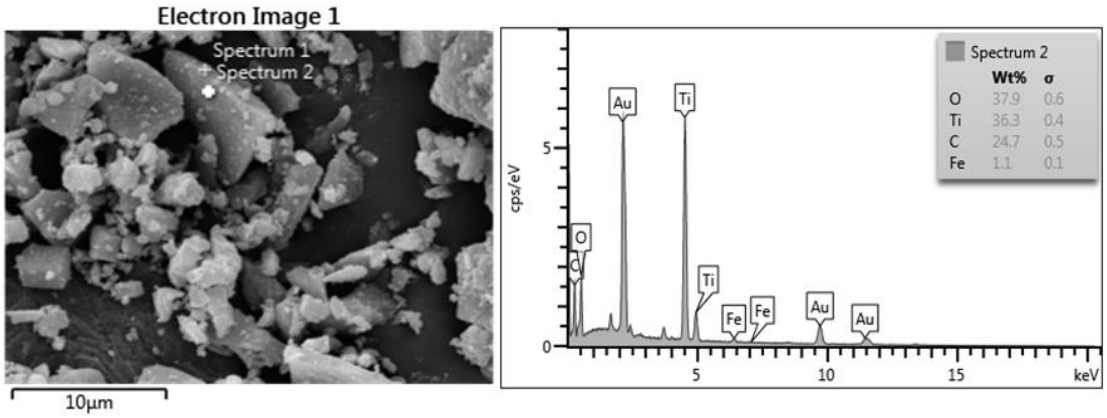

Figure 4.6 EDX of Synthesized Fe-TiO2

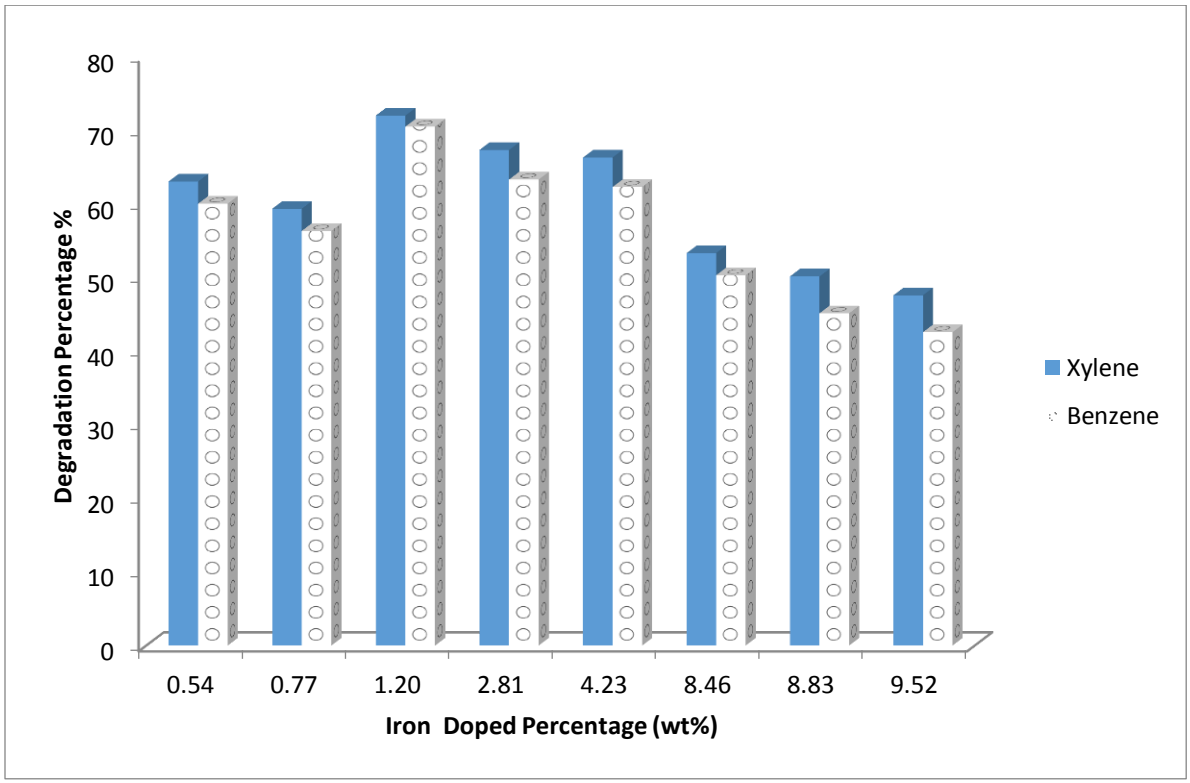

Figure 4.7 Effect of doping percentage on photo-Degradation

generation life time thus photo catalytic degradation efficiency, in addition to improving the interfacial charge transfer for pollutants degradation in attention of proper percentage of doped iron. Otherwise, iron content beyond 1 % results undesired recombination centers due to narrow distance between dopant trap, retarding charge transfer to the surface as a sequence, dwindling photo-catalytic activity of TiO_2 then degradation rate of the pollutants (Cong et. al., 2007; Xin et. al., 2007; Yang et. al., 2009; Lu et. al., 2011). EDX analysis **Fig 4.6** further confirms the incorporation of iron into in titanium dioxide lattice because of the resemblance in ionic radii. (Fe^{3+} = 0.79Å, Ti^{4+} = 0.75 Å) enabling iron substitution of Ti ions into semiconductor (Jo and Lee 2013).

4.2.2 Adsorption Equilibrium Isotherms of Benzene and Xylenes

4.2.2.1 Mono equilibrium adsorption

The photo catalytic process occurs on the surface of Fe-TiO_2, pointing out the importance of examining adsorption of benzene and xylenes from aqueous solution onto catalyst surface to determine equilibrium concentrations (C_e) that represent the initiative concentration for photo-catalytic process. The quantity of benzene and xylenes adsorbed, q_e (mg/g) onto the surface is calculated through mass balance with the assumption that decrease of contaminants in liquid phase is related to adsorption onto catalyst solid surface.

$$q_e = \frac{(C_o - C_e)V}{M} \qquad \textbf{Equation 6}$$

Where C_o (mg/L) is pollutants initial concentration in solution, C_e (mg/L) equilibrium concentration, V (L) volume of solution and M (g) mass of adsorbent added for experiment. Langmuir, Freundlich and Redlich–Peterson equations are famous adsorption isotherm models **Table 4.3**, were applied to the experimental data of mono benzene and xylenes individually. The

parameters obtained from suggested adsorption isotherms were fitted using Wolfram Mathematica 8. The constants and correlation coefficient (R^2) were listed in **Table 4.4**. **Fig 4.8** and **Fig 4.9** reveal the fitted adsorption models isotherm and experimental data simultaneously, the fitted isotherm models quite represented the experimental data which is confirmed through correlation coefficient clearly near to unity. Adsorption capacities were determined for benzene and xylenes $[13.5508 - 92.1083]$ (mg/g) respectively. The adsorption capacity of xylenes was found to be superior to benzene (de Souza et. al., 2012; Shahalam et. al., 1997), it can be related to xylenes greater molecular mass compared to benzene and less solubility towards water contributing its adsorption tendency to Fe-TiO_2. Seeing that the proposed isotherms clearly fitted the experimental points, more investigation is needed to determine the best among chosen models. Introducing a dimensionless constant named separation factor or equilibrium factor defined in **Table 4.2**. Benzene and xylenes R_L values in range $0.6770 - 0.9129$ and $0.7263 - 0.9299$ respectively. Therefore, the adsorption processes were favorable. On the other hand, the value of Freundlich's n_F parameter an index relates adsorption affinity and capacity between adsorbent and adsorbate. Weak interaction adsorbate to adsorbent appears when n_F lower than 1 while the conversely at n_F greater than 1. Nonetheless, , at value close to unity, an assumption to equivalent energetic sites take place promotes experimental data likely be fitted to Langmuir adsorption model, was the case for benzene and Xylenes (Valente et al. 2006). The Redlich–Peterson model is combination of Langmuir and Freundlich aspects with parameter b as limiting factor; when b approaches zero indicates the model follows Henry's law thereby, the parameter almost unity strongly suggests Langmuir model fitting the experimental data (Moura et al. 2011).

Table 4.2 Dimensionless Constant Separation Factor or Equilibrium Factor, R_L

Langmuir equilibrium parameter	$R_L = \frac{1}{1 + b_L\, C_o}$
$R_L > 1$	Unfavorable
$R_L = 1$	Linear
$0 < R_L < 1$	Favorable
$R_L = 0$	irreversible

Table 4.3 Adsorption Isotherm Models used for Mono component adsorption

Isotherm Model	Equation
Langmuir	$q_e = \frac{q_{max} b_L C_e}{1 + b_L C_e}$
Freundlich	$q_e = k_F\, C_e^{\,1/n_F}$
Redlich–Peterson	$q_e = \frac{K_{PR}\, C_e}{\left(1 + C_e^b\, a_{PR}\right)}$

Table 4.4 Values for Adsorption Isotherm Model fitted parameters of BTX in Mono Component System

	Benzene	Xylenes
Langmuir		
$q_{max}\ (mg/g)$	13.5508	92.1083
$b_L\ (L/mg)$	0.00477	0.00376
R^2	0.99904	0.9998
R_L	$0.6770 - 0.9129$	0.7263
Freundlich		
k_F	5.5992	20.5321
n_F	1.24566	1.0886
R^2	0.9987	0.9997
Redlich–Peterson		
$K_{PR}\ (L/mg)$	3.2465	17.3585
$a_{PR}\ (L/mg)$	0.00520	0.00381
b	0.9834	0.9970
R^2	0.9990	0.9998

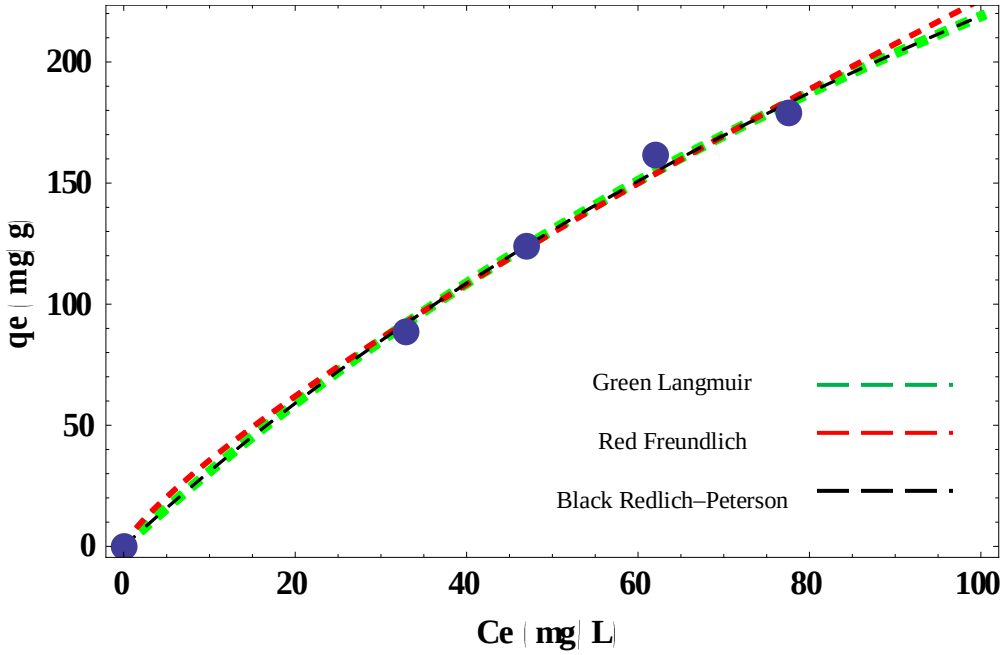

Figure 4.8 Fitting Experimental data of Benzene

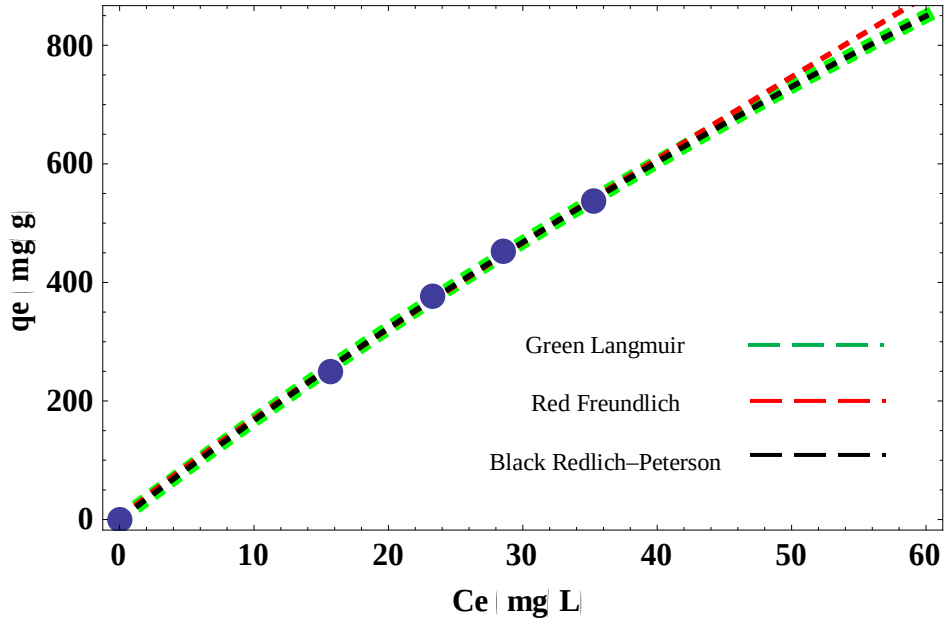

Figure 4.9 Fitting Experimental data of Xylene

4.2.2.2 Binary equilibrium adsorption

In the present study, a set of experiments on benzene and xylenes binary systems were carried out in a batch system at room temperature and neutral pH (≈ 7.00), the outcome of each set of experiment are shown in **Fig 4.10** and **Fig 4.11**. For comparison, single adsorption isotherm experimental data for correspondent components is also included within binary adsorption isotherms. Starting with xylenes adsorption isotherm in binary solution with benzene **Fig 4.10**, it can be observed adsorption capacity of pure xylene influenced by benzene presence, reducing adsorption capacity of individual pollutant almost 70 % in binary component system system (Al-Degs et al. 2007). More into experimental results showed effect of benzene over xylenes adsorption, competitive xylenes adsorption values occurred within benzene existence **Fig 4.10**, remarkably lower than relevant data in absence of benzene (circle). Therefore, within concentration range considered xylenes adsorption capacity is strongly influenced by increasing benzene concentration competitively. Furthermore, **Fig 4.11** illustrate benzene adsorption isotherms in binary solution with xylenes, it can be noticed no great influence upon mono adsorption benzene isotherm from xylenes presence in binary system. Moreover, it can be realized that benzene adsorption isotherm is clearly embedded into benzene and xylenes binary adsorption isotherms, benzene adsorption points (diamond) showing similar pattern to pollutants binary data and presumably coincide hence, along the investigated concentration range, benzene adsorption capacity is most probably independent on xylene presence. With mentioning that single and binary adsorption experiments are performed in the same conditions verifying the base of comparison (Erto et. al., 2012; Erto et. al., 2011; Erto et. al., 2010). That suggests adsorbate surface is covered with both pollutants independently on surface active sites, attraction of investigated pollutants is expected to have no effect towards each other adsorption capacities

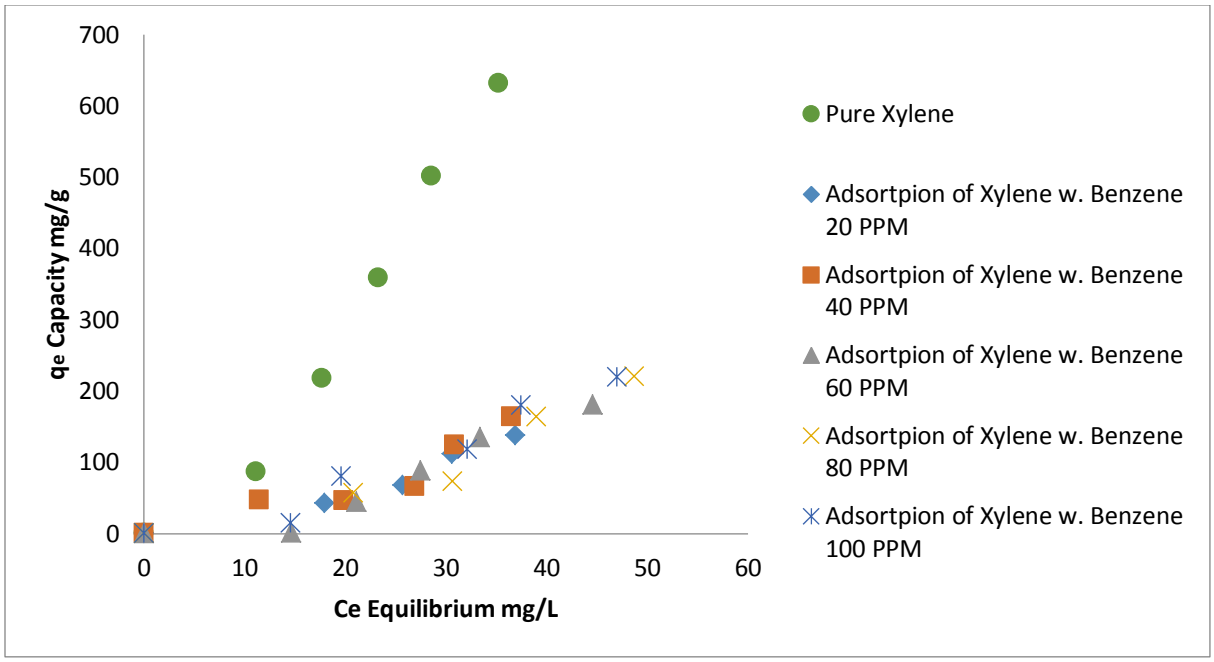

Figure 4.10 Binary Adsorption of Xylenes with Different Concentrations of Benzene

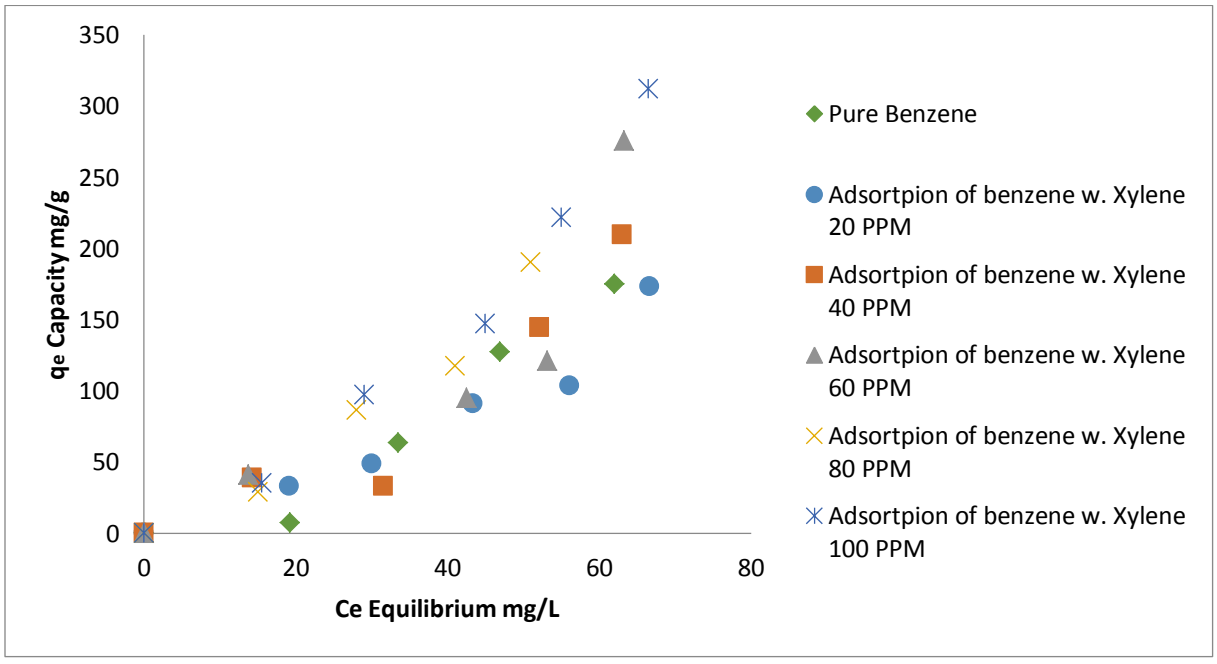

Figure 4.11 Binary Adsorption of Benzene with Different Concentrations of Xylenes

but rather independent and that equilibrium concentrations of the pollutants are related to its own affinity towards same active sites.

4.2.2.3 Photo-catalytic Degradation of Benzene and Xylenes

Results shown in **Fig 4.12** and **Fig 4.13** represent photo catalytic degradation of benzene and xylenes in binary system, the experiments were conducted at neutral pH (≈ 7.00) and room temperature, the degradation percentage was calculated by

$$Degradation\ Percentage\ Reduction\ \% = \left[\frac{C_o - C_e}{C_0}\right] * 100 \qquad \textbf{Equation 7}$$

Where C_o (mg/L) is pollutants initial concentration in solution and C_e (mg/L) is equilibrium concentration. **Fig 4.12** represent the degradation percentage reduction against equilibrium concentrations of xylenes within xylenes-benzene binary solution, it can be recognized pure xylenes reduction percentage is superior to binary xylenes and benzene degradation about 30 %. Deep monitoring into experimental points reveals similar tendency to adsorption isotherms, pure xylenes degradation values (circle) in **Fig 4.12** is obviously greater than corresponding data when benzene is existence. Since photo catalytic process occurs fundamentally on catalyst surface, there is a close relation between adsorption and degradation therefore, within tested range of concentrations benzene presence retarded degradation effectiveness of xylenes through increasing xylenes equilibrium concentration. Which complies with adsorption prediction, catalyst surface is suggested to be filled with portion of both pollutants simultaneously initiating the photo catalytic degradation and leaving the rest in solute, presuming no interaction between pollutants but rather related to its adsorption affinity to same active sites then degradation. As for **Fig 4.13**, illustrates benzene within xylenes-benzene binary solution photo catalytic degradation

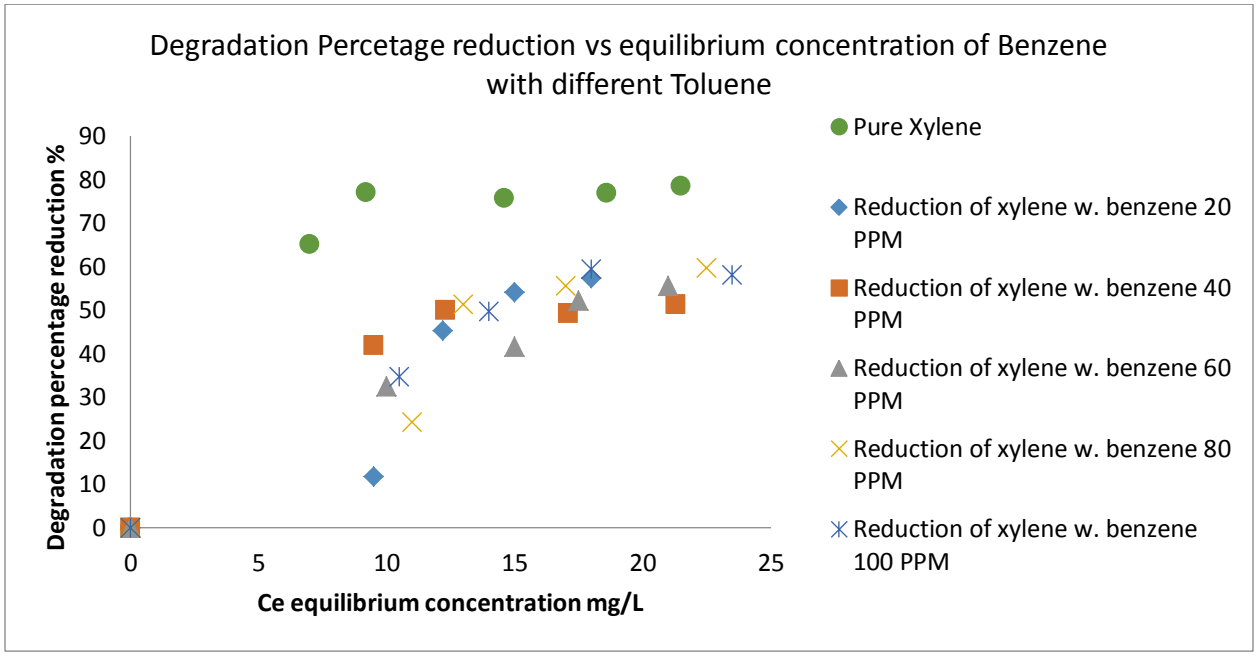

Figure 4.12 Binary Degradation of Xylenes with Different Concentrations of Benzene

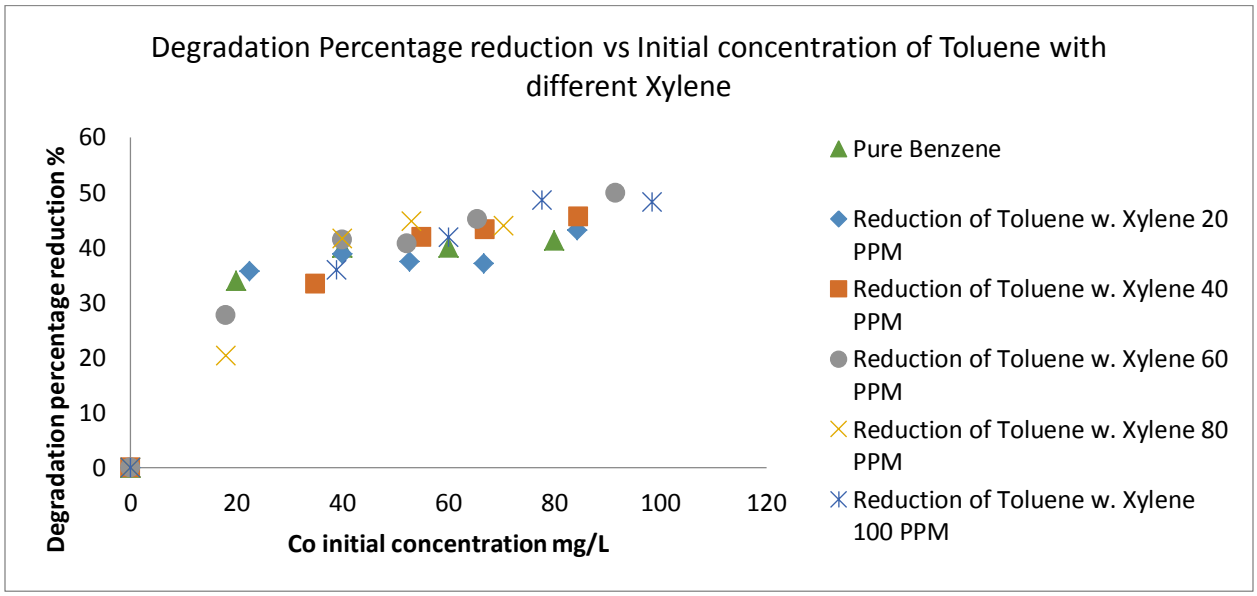

Figure 4.13 Binary Degradation of Benzene with Different Concentrations of Xylenes

reduction, experimental points strongly indicates the absence of xylenes influence over benzene degradation supporting the outcome of adsorption, benzene degradation data (triangle) are approximately embedded into xylenes and benzene degradation data. Conveniently supporting assumption made regarding adsorption, that benzene mono degradation is independent on xylenes presence in binary degradation system, possibly adsorbate surface is filled with both pollutants independently on same active sites for degradation, with no influence towards each other adsorption capacities as a result, degradation rate rather independent as pollutants are related to its own tendency to same active sites.

4.3 Conclusion

Benzene and xylenes photo catalytic degradation was achieved using meoporous iron doped titanium dioxide (Fe-TiO_2). The synthesis followed Sol-Gel method where iron content was found preferable almost 1 %, promoting catalyst activity through descending electron-hole combination, that improved catalyst photo catalytic life and creating nano size grains that enhanced surface area. Adsorption isotherms of examined pollutants quite fitted the selected isotherm models, while parameters strongly indicated Langmuir model fitting the experimental data and maximum capacity for xylenes. Moreover, binary mixture adsorption isotherms of benzene in xylenes-benzene mixture, showed almost similar adsorption isotherms in comparison to their corresponding individual equilibrium concentrations. On the other hand, xylenes adsorption capacity was about 70 % superior to xylenes-benzene adsorption isotherms. Indicating investigated pollutants are expected to have no influnce towards adsorption rate but rather independent, that equilibrium concentrations of the pollutants are related to its own affinity towards same active sites. Consequently photo catalytic degradation, as photo catalytic

reaction occurs on the surface of catalyst pointing out the critical role of adsorption to initiate degradation.

5 Chapter

Conclusions and Recommendations

Mesoporous iron doped titanium dioxide (Fe-TiO_2) was successfully synthesized using Sol-Gel method. The prepared catalyst achieved photo catalytic degradation of benzene, toluene and xylenes in aqueous solution. The photo catalytic activity was evaluated for liquid phase photo catalytic degradation of benzene, toluene and xylenes under ultraviolet illumination and found to be enhanced via doping iron into titania lattice, as the optimum percentage about 1 %, that enabled the dopant to act properly as charge trap hindering electron-hole combination. XRD verified small grain size of catalyst possessing both Anatase and Rutile phases. Nitrogen adsorption/desorption confirmed mesoporousity structure, narrow pore size distribution and relatively high surface area. SEM-EDX showed synthesized catalyst is clusters of irregular shapes in diverse sizes and dimensions mostly possess sharp corners and straight edges. Furthermore, adsorption isotherm of benzene, toluene and xylenes was fitted to common adsorption isotherm models, the fitted parameters strongly suggested Langmuir model with xylenes gaining the highest adsorption capacity. Moreover, binary mixture adsorption isotherms was carried out for xylenes-toluene, benzene-toluene and benzene-xylene couples. Xylenes-toluene binary adsorption isotherm revealed adsorption capacity of pure Toluene was affected by existence of Xylenes reducing individual pollutant adsorption capacity about 40 % in multi component system, which was also the case for xylenes adsorption isotherms in binary solution with Toluene, reducing the adsorption capacity about 50 %. Observing benzene-toluene binary mixture adsorption isotherms, no influence was noticed upon neither Benzene nor toluene mono adsorption isotherm in binary component system. Finally, investigation of benzene-xylenes in

binary mixture adsorption isotherms, adsorption capacity of pure xylene was affected by benzene presence, reducing adsorption capacity of individual pollutant almost 70 % in binary component system. On the other hand, no great influence upon mono adsorption benzene isotherm from xylenes presence in binary system. As for photo catalytic degradation of pollutants in binary mixture, the degradation followed the same pattern of adsorption since photo catalytic process fundamentally takes place on catalyst surface, conveniently supporting assumption made regarding adsorption. Hence, investigated pollutants have no interaction influencing adsorption capacities and degradation rate is rather independent as pollutants are related to its own affinity towards same active sites.

For future work, the following points are strongly recommended:

- Investigate photo-catalytic degradation and adsorption for benzene, toluene and xylenes in tertiary system as the thesis covered the mono and binary system.
- Study the effect of parameters on photo-catalytic degradation and adsorption such light intensity, temperature, catalysis amount, pH and shaker speed.
- Perform kinetic study for photo-catalytic degradation of benzene, toluene and xylenes.
- Apply photo-catalytic degradation to other pollutants.

References

Adán, C. et al., 2007. Structure and activity of nanosized iron-doped anatase TiO2 catalysts for phenol photocatalytic degradation. *Applied Catalysis B: Environmental*, 72(1-2), pp.11–17. Available at: http://linkinghub.elsevier.com/retrieve/pii/S0926337306004206 [Accessed March 9, 2014].

Al-Degs, Y. et al., 2007. Competitive adsorption of reactive dyes from solution: Equilibrium isotherm studies in single and multisolute systems. *Chemical Engineering Journal*, 128(2-3), pp.163–167. Available at: http://linkinghub.elsevier.com/retrieve/pii/S1385894706004402 [Accessed September 21, 2014].

Ambrus, Z. et al., 2008. Synthesis, structure and photocatalytic properties of Fe(III)-doped TiO2 prepared from TiCl3. *Applied Catalysis B: Environmental*, 81(1-2), pp.27–37. Available at: http://linkinghub.elsevier.com/retrieve/pii/S0926337307004249 [Accessed January 30, 2014].

An, T. et al., 2011. Photocatalytic degradation kinetics and mechanism of antivirus drug-lamivudine in TiO< sub> 2</sub> dispersion. *Journal of hazardous materials*. Available at: http://www.sciencedirect.com/science/article/pii/S0304389411011885 [Accessed April 11, 2014].

Anipsitakis, G.P. & Dionysiou, D.D., 2004. Radical generation by the interaction of transition metals with common oxidants. *Environmental science & technology*, 38(13), pp.3705–12. Available at: http://www.ncbi.nlm.nih.gov/pubmed/15296324.

Arslan, I., Balcioğlu, I. & Bahnemann, D., 2000. Advanced chemical oxidation of reactive dyes in simulated dyehouse effluents by ferrioxalate-Fenton/UV-A and TiO 2/UV-A processes. *Dyes and pigments*, 47(3), pp.207–218. Available at: http://linkinghub.elsevier.com/retrieve/pii/S0143720800000826 [Accessed June 18, 2014].

Augugliaro, V. et al., 1999. Photocatalytic oxidation of gaseous toluene on anatase TiO2 catalyst: Mechanistic aspects and FT-IR investigation. *Applied Catalysis B: Environmental*, 20(1), pp.15–27. Available at: http://www.sciencedirect.com/science/article/pii/S0926337398000885 [Accessed June 18, 2014].

Bahnemann, D., 1987. Preparation and characterization of quantum size zinc oxide: a detailed spectroscopic study. *Journal of Physical …*. Available at: http://pubs.acs.org/doi/abs/10.1021/j100298a015 [Accessed April 8, 2014].

Blanco, J. et al., 1996. Photocatalytic destruction of toluene and xylene at gas phase on a titania based monolithic catalyst. *Catalysis Today*, 29(1-4), pp.437–442. Available at:

http://www.sciencedirect.com/science/article/pii/0920586195003177 [Accessed April 11, 2014].

Breu, F., Guggenbichler, S. & Wollmann, J., 2008a. Benzene IPCS_INCHEM. *Vasa*, pp.1–73. Available at: http://medcontent.metapress.com/index/A65RM03P4874243N.pdf [Accessed March 31, 2014].

Breu, F., Guggenbichler, S. & Wollmann, J., 2008b. Toluene IPCS_INCHEM. *Vasa*, pp.1–83. Available at: http://medcontent.metapress.com/index/A65RM03P4874243N.pdf [Accessed March 31, 2014].

Breu, F., Guggenbichler, S. & Wollmann, J., 2008c. Xylenes IPCS_INCHEM. *Vasa*, pp.1–81. Available at: http://medcontent.metapress.com/index/A65RM03P4874243N.pdf [Accessed March 31, 2014].

Carp, O., 2004. Photoinduced reactivity of titanium dioxide. *Progress in Solid State Chemistry*, 32(1-2), pp.33–177. Available at: http://linkinghub.elsevier.com/retrieve/pii/S0079678604000123 [Accessed February 19, 2014].

Choina, J. & Duwensee, H., 2010. Removal of hazardous pharmaceutical from water by photocatalytic treatment. *... European Journal of ...*. Available at: http://link.springer.com/article/10.2478/s11532-010-0109-9 [Accessed April 11, 2014].

Chung, Y.-C. & Chen, C.-Y., 2008. Degradation of azo dye reactive violet 5 by TiO2 photocatalysis. *Environmental Chemistry Letters*, 7(4), pp.347–352. Available at: http://link.springer.com/10.1007/s10311-008-0178-6 [Accessed March 26, 2014].

Comninellis, C. et al., 2008. Advanced oxidation processes for water treatment: advances and trends for R&D. *Journal of Chemical ...*, 776(October 2007), pp.769–776. Available at: http://onlinelibrary.wiley.com/doi/10.1002/jctb.1873/full [Accessed March 26, 2014].

Cong, Y. et al., 2007. Preparation, photocatalytic activity, and mechanism of nano-TiO2 Co-doped with nitrogen and iron (III). *Journal of Physical Chemistry C*, 111(Iii), pp.10618–10623.

Crittenden, J. et al., 1997. Photocatalytic oxidation of chlorinated hydrocarbons in water. *Water Research*, 31(3), pp.429–438. Available at: http://linkinghub.elsevier.com/retrieve/pii/S0043135496002679 [Accessed March 2, 2014].

Dias, J.M. et al., 2007. Waste materials for activated carbon preparation and its use in aqueous-phase treatment: a review. *Journal of environmental management*, 85(4), pp.833–46. Available at: http://www.sciencedirect.com/science/article/pii/S0301479707002964 [Accessed July 16, 2014].

Dias, M. & Azevedo, E., 2009. Photocatalytic decolorization of commercial acid dyes using solar irradiation. *Water, air, and soil pollution*. Available at: http://link.springer.com/article/10.1007/s11270-009-0028-6 [Accessed March 26, 2014].

Dorsey, A. & McClure, P.R., 1989. Toxicological profile for toluene. *Agency for Toxic Substances and Disease Registry, US …*, (September). Available at: http://scholar.google.com/scholar?hl=en&btnG=Search&q=intitle:TOXICOLOGICAL+PROFILE+FOR+TOLUENE#0 [Accessed April 1, 2014].

Echavia, G., Matzusawa, F. & Negishi, N., 2009. Photocatalytic degradation of organophosphate and phosphonoglycine pesticides using TiO< sub> 2</sub> immobilized on silica gel. *Chemosphere*. Available at: http://www.sciencedirect.com/science/article/pii/S0045653509005724 [Accessed April 11, 2014].

Erto, a. et al., 2010. Experimental and statistical analysis of trichloroethylene adsorption onto activated carbon. *Chemical Engineering Journal*, 156(2), pp.353–359. Available at: http://linkinghub.elsevier.com/retrieve/pii/S1385894709007268 [Accessed January 17, 2015].

Erto, a., Lancia, a. & Musmarra, D., 2011. A modelling analysis of PCE/TCE mixture adsorption based on Ideal Adsorbed Solution Theory. *Separation and Purification Technology*, 80(1), pp.140–147. Available at: http://linkinghub.elsevier.com/retrieve/pii/S1383586611002450 [Accessed January 8, 2015].

Erto, a., Lancia, a. & Musmarra, D., 2012. A Real Adsorbed Solution Theory model for competitive multicomponent liquid adsorption onto granular activated carbon. *Microporous and Mesoporous Materials*, 154, pp.45–50. Available at: http://linkinghub.elsevier.com/retrieve/pii/S1387181111005221 [Accessed January 8, 2015].

Fabbri, D., Crime, A. & Davezza, M., 2009. Surfactant-assisted removal of swep residues from soil and photocatalytic treatment of the washing wastes. *Applied Catalysis B: …*. Available at: http://www.sciencedirect.com/science/article/pii/S0926337309003245 [Accessed April 11, 2014].

Fahim, M., Al-Sahhaf, T. & Elkilani, A., 2009. *Fundamentals of petroleum refining*, Available at: http://books.google.com/books?hl=en&lr=&id=UcFsv1mMFHIC&oi=fnd&pg=PP1&dq=Chapter+17+–+Environmental+Aspects+in+Refining+Mohamed+A.+Fahim,+Taher+A.+Alsahhaf,+Amal+Elkilani&ots=E04na-xDny&sig=CR-5YnMzpq-1jZYqkkQdf2fL0fQ [Accessed September 17, 2014].

Fay, M. & Risher, J.F., 2007. Toxicological Profile for Xylene. , (August). Available at: http://scholar.google.com/scholar?hl=en&btnG=Search&q=intitle:TOXICOLOGICAL+PROFILE+FOR+XYLENES#2 [Accessed March 31, 2014].

Ferrari-Lima, a. M. et al., 2014. Photodegradation of benzene, toluene and xylenes under visible light applying N-doped mixed TiO2 and ZnO catalysts. *Catalysis Today*. Available at: http://linkinghub.elsevier.com/retrieve/pii/S0920586114002727 [Accessed September 28, 2014].

Fu, X., Zeltner, W. a. & Anderson, M. a., 1995. The gas-phase photocatalytic mineralization of benzene on porous titania-based catalysts. *Applied Catalysis B: Environmental*, 6(3), pp.209–224. Available at: http://linkinghub.elsevier.com/retrieve/pii/0926337395000178.

Fujishima, A., 1972. Electrochemical photolysis of water at a semiconductor electrode. *nature*. Available at: http://adsabs.harvard.edu/abs/1972Natur.238...37F [Accessed April 3, 2014].

Gaya, U.I. & Abdullah, A.H., 2008. Heterogeneous photocatalytic degradation of organic contaminants over titanium dioxide: A review of fundamentals, progress and problems. *Journal of Photochemistry and Photobiology C: Photochemistry Reviews*, 9(1), pp.1–12. Available at: http://linkinghub.elsevier.com/retrieve/pii/S1389556708000300 [Accessed January 22, 2014].

Gibson, L., 2014. Mesosilica materials and organic pollutant adsorption: part B removal from aqueous solution. *Chemical Society reviews*. Available at: http://pubs.rsc.org/en/content/articlehtml/2014/cs/c3cs60095e [Accessed September 20, 2014].

Guelli Ulson de Souza, S.M. de A. et al., 2012. Removal of Mono- and Multicomponent BTX Compounds from Effluents Using Activated Carbon from Coconut Shell as the Adsorbent. *Industrial & Engineering Chemistry Research*, 51(18), pp.6461–6469. Available at: http://pubs.acs.org/doi/abs/10.1021/ie2026772 [Accessed October 14, 2014].

Gupta, S.M. & Tripathi, M., 2011. A review of TiO2 nanoparticles. *Chinese Science Bulletin*, 56(16), pp.1639–1657. Available at: http://link.springer.com/10.1007/s11434-011-4476-1 [Accessed February 3, 2014].

Hackbarth, F. V. et al., 2014. Benzene, toluene and o-xylene (BTX) removal from aqueous solutions through adsorptive processes. *Adsorption*, pp.577–590. Available at: http://link.springer.com/10.1007/s10450-014-9602-3 [Accessed September 13, 2014].

Hapeshi, E., Achilleos, A. & Vasquez, M., 2010. Drugs degrading photocatalytically: kinetics and mechanisms of ofloxacin and atenolol removal on titania suspensions. *Water research*. Available at: http://www.sciencedirect.com/science/article/pii/S0043135409007994 [Accessed April 11, 2014].

Hir, Z.A.M., Ali, R. & Bakar, W.A.W.A., 2011. PHOTODEGRADATION OF BENZENE-TOLUENE-XYLENE IN PETROLEUM REFINERY WASTE WATER BY ZnO / SnO 2 / WO 3 AND. , pp.54–61.

Hoffmann, M.R. et al., 1995. Environmental Applications of Semiconductor Photocatalysis. *Chemical Reviews*, 95(1), pp.69–96. Available at: http://pubs.acs.org/doi/abs/10.1021/cr00033a004 [Accessed March 24, 2014].

Ibhadon, A. & Fitzpatrick, P., 2013. Heterogeneous Photocatalysis: Recent Advances and Applications. *Catalysts*, 3(1), pp.189–218. Available at: http://www.mdpi.com/2073-4344/3/1/189/ [Accessed March 21, 2014].

Jeong, J., Sekiguchi, K. & Sakamoto, K., 2004. Photochemical and photocatalytic degradation of gaseous toluene using short-wavelength UV irradiation with TiO2 catalyst: comparison of three UV sources. *Chemosphere*, 57(7), pp.663–71. Available at: http://www.ncbi.nlm.nih.gov/pubmed/15488929 [Accessed April 3, 2014].

Jo, W.-K. & Lee, J.Y., 2013. Iron-impregnated titania composites for the decomposition of low-concentration aromatic organic pollutants under UV and visible light irradiation. *Chinese Journal of Catalysis*, 34(12), pp.2209–2216. Available at: http://linkinghub.elsevier.com/retrieve/pii/S1872206712606883 [Accessed March 2, 2014].

Laokiat, L. et al., 2011. Photocatalytic degradation of benzene, toluene, ethylbenzene, and xylene (BTEX) using transition metal-doped titanium dioxide immobilized on fiberglass cloth. *Korean Journal of Chemical Engineering*, 29(3), pp.377–383. Available at: http://link.springer.com/10.1007/s11814-011-0179-1 [Accessed February 25, 2014].

Lee, B. et al., 2003. Optical properties of Pt-TiO2 catalyst and photocatalytic activities for benzene decomposition. *Korean Journal of …*. Available at: http://link.springer.com/article/10.1007/BF02697281 [Accessed April 11, 2014].

Li, Z. et al., 2008. Effect of Fe-doped TiO2 nanoparticle derived from modified hydrothermal process on the photocatalytic degradation performance on methylene blue. *Journal of hazardous materials*, 155(3), pp.590–4. Available at: http://www.ncbi.nlm.nih.gov/pubmed/18179869 [Accessed March 26, 2014].

Lin, Y. et al., 2011. Study of benzylparaben photocatalytic degradation by TiO< sub> 2</sub>. *Applied Catalysis B: …*. Available at: http://www.sciencedirect.com/science/article/pii/S0926337311001093 [Accessed April 11, 2014].

Lu, X. et al., 2011. Preparation and characterization of Fe-TiO2 films with high visible photoactivity by autoclaved-sol method at low temperature. *Solid State Sciences*, 13(3), pp.625–629. Available at: http://dx.doi.org/10.1016/j.solidstatesciences.2010.12.036.

Maira, A.J. et al., 2001. Gas-phase photo-oxidation of toluene using nanometer-size TiO2 catalysts. *Applied Catalysis B: Environmental*, 29(4), pp.327–336. Available at: http://www.sciencedirect.com/science/article/pii/S0926337300002113 [Accessed April 13, 2014].

Mills, A. & Hunte, S. Le, 1997. An overview of semiconductor photocatalysis. *... of photochemistry and photobiology A: Chemistry*. Available at: http://www.sciencedirect.com/science/article/pii/S1010603097001184 [Accessed April 8, 2014].

Moura, C.P. et al., 2011. Adsorption of BTX (benzene, toluene, o-xylene, and p-xylene) from aqueous solutions by modified periodic mesoporous organosilica. *Journal of colloid and interface science*, 363(2), pp.626–34. Available at: http://www.ncbi.nlm.nih.gov/pubmed/21868024 [Accessed September 13, 2014].

Mwangi, I.W. et al., 2013. Immobilized Fe (III)-doped titanium dioxide for photodegradation of dissolved organic compounds in water. *Environmental science and pollution research international*, 20(9), pp.6028–38. Available at: http://www.ncbi.nlm.nih.gov/pubmed/23526310 [Accessed September 13, 2014].

Nasralla, N. et al., 2013. Structural and spectroscopic study of Fe-doped TiO2 nanoparticles prepared by sol-gel method. *Scientia Iranica*, 20(3), pp.1018–1022. Available at: http://dx.doi.org/10.1016/j.scient.2013.05.017.

Navío, J. a et al., 1999. Iron-doped titania semiconductor powders prepared by a sol-gel method. Part I : synthesis and characterization. *Applied Catalysis A: General*, 177(1), pp.111–120. Available at: http://www.sciencedirect.com/science/article/pii/S0926860X98002555\npapers://d1ebd311-64c1-4c1d-9832-9631d7abf4b4/Paper/p11933.

Newsam, J., 1988. Structural characterization of zeolite beta. *... of the Royal ...*. Available at: http://rspa.royalsocietypublishing.org/content/420/1859/375.short [Accessed June 16, 2015].

Oc, C.O.C. & Ioc, I.O.C., National Primary Drinking Water Regulations.

Ohno, T. et al., 2003. Synergism between rutile and anatase TiO 2 particles in photocatalytic oxidation of naphthalene. , 244, pp.383–391.

Ohno, T., Akiyoshi, M. & Umebayashi, T., 2004. Preparation of S-doped TiO< sub> 2</sub> photocatalysts and their photocatalytic activities under visible light. *Applied Catalysis A: ...*. Available at: http://www.sciencedirect.com/science/article/pii/S0926860X0400050X [Accessed April 11, 2014].

Palau, J. et al., 2012. Photodegradation of Toluene, m -Xylene, and n -Butyl Acetate and Their Mixtures over TiO 2 Catalyst on Glass Fibers. *Industrial & Engineering Chemistry*

Research, 51(17), pp.5986–5994. Available at: http://pubs.acs.org/doi/abs/10.1021/ie300357x [Accessed September 13, 2014].

Di Paola, A. et al., 2002. Photocatalytic degradation of organic compounds in aqueous systems by transition metal doped polycrystalline TiO2. *Catalysis Today*, 75(1-4), pp.87–93. Available at: http://www.sciencedirect.com/science/article/pii/S0920586102000482 [Accessed June 2, 2014].

Ranjit, K.T. & Viswanathan, B., 1997. Photocatalytic reduction of nitrite and nitrate ions over doped TiO2 catalysts. *Journal of Photochemistry and Photobiology A: Chemistry*, 107(1-3), pp.215–220. Available at: http://linkinghub.elsevier.com/retrieve/pii/S1010603097000257.

Ruthven, D.M., Eic, M. & Xu, Z., 1991. *Proceedings of ZEOCAT 90*, Elsevier. Available at: http://www.sciencedirect.com/science/article/pii/S0167299108629092 [Accessed June 16, 2015].

Shahalam, A.B. et al., 1997. Competitive adsorption phenomena adsorption phenomena of petrochemicals — benzene, toluene, and xylene in hexane in fixed-beds of sands. *Water, Air, & Soil Pollution*, 95(1-4), pp.221–235. Available at: http://link.springer.com/10.1007/BF02406167 [Accessed September 28, 2014].

Sing, K.S.W. et al., 1985. INTERNATIONAL UNION OF PURE COMMISSION ON COLLOID AND SURFACE CHEMISTRY INCLUDING CATALYSIS * REPORTING PHYSISORPTION DATA FOR GAS / SOLID SYSTEMS with Special Reference to the Determination of Surface Area and Porosity. *Pure & Appl. Chem.*, 57(4), pp.603–619.

Sivula, K., Formal, F. & Grätzel, M., 2009. WO3− Fe2O3 Photoanodes for Water Splitting: A Host Scaffold, Guest Absorber Approach. *Chemistry of Materials*. Available at: http://pubs.acs.org/doi/abs/10.1021/cm900565a [Accessed April 8, 2014].

Su, B. et al., 2007. Photocatalytic degradation of methylene blue on Fe3+-doped TiO2 nanoparticles under visible light irradiation. *Frontiers of Chemistry in China*, 2(4), pp.364–368. Available at: http://link.springer.com/10.1007/s11458-007-0069-6 [Accessed March 3, 2014].

Sun, S. et al., 2011. Photocatalytic degradation of gaseous o-xylene over M-TiO 2 (M=Ag, Fe, Cu, Co) in different humidity levels under visible-light irradiation: Activity and kinetic study. *Rare Metals*, 30(SUPPL.1), pp.147–152.

Sun, S. et al., 2012. Photocatalytic degradation of gaseous toluene on Fe-TiO2 under visible light irradiation: A study on the structure, activity and deactivation mechanism. *Applied Surface Science*, 258(12), pp.5031–5037. Available at: http://linkinghub.elsevier.com/retrieve/pii/S0169433212001055 [Accessed October 31, 2014].

Thiruvenkatachari, R., 2008. A review on UV/TiO2 photocatalytic oxidation process (Journal Review). *Korean Journal of …*. Available at: http://link.springer.com/article/10.1007/s11814-008-0011-8 [Accessed April 11, 2014].

Tong, T. et al., 2008. Preparation of Fe3+-doped TiO2 catalysts by controlled hydrolysis of titanium alkoxide and study on their photocatalytic activity for methyl orange degradation. *Journal of hazardous materials*, 155(3), pp.572–9. Available at: http://www.ncbi.nlm.nih.gov/pubmed/18191326 [Accessed September 13, 2014].

Tsoukleris, D.S. et al., 2007. Photocatalytic degradation of volatile organics on TiO2 embedded glass spherules. *Catalysis Today*, 129(1-2), pp.96–101. Available at: http://linkinghub.elsevier.com/retrieve/pii/S0920586107004117 [Accessed March 26, 2014].

Valente, J.P.S., Padilha, P.M. & Florentino, A.O., 2006. Studies on the adsorption and kinetics of photodegradation of a model compound for heterogeneous photocatalysis onto TiO(2). *Chemosphere*, 64(7), pp.1128–33. Available at: http://www.ncbi.nlm.nih.gov/pubmed/16405950 [Accessed October 9, 2014].

Vidal, C.B. et al., 2012. BTEX removal from aqueous solutions by HDTMA-modified Y zeolite. *Journal of environmental management*, 112, pp.178–85. Available at: http://www.sciencedirect.com/science/article/pii/S0301479712003908 [Accessed September 18, 2014].

Vidal, N.C. & Volzone, C., 2009. Analysis of tetramethylammonium–montmorillonite and retention of toluene from aqueous solution. *Applied Clay Science*, 45(4), pp.227–231. Available at: http://www.sciencedirect.com/science/article/pii/S016913170900132X [Accessed September 18, 2014].

Wang, W., Chiang, L.-W. & Ku, Y., 2003. Decomposition of benzene in air streams by UV/TiO2 process. *Journal of Hazardous Materials*, 101(2), pp.133–146. Available at: http://linkinghub.elsevier.com/retrieve/pii/S0304389403001699 [Accessed April 11, 2014].

Wang, Y., Jiang, Z.H. & Yang, F.J., 2006. Effect of Fe-doping on the pore structure of mesoporous titania. *Materials Science and Engineering B: Solid-State Materials for Advanced Technology*, 134(July), pp.76–79.

Wilbur, S. & Keith, S., 2007. Toxicological profile for benzene. *Atlanta, Ga, USA: US …*, (August). Available at: http://stacks.cdc.gov/view/cdc/6992/SMR=9.26 [Accessed March 31, 2014].

Xin, B. et al., 2007. Study on the mechanisms of photoinduced carriers separation and recombination for Fe3+–TiO2 photocatalysts. *Applied Surface Science*, 253(9), pp.4390–4395. Available at: http://linkinghub.elsevier.com/retrieve/pii/S0169433206012591 [Accessed March 1, 2014].

Xu, Y.-J., Zhuang, Y. & Fu, X., 2010. New Insight for Enhanced Photocatalytic Activity of TiO 2 by Doping Carbon Nanotubes: A Case Study on Degradation of Benzene and Methyl Orange. *The Journal of Physical Chemistry C*, 114(6), pp.2669–2676. Available at: http://pubs.acs.org/doi/abs/10.1021/jp909855p [Accessed April 12, 2014].

Yang, X. et al., 2009. Photo-catalytic degradation of Rhodamine B on C-, S-, N-, and Fe-doped TiO2 under visible-light irradiation. *Applied Catalysis B: Environmental*, 91, pp.657–662.

Zaleska, A., 2008. Doped-TiO 2 : A Review. , (1), pp.157–164.

Zhu, J. et al., 2004. Characterization of Fe–TiO2 photocatalysts synthesized by hydrothermal method and their photocatalytic reactivity for photodegradation of XRG dye diluted in water. *Journal of Molecular Catalysis A: Chemical*, 216(1), pp.35–43. Available at: http://linkinghub.elsevier.com/retrieve/pii/S1381116904000056 [Accessed February 10, 2014].

Zuo, G.-M. et al., 2006. Study on photocatalytic degradation of several volatile organic compounds. *Journal of hazardous materials*, 128(2-3), pp.158–63. Available at: http://www.ncbi.nlm.nih.gov/pubmed/16157448 [Accessed February 25, 2014].

Vitae

Personal Information:

Name: Abdulla Musbah Abdulla Mohammed Khair
Gender: Male
Religion: Muslim
Nationality: Sudanese
Date of Birth: 4/12/1986
Place of Birth: Abu Dhabi, UAE
Email Address: eng-musbah@hotmail.com
Marital status: Single

Education:

Graduate Level

- King Fahd University of Petroleum & Minerals, Chemical Engineering Department, M.Sc., June 2015, 3.46/4.00

Undergraduate Level

- University of Khartoum, Faculty of Engineering, Chemical Engineering Department, B.Sc., 2010, First Class (honours), 7.23/10

Academic Projects:

- ***Photo-catalytic degradation of Benzene, Toluene and Xylenes in aqueous solution*** 'Master thesis'

In this thesis, I synthesized and characterized TiO_2 for photo-catalytic degradation of BTX in aqueous Solution using UV light, where I succeeded in removal quite percentage of pollutants

- ***Design of Natural Gas Condensate Production Facility*** 'senior year'

It was senior year project were as a team work we were able to design Natural Gas Condensate Production Facility, going through Mass and Energy balances, thermodynamics, simulation, equipment design, safety analysis and cost estimation

- ***HYSYS simulation program in Chemical Engineering applications***.

It was for exploration and learning the program for chemical engineering application, applying industrial case studies for more understanding.

Vocational Experience:

- ***King Fahd University of Petroleum & Minerals, Research Institute, Center of environment and water*** [part time] ***1/4/2014 – 1/6/2014***

For the mentioned period, I prepared samples for analysis where some chemical and physical treatment needed for further analysis of the samples, to observe the effect of pollution on environment and make sure that not exceed the limit appointed by environmental agencies.

- ***University of Khartoum, Faculty of Engineering, Mathematical Engineering, Teaching Assistant*** ***13/10/2010 - 13/8/2011***

For the duration, I was responsible for teaching and marking the tutorials for about 200 students in addition to, marking and documentation of their exams, quizzes and tests. I even participate in my spare time to assist tutors in chemical engineering department in Heat Transfer tutorials.

Vocational Training:

- Khartoum Refining Company 23/10/2011 – 3/11/2011
- Nanotechnology IIUM 'International Islamic University of Malaysia' Three days
- Tappco / Al Managil Lubricants Blending Plant 30/8/2008 – 4/9/2008
- Savola edible oil Factory 7/7/2007 – 7/8/2007
- Tajoug Soap Factory 22/7/2006 – 24/8/2006

Professional Membership:

- Fellow of the Sudanese Engineering Society

Skills:

- English '**IELTS (6.5)**'

- Arabic '**mother tongue**'
- Microsoft Office '**word, excel & power point**'
- Simulation Package '**HYSYS & ChemCAD**
- Mathematica
- High performance liquid chromatography 'HPLC'
- Gas chromatography 'GC'
- Purge and Trap
- BET surface analyzer

Awards:

- **Scholarship** King Fahd University of Petroleum & Minerals **M.Sc. Program**

Extracurricular Activities:

- Brother's Wedding Planning 'April 2012'
- Head of academic trip to Malaysia 'September 2009'
- Active participant in University of Khartoum Engineering Fair, through (CHESS) Chemical Engineering Student Society '2007 & 2009'

Publication:

1. Multi component degradation of Toluene and Xylenes using iron doped titanium dioxide [**under preparation**]
2. Multi component degradation of Benzene and Xylenes using iron doped titanium dioxide [**under preparation**]
3. Multi component degradation of Benzene and Toluene using iron doped titanium dioxide [**under preparation**]